



저작자표시 2.0 대한민국

이용자는 아래의 조건을 따르는 경우에 한하여 자유롭게

- 이 저작물을 복제, 배포, 전송, 전시, 공연 및 방송할 수 있습니다.
- 이차적 저작물을 작성할 수 있습니다.
- 이 저작물을 영리 목적으로 이용할 수 있습니다.

다음과 같은 조건을 따라야 합니다:



저작자표시. 귀하는 원저작자를 표시하여야 합니다.

- 귀하는, 이 저작물의 재이용이나 배포의 경우, 이 저작물에 적용된 이용허락조건을 명확하게 나타내어야 합니다.
- 저작권자로부터 별도의 허가를 받으면 이러한 조건들은 적용되지 않습니다.

저작권법에 따른 이용자의 권리는 위의 내용에 의하여 영향을 받지 않습니다.

이것은 [이용허락규약\(Legal Code\)](#)을 이해하기 쉽게 요약한 것입니다.

[Disclaimer](#) 

공학석사 학위논문

An Investigation on Structural Design of Reinforced Concrete Slabs with Steps

단차가 있는 철근콘크리트 슬래브의
구조설계에 관한 연구

2014년 2월

서울대학교 대학원

건축학과

김 상 희

An Investigation on Structural Design of Reinforced Concrete Slabs with Steps

지도 교수 강 현 구

이 논문을 공학석사 학위논문으로 제출함

2014년 2월

서울대학교 대학원

건축학과

김 상 희

김상희의 공학석사 학위논문을 인준함

2014년 2월

위 원 장

홍성진

(인)

부위원장

강현구

(인)

위 원

박종근

(인)



Abstract

An Investigation on Structural Design of Reinforced Concrete Slabs with Steps

Kim, Sanghee

Dept. of Architecture & Architectural Engineering

The Graduate School

Seoul National University

Advisor: Prof. Thomas Kang

Reinforced concrete slabs with steps were experimentally studied to analyze their structural performance and to suggest reinforcing details of the step. Because the stepped slabs may behave very poorly in terms of bending strength, stiffness, deflection, cracking, etc., the study is aimed at suggesting proper reinforcing details so that the same bending strength as that without steps can be obtained. The bending strengths of 12 test specimens with a variety of different reinforcing detail types or other parameters were compared with one another. The specimen without any additional reinforcement in the step exhibited a very low bending strength and significant damage, and the specimens

with diagonal reinforcements in the step manifested substantial early cracks and hinging of the step as well as a substantial loss of the bending strength. On the contrary, the specimens with a combination of U-bars, revU-bars, L-bars, and revL-bars performed very well and reached up to 100 % of the slab bending strength. U-bars and revU-bars were effective in controlling diagonal cracks, while L-bars and revL-bars were effective in preventing the yielding of slab reinforcement near the step.

The second purpose of the analysis of this study was to propose a modification factor to reflect the stiffness modification of a step in flat plates. Reinforced concrete slabs with steps exhibit distinct structural characteristics that are determined by a series of structural experiment and nonlinear analysis. The corner of the step was weak and flexible, and thus the rotational stiffness at the corner of the step was investigated through the analyses with 6 types of models using a nonlinear finite element program. Then, a systematic analysis on the stiffness change was performed using a linear finite element procedure along with rotational springs. The stiffness of reinforced concrete flat plates with steps was mainly affected by the step length, location, thickness and height. First, a single modification factor for each of these variables was obtained, while other variables were constrained. When the influence of multiple variables were simultaneously considered, the single modification factor was multiplied by one another. This method was verified by a comparative analysis, and, finally, it was found that the complex modification factor as suggested in this study could be used

together with the existing effective beam width model.

Keywords: Step, Flat plate, Additional bar, Modification factor, Effective beam width

Student Number : 2012-20548

Table of Contents

Abstract	i
Table of Contents	iv
Figures	ix
Tables	xvi
Notations	xviii
Chapter 1 Introduction	1
1.1 Background of the Research	1
1.2 Purpose of the Research	3
1.3 Literature Review	5
1.3.1 Overview of details of step reinforcement in the overseas	5
1.3.2 Research of Kang et al.	6
1.3.3 Research of Grossman on effective beam width	8
1.3.4 Research of Hwang and Moehle on effective beam width	9
1.4 Research Scope and Contents	10

Chapter 2 Quantity Estimation of Additional Reinforcement in the Step	13
2.1 Stress Flow in the Step	13
2.2 Estimation Method for Additional Rebar Quantity	15
2.3 Estimation of Additional Rebar Quantity	17
2.3.1 Type-A model with 210 mm step thickness ..	17
2.3.2 Type-A model with 400 mm step thickness ..	17
2.3.3 Type-B model with 210 mm step thickness ..	18
2.4 Application of the Computed Additional Rebar Quantity to the Specimen	19
2.5 Summary of Results	20
 Chapter 3 Gravity Load Test	 21
3.1 Experimental Plan	21
3.2 Design of Test Specimen	24
3.3 Test Specimen Fabrication	42
3.4 Test Method	47

Chapter 4 Experimental Results and Proposal of Detailing Design for the Step	49
4.1 Material Test Result	49
4.1.1 Result of concrete material test	49
4.1.2 Result of rebar material test	50
4.2 Cracking of the Specimens and the Failure Mode	51
4.2.1 Cracking stages of the slab and the failure mode	51
4.2.2 Cracking of the specimens and the failure mode	54
4.3 Analysis of the Experimental Results	70
4.3.1 Overview of experimental result analysis	70
4.3.2 Analysis of experimental result	72
4.4 Concept of Step Reinforcement Design	83
4.4.1 Additional reinforcement quantity of revU-bar	85
4.4.2 Additional reinforcement quantity of U-bar	86
4.4.3 Additional reinforcement quantity of L-bar and revL-bar	86
4.5 Proposal of Step Reinforcement Design	86
4.5.1 Anchoring of main rebar in the slab	87

4.5.2 Design of revU-bar and U-bar	88
4.5.3 Design of revL-bar and L-bar	89
4.5.4 Construction sequence	91
4.6 Necessity of Stiffness Analysis based on the Experimental Result	96
4.7 Summary of Results	97

Chapter 5 Stiffness Analysis in Consideration of Steps 99

5.1 Input Method through Elastic Link	99
5.2 Computation and Application of Rotational Stiffness	102
5.3 Procedure and Condition for the Computation of Step Modification Factor	103
5.3.1 Rotational stiffness by the area of influence ..	103
5.3.2 Procedure of modification factor computation	104
5.4 Analysis Result of Step Modification Factor	106
5.4.1 Basics of stiffness analysis	106
5.4.2 Relationship between variables and single modification factor	107
5.4.3 Variables analysis and proposal of step modification factor	112

5.5 Summary of Results	121
Chapter 6 Conclusions	123
References	126
국 문 초 록 (Korean Abstract)	128

Figures

Fig. 1.1.1	Frequency characteristics of drainage noise	2
Fig. 1.1.2	Plane and sectional views of slabs with steps	3
Fig. 1.3.1	Exemplar reinforcement scheme for a large step at the top of a beam	5
Fig. 1.3.2	Step in the beam bottom located near a column ...	5
Fig. 1.3.3	A large step or elevation change in a beam can create a bent	6
Fig. 1.3.4	Slabs with steps	6
Fig. 1.3.5	Initial stiffness and deformation of each specimen during maximum bearing	8
Fig. 1.4.1	Concept of modification factor (γ) computation through stiffness analysis	12
Fig. 2.1.1	Stress flow in the step within a slab	14
Fig. 2.1.2	Stress in the step	14
Fig. 2.1.3	Proposals with strut-tie	14
Fig. 2.2.1	Location of the rebar from the step	15
Fig. 2.2.2	Type-A strut-tie model with 210 mm step thickness	16
Fig. 2.2.3	Type-A strut-tie model with 400 mm step thickness	16
Fig. 2.2.4	Type-B strut-tie model with 210 mm step thickness	16
Fig. 2.3.1	Sectional force of Type-A model with 210 mm step thickness	17

Fig. 2.3.2	Sectional force of Type-A model with 400 mm step thickness	18
Fig. 2.3.3	Sectional force of Type-B model with 210 mm step thickness	18
Fig. 3.2.1	Drawing of specimen-1 image and the gauge location	28
Fig. 3.2.2	Drawing of specimen-2 image and the gauge location	29
Fig. 3.2.3	Drawing of specimen-3 image and the gauge location	30
Fig. 3.2.4	Drawing of specimen-4 image and the gauge location	31
Fig. 3.2.5	Drawing of specimen-5 image and the gauge location	32
Fig. 3.2.6	Drawing of specimen-6 image and the gauge location	33
Fig. 3.2.7	Drawing of specimen-7 image and the gauge location	34
Fig. 3.2.8	Drawing of specimen-8 image and the gauge location	35
Fig. 3.2.9	Drawing of specimen-9 image and the gauge location	36
Fig. 3.2.10	Drawing of specimen-10 image and the gauge location	37
Fig. 3.2.11	Drawing of specimen-11 image and the gauge location	38
Fig. 3.2.12	Drawing of specimen-12 image and the gauge location	39
Fig. 3.2.13	Detail of the step (specimen-2 ~ specimen-7)	40
Fig. 3.2.14	Detail of the step (specimen-8 ~ specimen-12)	40
Fig. 3.2.15	Detail of the end of specimen	40
Fig. 3.2.16	Detail of the hook	40
Fig. 3.2.17	Type-A additional rebar	41

Fig. 3.2.18 Type-B additional rebar	41
Fig. 3.2.19 Type-C additional rebar	41
Fig. 3.3.1 Process of rebar layout and gauge installation	44
Fig. 3.3.2 Form preparation and concrete placement process	45
Fig. 3.3.3 Laboratory table installation and testing process	46
Fig. 3.4.1 Test set-up	47
Fig. 3.4.2 Method 1 of installing line loading device	48
Fig. 3.4.3 Method 2 of installing line loading device	48
Fig. 3.4.4 Installation drawing of LVDT and wire gauge	48
Fig. 4.1.1 Compressive strength of specimens	50
Fig. 4.2.1 Stages of cracking and failure of the step	53
Fig. 4.2.2 Cracking of specimen-1 by loading stage	55
Fig. 4.2.3 Cracking of specimen-2 by loading stage	56
Fig. 4.2.4 Cracking of specimen-3 by loading stage	58
Fig. 4.2.5 Cracking of specimen-4 by loading stage	59
Fig. 4.2.6 Cracking of specimen-5 by loading stage	60
Fig. 4.2.7 Cracking of specimen-6 by loading stage	61
Fig. 4.2.8 Cracking of specimen-7 by loading stage	62
Fig. 4.2.9 Cracking of specimen-8 by loading stage	64

Fig. 4.2.10 Cracking of specimen-9 by loading stage	65
Fig. 4.2.11 Cracking of specimen-10 by loading stage	66
Fig. 4.2.12 Cracking of specimen-11 by loading stage	68
Fig. 4.2.13 Cracking of specimen-12 by loading stage	69
Fig. 4.3.1 Location of rotational angle	71
Fig. 4.3.2 Center applied load-displacement relations (specimens-1, 5, 9, 12)	73
Fig. 4.3.3 Center applied load-displacement relations (specimens-1 and 2)	74
Fig. 4.3.4 Comparison of load-angle of specimen-2	74
Fig. 4.3.5 Center applied load-displacement relations (specimens-1, 2, 6, 10, 11)	75
Fig. 4.3.6 Center applied load-displacement relations (specimens-1, 5, 10)	77
Fig. 4.3.7 Applied load-angle relations of SP-10	77
Fig. 4.3.8 Center applied load-displacement relations (specimens-1, 5, 9)	78
Fig. 4.3.9 Center applied load-displacement relations (specimens-1, 4, 7)	79
Fig. 4.3.10 Strain of specimen-4 with revU-bar	80
Fig. 4.3.11 Center applied load-displacement relations (specimens-1, 3, 4, 5)	80
Fig. 4.3.12 Center applied load-displacement relations (specimens-1, 4, 8)	81

Fig. 4.3.13 Strain of inclined rebar of specimen-4	82
Fig. 4.3.14 Strain of inclined rebar of specimen-8	82
Fig. 4.3.15 Center applied load-displacement relations (specimens-1, 9, 12)	83
Fig. 4.3.16 Strain of the main rebar of specimen-12	83
Fig. 4.4.1 Concept drawing of rebar placement at the step area	84
Fig. 4.4.2 Stress flow at upper step	85
Fig. 4.4.3 Stress flow at lower step	85
Fig. 4.5.1 Rebar termination #1	88
Fig. 4.5.2 Rebar termination #2	88
Fig. 4.5.3 revU-bar in upper slab	89
Fig. 4.5.4 U-bar in lower slab	89
Fig. 4.5.5 revL-bar of upper slab	90
Fig. 4.5.6 L-bar of lower slab	90
Fig. 4.5.7 revL-bar of upper slab	91
Fig. 4.5.8 L-bar of lower slab	91
Fig. 4.5.9 revL-bar of upper slab	91
Fig. 4.5.10 L-bar of lower slab	91
Fig. 4.5.11 Longitudinal placement of lower main rebar in lower slab	93

Fig. 4.5.12 Placement of U-bar	93
Fig. 4.5.13 Placement of L-bar	94
Fig. 4.5.14 Perpendicular placement of lower main rebar in lower slab	94
Fig. 4.5.15 Longitudinal placement of lower main rebar in upper slab	94
Fig. 4.5.16 Placement of revL-bar	94
Fig. 4.5.17 Perpendicular placement of upper main rebar in lower slab	95
Fig. 4.5.18 Longitudinal placement of upper main rebar in lower slab	95
Fig. 4.5.19 Perpendicular placement of lower main rebar in upper slab	95
Fig. 4.5.20 Perpendicular placement of lower main rebar in upper slab	95
Fig. 4.5.21 Longitudinal placement of upper main rebar in upper slab	96
Fig. 4.5.22 Placement of revU-bar	96
Fig. 5.1.1 Actual behavior of the step	100
Fig. 5.1.2 Behavior of stiffness analysis program	100
Fig. 5.1.3 Element coordinates	101
Fig. 5.1.4 Input form for rotational stiffness	101
Fig. 5.2.1 Relationship of moment-rotational angle (-) per unit length.....	102

Fig. 5.2.2	Relationship of moment-rotational angle (+) per unit length	102
Fig. 5.3.1	Frame modeling	104
Fig. 5.3.2	Concept of modification factor (γ) computation through stiffness analysis	106
Fig. 5.4.1	Basic plane view for stiffness analysis	107
Fig. 5.4.2	Location of the step	108

Tables

Table 1.1.1	SPL of existing drainage system	1
Table 1.1.2	Existing structure of slab and method of its improvement	3
Table 1.2.1	Comparison of wall-slab structure and flat slab hybrid structure	4
Table 1.3.1	List of specimens used in the research of Kang et al.	7
Table 2.4.1	Additional required rebar quantity	19
Table 2.4.2	Additional required rebar applied to actual specimen	19
Table 3.1.1	Basic specification of the specimen	22
Table 3.1.2	Plan for the specimens	22
Table 3.1.3	Plan for the specimen composition by variables ..	23
Table 3.3.1	Schedule of preliminary experiment (first test)	42
Table 3.3.2	Schedule of follow-up experiment (second test) ..	43
Table 4.1.1	Concrete mix design	49
Table 4.1.2	Concrete compressive strength	50
Table 4.1.3	Tensile strength of the rebars	51
Table 4.3.1	Maximum bending strength of each specimen	72
Table 4.3.2	Secant stiffness at the applied load of 20 kN and $(3/4)P_{\max}$	76

Table 5.4.1	Specification of the basic model for stiffness analysis	107
Table 5.4.2	Analysis result by the change of step length and location for strength design	115
Table 5.4.3	Analysis result by the change of step length and location for serviceability design	116
Table 5.4.4	Analysis result by the change of step thickness	117
Table 5.4.5	Analysis result by the change of step height	117
Table 5.4.6	Analysis result by the increase in the length of slab adjacent in both sides	118
Table 5.4.7	Analysis result by the increase in the length of slab adjacent in one side	118
Table 5.4.8	Analysis result by the increase in the column size	119
Table 5.4.9	Analysis result by the number of continuous slabs	119
Table 5.4.10	Complex analysis result in simultaneous consideration of several variables	120
Table 5.5.1	Single modification factor by step length and location	121
Table 5.5.2	Single modification factor by step thickness	122
Table 5.5.3	Single modification factor by step height	122

Notations

A_b	=	Cross area of one flexural tensile rebar placed in the slab, mm^2
A_{rU}	=	Cross area of one revU bar, mm^2
A_s	=	Total cross area per unit width of longitudinal flexural tensile rebar in the slab with step, mm^2/mm
A_{s_rU}	=	Total cross area per unit width of revU bar reinforcement in the joint panel area of the step, mm^2/mm
A_{s_U}	=	Total cross area per unit width of U bar reinforcement in the joint area of the step, mm^2/mm
b_i	=	Effective beam width of flat slab, satisfying the basic condition of stiffness design while controlling for the variables, mm
b'_k	=	Effective beam width of slab with step, satisfying the basic condition of stiffness design with the step length being 50 % of the slab length and the location of step being at the center of inner slab while controlling for the variables, mm
b_{cal}	=	Step effective beam width from multiplying step modification factor by the effective beam width of flat slab ($\gamma \times b_i$)
b_k	=	Effective beam width through stiffness analysis simultaneously with several variables
c	=	Dimension of a square column dimension

c_1	=	Width of the supporting column in the direction of the moment computation, mm
c_1	=	Column size, mm
c_2	=	Width of the supporting column in the direction perpendicular to the span of moment computation, mm
d	=	Effective depth of the slab, mm
f_{ck}	=	Concrete compressive design standard strength, MPa
f_y	=	Design standard yield strength of one rebar, MPa
f_{y-rU}	=	Design standard yield strength of one revU bar, MPa
$f_{y-U} :$	=	Design standard yield strength of U-bar reinforcement in the joint area of the step, MPa
h	=	Slab thickness, mm
K_d	=	Stiffness modification factor
K_{FP}	=	Location index of the column (inner column: 1.0, exterior column: 0.8, corner column: 0.6)
$K_{\text{sec}, 20\text{kN}}$	=	Secant stiffness at the load of 20 kN, kN/mm
$K_{\text{sec}, (3/4)P_{\text{max}}}$	=	Secant stiffness at 3/4 of maximum load, kN/mm
l	=	Length of a square slab
l_1	=	Distance between the center of columns in the direction of moment computation, mm

l_2	=	Distance between the center of columns in the direction perpendicular to the span of moment computation, mm
l_2'	=	Effective beam width (αl_2), mm
L	=	Size of loading capacity, lb/ft ²
$M_{actuator\ load}$	=	Moment produced by line load device and lading force, kN · m
M_{max}	=	Maximum moment measured in the experiment, kN · m
$M_{self\ weight}$	=	Moment at the center of the specimen produced by the weight of the specimen itself, kN · m
SDx	=	Stiffness in the x-axis direction of element coordinates
SDy	=	Stiffness in the y-axis direction of element coordinates
SDz	=	Stiffness in the z-axis direction of element coordinates
SRx	=	Rotational stiffness in the x-axis direction of element coordinates
SRy	=	Rotational stiffness in the y-axis direction of element coordinates
SRz	=	Rotational stiffness in the z-axis direction of element coordinates
α	=	Effective width coefficient
β	=	Stiffness reduction coefficient

$\Delta_{20\text{kN}}$	=	Deflection at the center with the load of 20 kN, mm
$\Delta_{3/4P_{\max}}$	=	Deflection at the center with 3/4 of maximum load, mm
γ	=	Step modification factor
γ'	=	Single modification factor
γ'_1	=	Single modification factor by the step length and location
γ'_2	=	Single modification factor by step thickness
γ'_3	=	Single modification factor by step height

Chapter 1

Introduction

1.1 Background of the Research

Apartments have been widely favored as a solution for housing market problem due to rapid urbanization and over-population. Additionally, they have been popular to the urban dwellers, who prefer more comfortable and convenient housing. They have been rapidly expanded in accordance with the government housing policy. However, there is a trade-off effect from the perspective of actual dwellers. Especially, noise problem is not just limited to the apartment dwellers but is a society issue. Moreover, the flushing in the toilet causes not only a noise problem but also a privacy invasion. The flushing noise records 38 dB(A) and 34 dB(A) but manifests the maximum noise level at the sound frequency of 1 kHz \sim 2 kHz, where people respond the most sensitively (Table 1.1.1, Fig. 1.1.1)^[1]. Thus, this study aims at stopping the noise transmission by installing the step in the slab. In other words, the usage of step would not follow the existing method of boring through the slab to connect to the lower floor but to place the drainage system in the step to contain the noise transmission within the floor.

Table 1.1.1 SPL of existing drainage system^[1] unit: dB(A)

Classification	Noise from the upper floor			Noise within the floor		
Ventilation fan	Bathroom	Living room	Bed room	Bathroom	Living room	Bed room
On	52-54	36-38	31-34	-	-	-
Off	50-52	35-37	31-33	78-80	54-57	44-49

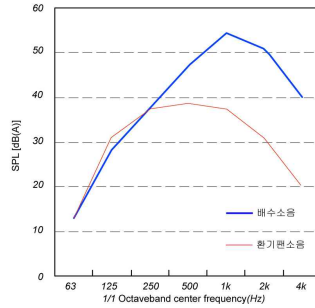


Fig. 1.1.1 Frequency characteristics of drainage noise^[1]

One of the serious problems that apartment buildings should solve is the maintenance and repair of bathroom drainage. The typical existing drainage of apartment bathroom has been to install the drainage system of the upper floor on the ceiling of lower floor. This type of drainage system requires the repair done from the bathroom of lower floor in case of the problems in the drainage of upper floor. This causes privacy invasion to the dwellers of lower floor and it is difficult to carry out the drainage repair in case of disagreement between the upper and lower floor residents.

Therefore, a method^[2] of installing the drainage within the same floor by placing a step of 230 mm height in the slab is considered to deal with this problem (Fig. 1.1.2). However, this design proposal involves step installation, which in turn causes the change of the slab height. Previous design limited the step height only to 60 mm, but this recent proposal will increase it to 230 mm, which will greatly affect the structural performance of the slab (Table 1.1.2). Additionally, the structural pattern of recent apartments changed from wall-slab structure to flat slab structure for its easiness of remodelling and flat slab-wall slab hybrid structure. Thus, it is important to investigate the influence of

large step on structural performance of flat slab structure in terms of gravity and flexural resistance. Then, it is necessary to carry out the analysis and reinforcement of the step in consideration of the influence.

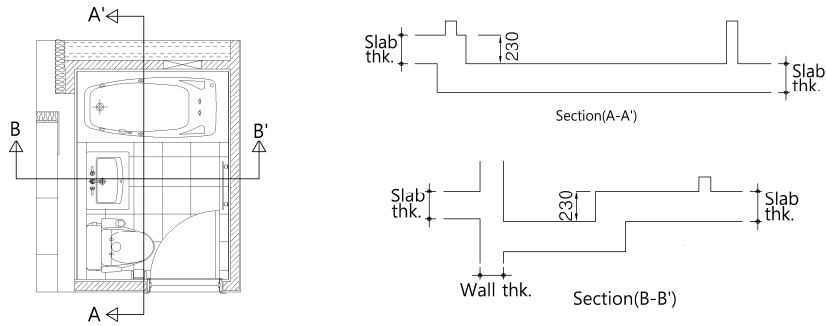


Fig. 1.1.2 Plane and sectional views of slabs with steps

Table 1.1.2 Existing structure of slab and method of its improvement

Classification	Wall-slab structure	Flat slab hybrid structure
Current		
Proposed		

1.2 Purpose of the Research

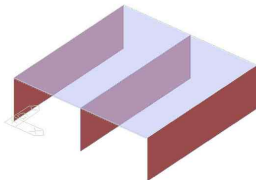
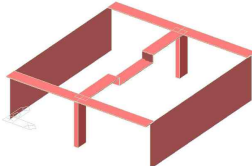
The purpose of this research is to comprehensively examine the structural performance of slabs with steps such as strength, stiffness change, deflection, cracking, etc. and to suggest stiffness modification factor and methods of reinforcing the step. The purpose coincides with the objective of flexible design of slabs and lowering of bathroom flushing noise as well as the

maintenance and repair of drainage system of apartments. The details of this research are as follows.

- 1) Methods of reinforcing the step for lowering of cracking and manifestation of flexural strength equivalent to the flat slab without step.
- 2) Proposal of effective beam width in consideration of the slab with step (Table 1.2.1)
- 3) Suggestion of methods of reinforcing the step through experiment and analytical research.

The study carried out experiments on slabs with steps and derived new relational equations with a variety of variables (step length, step thickness, concrete strength, etc.) based on the experimental result. That is, the structural performance of flat slab against gravity load and flexural load is examined in consideration of the step in the slab, and the methods of reinforcing flat slab with step and effective stiffness modification factor are suggested based on the experimental result.

Table 1.2.1 Comparison of wall-slab structure and flat slab hybrid structure

Classi- fication	Wall-slab structure	Flat slab hybrid structure
Flexural load support	 <p>[Bearing wall + Slab]</p>	 <p>[Bearing wall + Effective beam (replacing of slab)]</p>
	Slab transfers flexural load to wall	Support flexural load with effective beam replacing slab

1.3 Literature Review

1.3.1 Overview of details of step reinforcement in the overseas

When the cross section of the beam is reduced from D2 to D1 as shown in Fig. 1.3.1, the upper main rebar of D2 is anchored with 90° hook, and the upper main rebar of D1 is affixed to D2.^[3] If necessary, additional reinforcement rebar is installed around the step. If the step is located near the shear, support or at the place of large moment, structural analysis should be performed. Additionally, if the step is located near the column, the small beam of D1 can be extended to the column (Fig. 1.3.2).

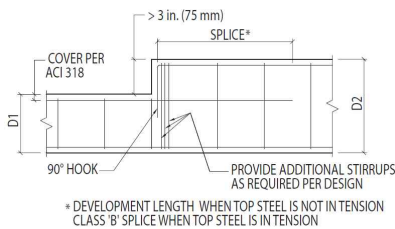


Fig. 1.3.1 Exemplar reinforcement scheme for a large step at the top of a beam

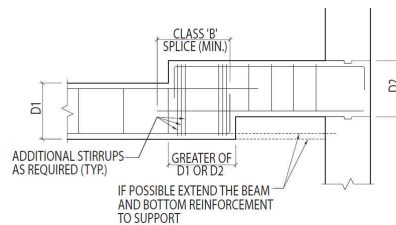


Fig. 1.3.2 Step in the beam bottom located near a column

Moreover, if the steps of D1 and D2 are large as shown in Fig. 1.3.3, the step is subjected to bending and requires the analysis of moment and shear at the critical cross section. The vertical member is tension strut, and vertical reinforcement should be accompanied.

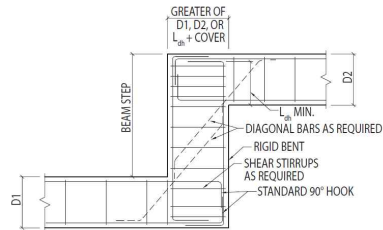


Fig. 1.3.3 A large step or elevation change in a beam can create a bent

1.3.2 Research of Kang et al.^[4]

The research of Kang et al.^[4] formed a partial ramen structure by placing a beam at the frame area such as wall and column (Fig. 1.3.4) to make the construction of step easier. This was an effort to deal some of the horizontal force with by the beam as a resistance to the flexural force. The safety of beam-slab is very important in securing the safety of the compound structure, and its structural performance was investigated.

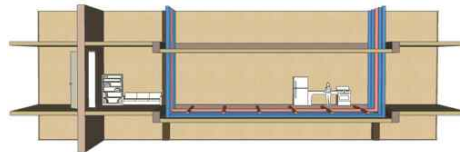


Fig. 1.3.4 Slabs with steps

An experiment was carried out to examine the structural performance of the beam-slab (Table 1.3.1). The beam with step possesses the same shear reinforcement (150 mm spacing between the shear reinforcement) as T-beam, and if there is no bending at the anchor, the bearing capacity rapidly decreased after maximum bearing force. However,

the bearing of the bent beam decreased more stably. When the spacing of the shear reinforcement was set at 75 mm, the stiffness or maximum bearing capacity manifested the same level as the case of 140 mm spacing. However, the bearing decreased more stably after the maximum bearing. When the spacing of shear reinforcement was set at 200 mm, the maximum bearing exhibited the similar behavior as the case of 150 mm spacing, but its bearing decrease was relatively larger after the maximum bearing. Examining HT3 and HT1-1, the shear reinforcement was spaced at 75 mm and 200 mm, respectively, and the stiffness and the behavior after the maximum bearing were more stable with more shear reinforcement (Fig. 1.3.5).

Table 1.3.1 List of specimens used in the research of Kang et al.^[4]

Specimen	Experimental variable	Remark
GB1	Standard	Oblong double reinforcement beam
GT1	T-beam	Ordinary T-beam
HT1	Half T-beam, shear reinforcement	Beam with step
HT2	Half T-beam, shear reinforcement	Beam with step
HT3	Half T-beam, shear reinforcement	Beam with step
HT1-1	Half T-beam, anchoring rebar detail	Beam with step
RT1	Reverse T-beam	Reverse T-beam

GB1 : 600×450×6500 mm, GT1 ~ RT1 : 2600×450×6500 mm

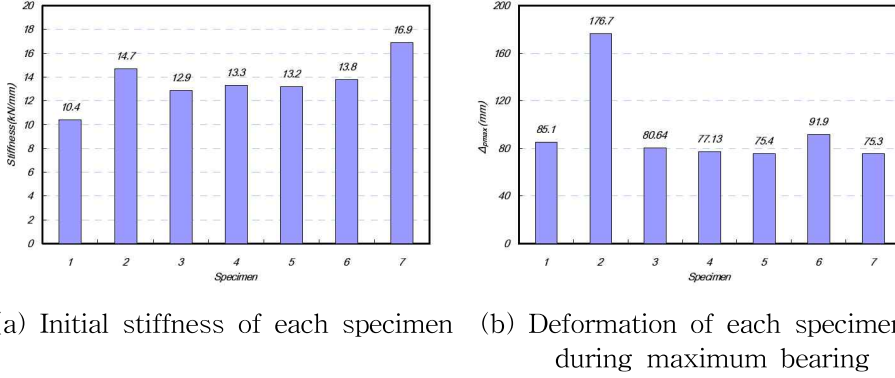


Fig. 1.3.5 Initial stiffness and deformation of each specimen during maximum bearing

1.3.3 Research of Grossman^[5] on effective beam width

The effective beam width method of Grossman^[5] computes the effective beam width so that the effect of stiffness reduction of the slab in response to the story drift can be more accurately predicted by using a stiffness reduction coefficient based on the result of U.C. Berkeley experiment. However, this computational equation was derived based on the assumption of square column with regular layout, greatly limiting its application to other structures. The elastic effective beam width of the exterior frame composed of corner joint and exterior joint parallel to the load direction is computed by multiplying the elastic effective width of interior frame by $[l_3 + (l_2/2)]l_2$. This means the slab part from the center of the column parallel to the load direction to the slab end. The elastic effective beam width of exterior frame, $\alpha l_3 + l_e/2$, is obtained by multiplying the modification factor of Grossman^[5] to the elastic effective beam width of interior

frame. This means the coefficient of α , the change of moment of entire slab, should be applied to l_3 . where α is the effective beam width coefficient and is the ratio of the elastic effective beam width to the slab width. This proposed equation is the computational equation of interior frame effective beam width. Additionally, the boundary between elastic and inelastic behavior is not clear. The method of effective beam width computation of Grossman^[5] for interior frame is shown below.

$$l_2' = \alpha l_2 = K_d [0.3l_1 + c_1(l_2/l_1) + (c_2 - c_1)/2] (d/r)(0.9h)(K_{FP}) \quad (\text{Eq. 1.3.1})$$

where $0.2K_d K_{FP} l_2 \leq l_2' \leq 0.5K_d K_{FP} l_2$

1.3.4 Research of Hwang and Moehle^[6] on effective beam width

Hwang and Moehle^[6] suggested stiffness reduction coefficient (at slab rotation of 0.5 %) for rectangle slab with rectangle column with the variable of load capacity size. Especially, they performed the experiment with 40 % reduced scale model of 3×3 span of one floor. Their equation (Eq. 1.3.2) is based on rigid joint assumption, and $1(1 - c_1/l_1)^3$ is multiplied for the case of flexible joint. Hwang and Moehle^[6] proposed 1/3 modification factor for the computation of elastic effective beam width of the exterior frame composed of corner joint and joint parallel to the load direction. Finally, the proposed equation of effective beam width is for the slab connected to the column and cannot be used for the case of slab being supported by structural wall.

$$\beta = 5c/l - 0.1(L/40 - 1) \geq 1/3 \quad (\text{Eq. 1.3.2})$$

1.4 Research Scope and Contents

The research on the flat slab with step structure can be largely grouped into three categories as shown below.

- 1) Computation of additional reinforcement rebar quantity in the step prior to the experiment
- 2) Gravity load test
- 3) Investigation of step modification factor

There are not previous studies on the slab with high step, and it is a customary practice to apply details based on the experience at the field site. However, it was noted that reinforcement against the stress concentration on the step was necessary based on preliminary nonlinear analysis. Thus, this study aimed at developing the rational reinforcement detail with strut-tie model.

The purpose of gravity load test is to analyze the structural performance change of slab with step with respect to gravity load on the basis of existing flat slab and to propose a reinforcement detail. The experiment involved 4-point loading on the slab specimen with both end simple supports in one direction, and the test data were compared with the data of finite element analysis so that the reliability of finite element analysis result could be examined.

The items of the experiment are shown below.

- 1) Failure mode of the slab specimen
- 2) Behavior of the step during failure
- 3) Maximum flexural strength of the slab specimen
- 4) Slab stiffness due to load-deflection relation and influence on the step
- 5) Ductility evaluation of the specimen by each variable

A method of reinforcing the step in the slab is proposed based on the result of test and analysis of such structural performance of the slab with step as flexural strength, stiffness, and deflection, etc. The step reinforcement method examined the flexural strength of the slab with step and is based on a strut-tie model.

The force flow around the step is examined to apply the strut-tie method so as to compute the quantity of necessary reinforcement rebar. Various reinforcement details are evaluated through experiments, and variable analysis is carried out afterwards. All these research results are used to propose the step reinforcement method for the flat slab with step.

Since nonlinear analysis requires a great deal of time and effort, effective beam width model analysis is performed from the practical point of view so that the relationship between various variables and stiffness, which has not been subjected to nonlinear analysis, is analyzed.

The relationship between stiffness and the variables of effective beam width model analysis is used as the basic data for the establishment of the effective beam width equation for the flat slab structure with step.

The concept of effective beam width for a slab with step in two directions is to replace with effective beam width of flat slab of the same lateral displacement against the same lateral force. In other words, the effective beam width of the slab with step is to replace with the flat slab of the same lateral displacement by multiplying modification factor to the effective beam width, which was obtained from the flat slab with step ($b_k = b_i \times \gamma$) as shown in Fig. 1.4.1. The modification factor differs with the condition of the step. The main variables of the stiffness analysis for the modification factor computation are the entire length of the slab, the length and depth of the step, concrete strength, rebar detail, etc., and the modification factor is determined by analyzing a variety of variable analyses. Additionally, the stiffness difference between the structure with step and without step is analyzed to reflect the result to the modification factor computation.

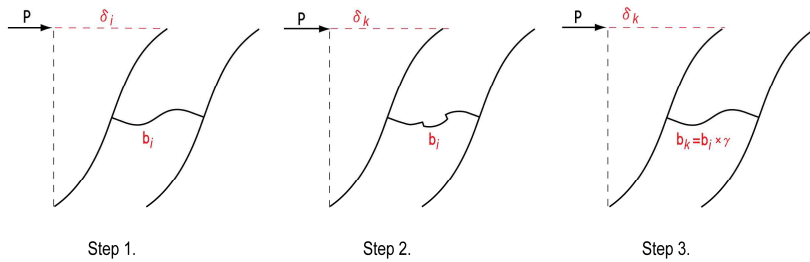


Fig. 1.4.1 Concept of modification factor (γ) computation through stiffness analysis

Chapter 2

Quantity Estimation of Additional Reinforcement in the Step

It is not easy to apply a complex analytical method for the limit design of concrete structure member, which possesses geometric or static discontinuity, or typical rebar layout details in a limited case to new and unfamiliar design environment. Strut-tie Model^[7] is a fundamental approach to visually display the load transfer route with the strut (representing the compressive strength on the concrete), tie (representing the tensile strength on the rebar) and the nodal area of strut-tie joint. In other words, it is a design tool to determine the required rebar quantity, the location of rebar layout, and the concentrated stress on the concrete.

This study applied the strut-tie method to identify the stress flow in the step and aimed at computing the required rebar quantity. The strut-tie method was applied through a simple truss modelling as shown in the next section.

2.1 Stress Flow in the Step

The stress flow in the step of the slab specimen was examined through stiffness analysis as shown in Figs. 2.1.1 and 2.1.2. It can be seen that the tensile stress is concentrated in the exterior bent area while compressive stress is concentrated in the interior bent area.

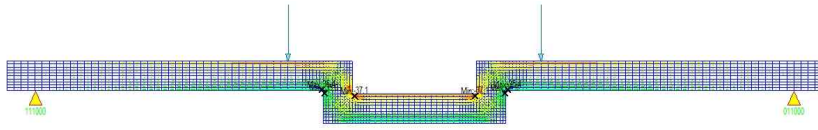


Fig. 2.1.1 Stress flow in the step within a slab

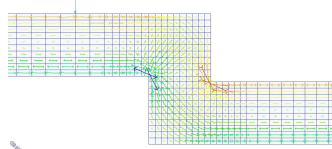
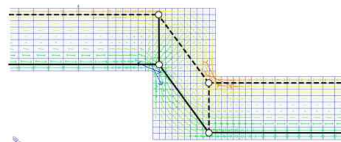
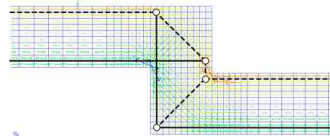


Fig. 2.1.2 Stress in the step

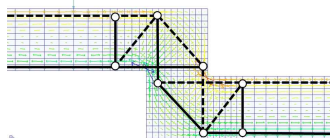
A strut-tie model was developed based on the analysis of the figures of stress flow as shown in Fig. 2.1.3. Proposals 2 and 3 were applied among various proposals to compute the required rebar quantity based on their appropriateness for this design.



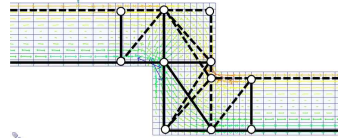
(a) Proposal 1



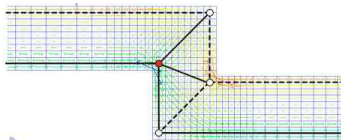
(b) Proposal 2



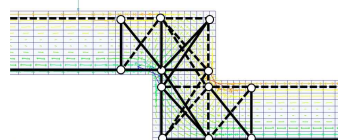
(c) Proposal 3



(d) Proposal 4



(e) Proposal 5



(f) Proposal 6

Fig. 2.1.3 Proposals with strut-tie

2.2 Estimation Method for Additional Rebar Quantity

The aforementioned proposals 2 and 3 in the previous section were renamed as Type-A and Type-B, respectively. Type-A is chosen for the necessary quantity computation of U-bar and revU-bar while Type-B is the model for the computation of necessary quantity of diagonal rebar. Each of these models was subjected to stiffness analysis. The additional required rebar quantity could be computed based on the force exerted on the strut and tie through elastic analysis.

The distance from the upper and lower surface to the center of the main rebar (d, d') is 36.5 mm as shown in Fig. 2.2.1. The location was set to be rotational section, and 443.45 kN of T and C was exerted to the right main rebar, followed by shear force of 33.75 kN.

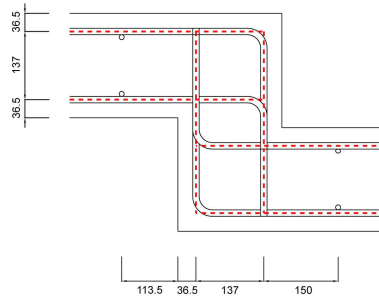


Fig. 2.2.1 Location of the rebar from the step (mm)

The loads based on strut-tie method were classified as Type-A and Type-B. Type-A involved step thickness of 210 mm (Fig. 2.2.2) and 400 mm (Fig. 2.2.3), and the step thickness of Type-B was 210 mm (Fig. 2.2.4).

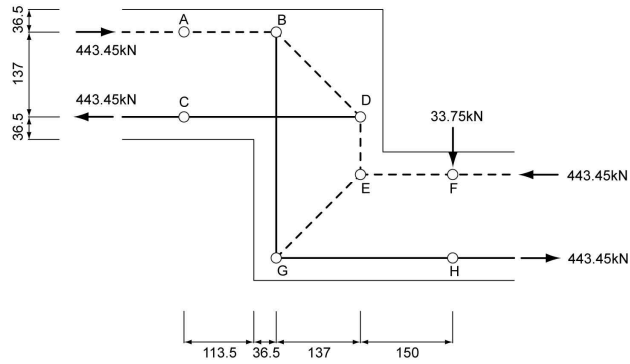


Fig. 2.2.2 Type-A strut-tie model with 210 mm step thickness

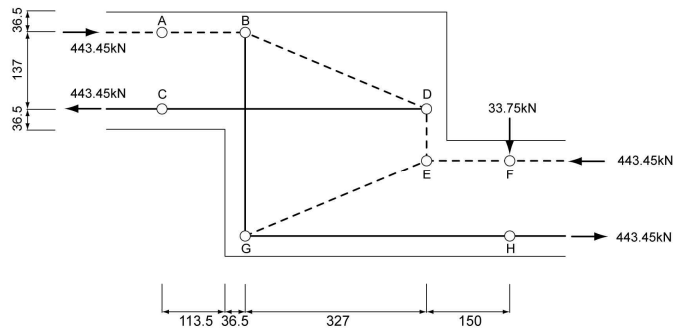


Fig. 2.2.3 Type-A strut-tie model with 400 mm step thickness

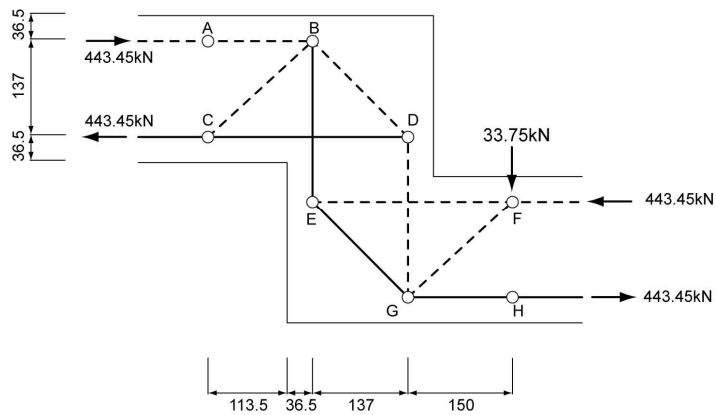


Fig. 2.2.4 Type-B strut-tie model with 210 mm step thickness

2.3 Estimation of Additional Rebar Quantity

2.3.1 Type-A model with step 210 mm thickness

Fig. 2.3.1 shows the sectional force of Type-A strut-tie model of the 210 mm step thickness in a slab. Since the specimen with 210 mm step thickness was to be reinforced with U-bar and revU-bar, the additional required rebar quantity could be computed with BG member. Because the sectional force of BG member is 443.4 kN, the sectional force could be divided into $A_s f_y$ to find out the required rebar quantity. This study planned to reinforce the step with seven SD500 D13 and four SD600 D16.

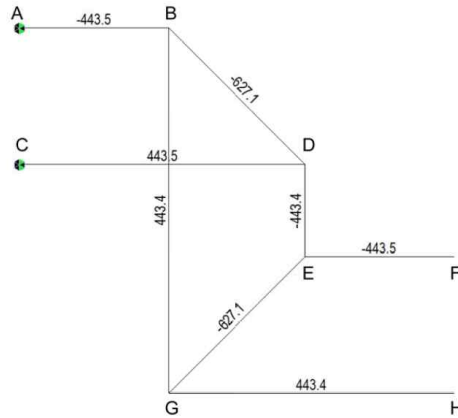


Fig. 2.3.1 Sectional force (kN) of Type-A model with 210 mm step thickness

2.3.2 Type-A model with 400 mm step thickness

The sectional force of Type-A strut-tie model of 400 mm step thickness is shown in Fig. 2.3.2. Since the specimen of 400 mm step thickness was to be reinforced with revU-bar, the additional rebar quantity could be computed with BG member.

Because the sectional force of BG member was 185.8 kN, the reinforcement required three SD500 D13 and two SD600 D16.

2.3.3 Type-B model with 210 mm step thickness

The sectional force of Type-B strut-tie model of 210 mm step thickness is shown in Fig. 2.3.3. Since the specimen of 210 mm step thickness was to be reinforced with inclined rebar, the additional rebar quantity could also be computed with EG member. Because the sectional force of EG member was 574.9 kN, the reinforcement required ten SD500 D13 and five SD600 D16.

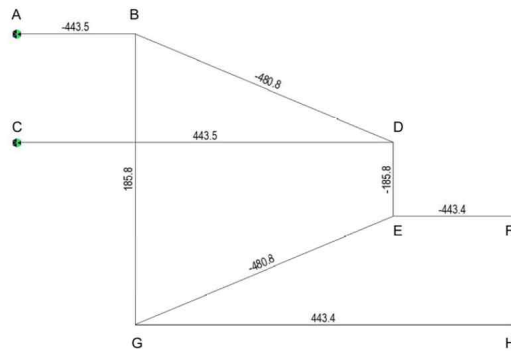


Fig. 2.3.2 Sectional force (kN) of Type-A model with 400 mm step thickness

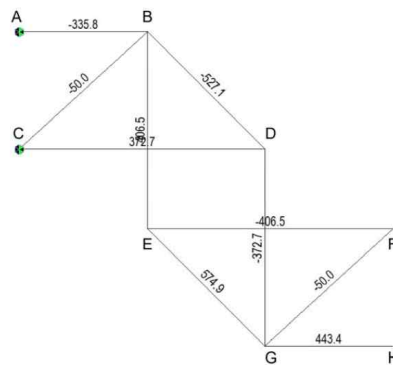


Fig. 2.3.3 Sectional force (kN) of Type-B model with 210 mm step thickness

2.4 Application of the Estimated Additional Rebar Quantity to the Specimen

Table 2.4.1 summarizes the additional required rebar quantity, which was computed in the previous 2.3 section, and Table 2.4.2 shows the actual application of the computed additional rebar quantity to specimens based on Table 2.4.1.

Table 2.4.1 Additional required rebar quantity

Strut-tie model	Step thickness	D13	D16	Remarks
Type-A	210 mm	7	4	
	400 mm	3	2	
Type-B	210 mm	10	5	

Table 2.4.2 Additional required rebar applied to actual specimen

Specimen	Additional rebar	Specimen	Additional rebar
Specimen-3 (Type-B, 200 mm)	Six inclined rebar, Six revU-bar	Specimen-8 (Type-B, 200 mm)	Six inclined rebar, Six revU-bar
Specimen-4 (Type-B, 200 mm)	Six inclined rebar, Six revU-bar	Specimen-9 (Type-A, 200 mm)	Six revU-bar
Specimen-5 (Type-A, 200 mm)	six revU-bar	Specimen-11 (Type-A, 400 mm)	Six revU-bar
Specimen-7 (Type-B, 200 mm)	Six revU-bar		

2.5 Summary of Results

Additional rebar quantity necessary for the step reinforcement was computed by applying strut-tie method. the computational result points to the conclusion that additional rebars are necessary in the similar quantity as the longitudinal reinforcement quantity. This result was reflected to actual specimens. Nonetheless, although strut-tie model assumed complete anchoring of the rebar, it was not possible in reality. Thus, some specimens were designed with more rebars than the quantity computed from the strut-tie model.

Chapter 3

Gravity Load Test

3.1 Experimental Plan

A slab specimen of 1000 mm width, 5800 mm length, and 210 mm thickness as shown in Table 3.1.1 was prepared in order to analyze the behavior of the slab with step and establish its improvement. The height of the step was fixed at 230 mm, and the length and thickness of the step were varied as experimental variables. The cover thickness was designed to be 30 mm for the top and bottom and 10 mm for the side.

Upper and lower main rebars were used as the rebar for the experiment, and SD500 D13 rebars were spaced at 150 mm interval as reinforcement around the step. However, SD600 D16 rebars were used in some cases in order to increase the reinforcement rebar for specimen-8. Three types of reinforcement, Type-A, Type-B, and Type-C were applied to each specimen according to the variable plan. The design standard for the concrete strength was set to be 24 MPa, and concrete specimens for strength test was prepared to measure the compressive strength.

Gravity load test was carried out with the first trend analysis as preliminary test, followed by a second test as the follow-up. Accordingly, there were a total of twelve specimens prepared as shown in Table 3.1.2, and the composition of the planned specimens with respect to the experimental variables is shown in Table 3.1.3.

Table 3.1.1 Basic specification of the specimen

Concrete design strength	$f_{ck} = 24 \text{ MPa}$	Rebar strength	$f_y = \text{SD500}$ (D13 and below)
Slab thickness	210 mm		$f_y = \text{SD600}$ (D16 and above)
Step height	230 mm	Cover	top and bottom : 30 mm side : 10 mm
Slab width	1000 mm	Main rebar	7-D13@150

Table 3.1.2 Plan for the specimens

Test	Specimen	Step length (mm)	Step thk. (mm)	Add. rebar	Rebar ratio	a/d	M_n (kN · m)	$V@M_n$ (kN)	V_n (kN)
1 st preli-minary test	Specimen -1	-	-	-	0.00535	10.37	75.2	41.8	141
	Specimen -2	1090	210	-	0.00535	10.37	75.2	41.8	141
	Specimen -3	1090	210	D13 @150	0.00535	10.37	75.2	41.8	141
	Specimen -4	1090	210	D13 @150	0.00535	10.37	75.2	41.8	141
	Specimen -5	1090	210	D13 @150	0.00535	10.37	75.2	41.8	141
	Specimen -6	1090	250	-	0.00535	10.37	75.2	41.8	141
	Specimen -7	1090	210	D13 @150	0.00535	10.37	75.2	41.8	141

Test	Specimen	Step length (mm)	Step thk. (mm)	Add. rebar	Rebar ratio	a/d	M_n (kN · m)	$V@M_n$ (kN)	V_n (kN)
2 nd follow-up test	Specimen -8	1090	210	D13+ D16 @150	0.00535	10.37	75.2	41.8	141
	Specimen -9	1090	210	D13 @150	0.00535	10.37	75.2	41.8	141
	Specimen -10	1090	210+ 180 (Slope)	D13 @150	0.00535	10.37	75.2	41.8	141
	Specimen -11	1090	400	D13 @150	0.00535	10.37	75.2	41.8	141
	Specimen -12	2700	210	D13 @150	0.00535	10.37	75.2	41.8	141

Table 3.1.3 Plan for the specimen composition by variables

With or w/o hook	Ordinary slab	Step thickness	Additional rebar		
			Type-A	Type-B	Type-C
Hook of 135° at the end of the main rebar	Specimen-1	Specimen-2 (210 mm)	Specimen-3 (revU-bar)	Specimen-4 (revU-bar)	Specimen-5
		Specimen-6 (250 mm)		Specimen-7	
Straight end of the main rebar		Specimen-10 (inclined step)		Specimen-8 (revU-bar, inclined rebar D16)	Specimen-9
		Specimen-11 (400 mm)			Specimen-12 (Step length : 2700 mm)

3.2 Design of Test Specimen

Specimen-1 (Table 3.2.1) is the standard specimen for the comparison of test results of the slabs with steps and is a typical RC flat slab of 1000 mm unit width without a step. SD500 D13 was used as the main rebar, and seven of those were spaced at 150 mm interval.

Specimen-2 (Fig. 3.2.2) is a slab with step and is designed with anchoring of the main rebar only and without additional reinforcement around the step. This specimen is used for the direct comparison with the existing method of specimen-1 by the presence or absence of the step in terms of cracking around the step, deflection and flexural strength, etc. The main rebar at right and left upper slab is anchored with a hook of 90° angle from the step toward lower slab and is finished with a hook of 135° angle at the end (Fig. 3.2.13). The main rebar at the center lower slab is anchored with a hook of 90° angle from the step toward upper slab and is finished with a hook of 135° angle at the end. The main rebar at both ends of the specimen is anchored with a hook of 180° (Fig. 3.2.15).

The step of specimen-3 (Fig. 3.2.3) was reinforced with Type-A (Fig. 3.2.17) and revU-bar. There are two inclined rebars laid out in the step as reinforcement (Fig. 3.5.1), and the one side of the inclined rebar was anchored to the upper main rebar of upper slab, and the other side was anchored at the lower main rebar of lower slab. revU-bar was installed as additional reinforcement.

The step of specimen-4 (Fig. 3.2.4) was reinforced with Type-B (Fig. 3.2.18) and revU-bar. There are two inclined rebars laid out in the step as reinforcement, and each of the inclined rebar at upper step is anchored at the upper main rebar of upper slab and upper main rebar of lower slab. Likewise, each of the inclined rebar laid out at the lower step is anchored at the lower main rebar of upper slab and lower main rebar of lower slab. revU-bar was installed as additional reinforcement of the step.

The step of specimen-5 (Fig. 3.2.5) was reinforced with Type-C additional rebar (Fig. 3.2.19). revU-bar reinforced the step and upper slab, and L-bar was used as a reinforcement of the lower slab and step. Moreover, U-bar and revU-bar were installed in the step as reinforcement.

Specimen-6 (Fig. 3.2.6) possesses the same form and layout as the specimen-2. The only difference is the thickness of the step. The step thickness of specimen-2 is the same 210 mm as the basic slab thickness, but the step thickness of specimen-6 is 250 mm. It was intended to examine the influence of change of the step thickness on the flexural behavior of the slab.

The step of specimen-7 (Fig. 3.2.7) was reinforced with Type-B additional rebar. Two inclined rebars were diagonally laid out between the step and main rebar. The inclined rebar laid out in the upper step is connected to upper main rebar of upper slab or upper main rebar of lower slab. Likewise, the inclined rebar laid out in the lower step is connected to the lower main rebar of upper slab or lower main rebar of lower slab. Although

specimen-4 was reinforced with revU-bar, specimen-7 is reinforced with inclined rebar only, and there is no reinforcement of revU-bar. This experimental plan was to evaluate the performance of revU-bar.

Specimen-8 (Fig. 3.2.8) possesses the same form, layout and additional rebar reinforcement as specimen-4. The only difference was there is no hook of 135° angle at the end of the main rebar anchoring inside the step (Fig. 3.2.14). SD600 D16 was used as diagonal reinforcement, enabling the comparison of the performance of the inclined rebars anchoring inside the step according to $A_s f_y$ with that of specimen-4.

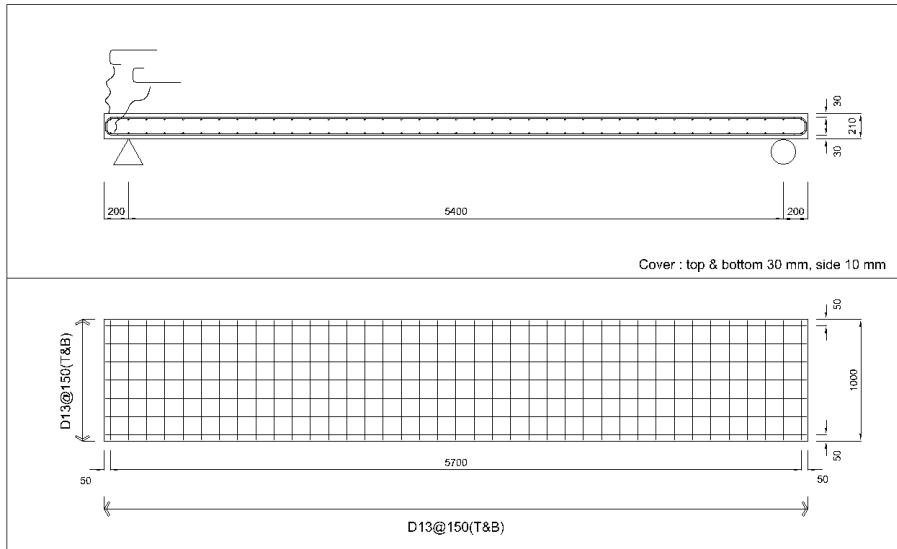
Specimen-9 (Fig. 3.2.9) has the same basic form, layout, and additional rebar reinforcement as specimen-5. The only difference was there is no hook of 135° angle at the end of the main rebar anchoring inside the step, enabling the comparison of the performance according to the presence or absence of the 135° hook at the end of the main rebar anchoring inside the step with that of specimen-5.

Specimen-10 (Fig. 3.2.10) encompasses a total of 390 mm step composed of 210 mm step and 180 mm inclined step. Although the main rebar of in the slab of all other specimens except for specimen-10 is anchored to the step. the lower main rebar of left upper slab, upper main rebar of lower slab, and lower main rebar of right upper slab is just one continuous rebar for the case of specimen-10. The lower main rebar of lower slab is laid out along the 180 mm inclined step, and there is no 135° hook at the

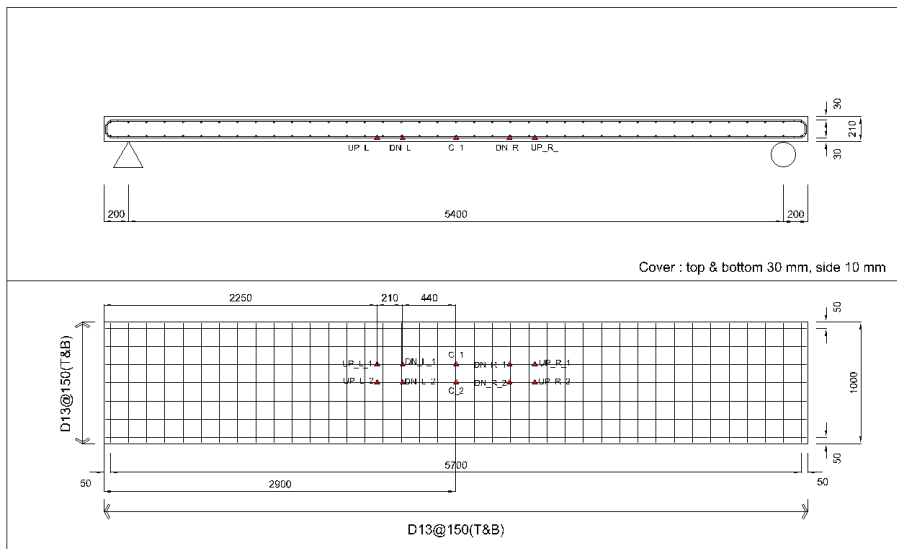
end of the main rebar. The step is reinforced with revU-bar.

Although specimen-11 (Fig. 3.2.11) is similar to specimen-2, its step thickness is larger at 400 mm. The basic layout is the same as specimen-2, and revU bar was installed in the step. The main rebar anchoring in the step does not have a hook at the end. The revU-bar of the specimen-11 has the dimension of 340 mm width and 380 mm height in accordance with the 400 mm step thickness.

Specimen-12 (Fig. 3.2.12) has the same upper and lower main rebar and the same additional rebar reinforcement of the step as specimen-9 with the only difference of the step length. Although other specimens have the step length of 1090 mm and 20 % length ratio of the step length to clear span, the step length of specimen-12 is 2700 mm with 50 % length ratio of the step length to clear span. This experimental set-up was planned to examine the difference of the behavior in response to shear span and to evaluate the performance during simultaneous exertion of shear force and moment. Additionally, although the loading point of other specimens was located outside the lower slab, i.e. upper slab, the loading point of specimen-12 was within the lower slab.

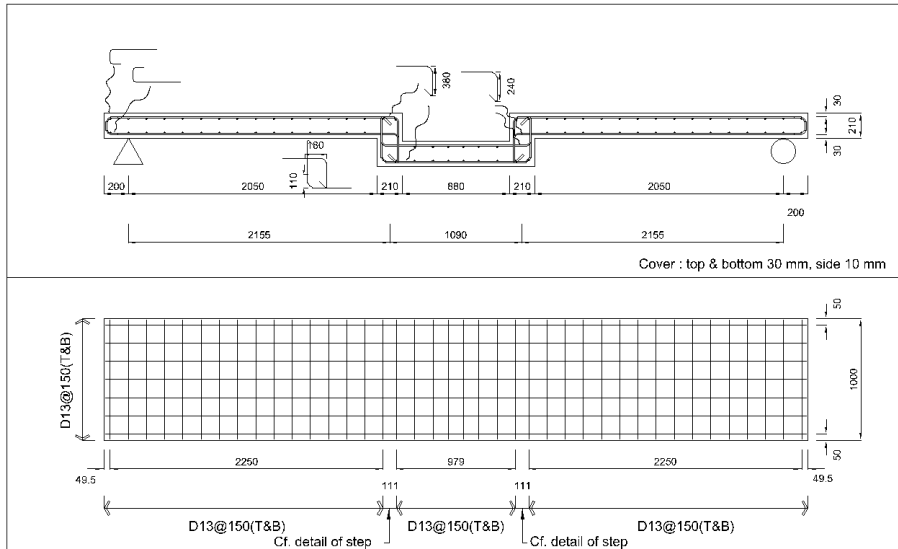


(a) Plane and sectional views of specimen-1

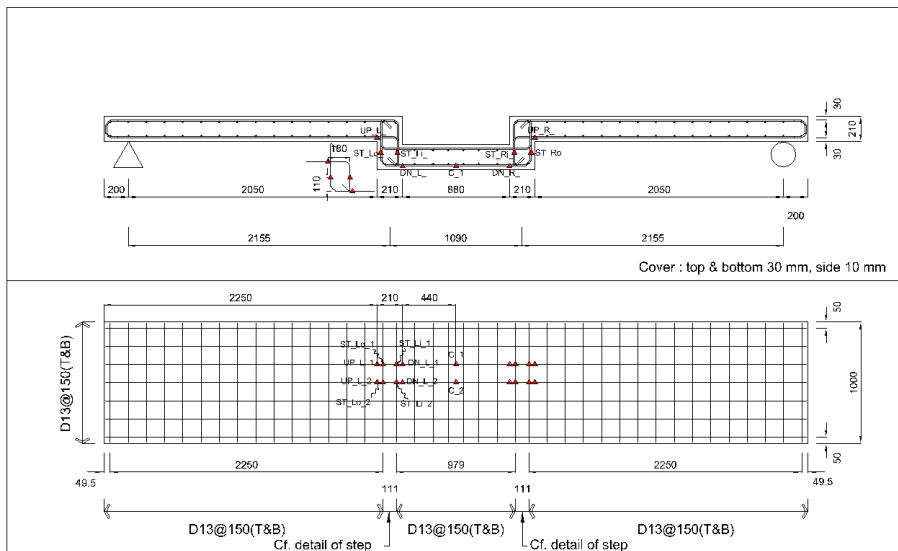


(b) Gauge location of specimen-1

Fig. 3.2.1 Drawing of specimen-1 image and the gauge location (mm)

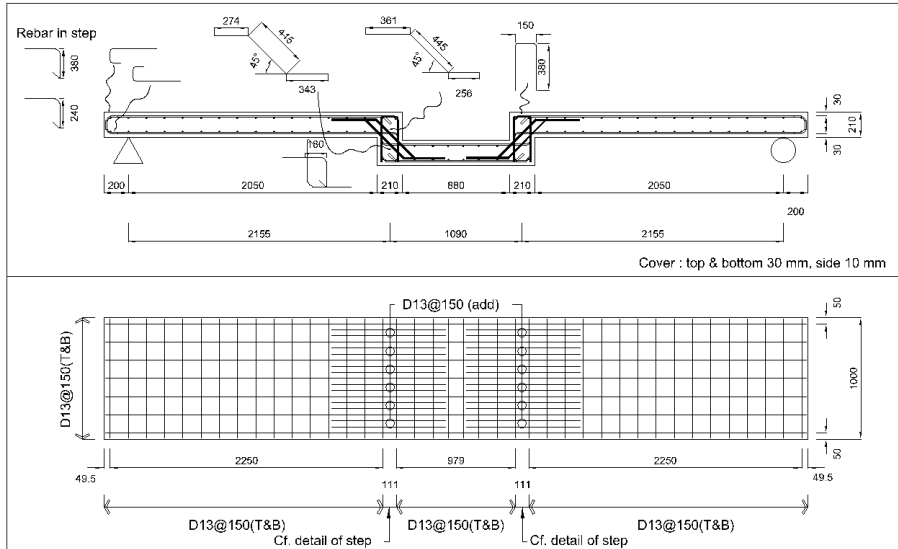


(a) Plane and sectional views of specimen-2

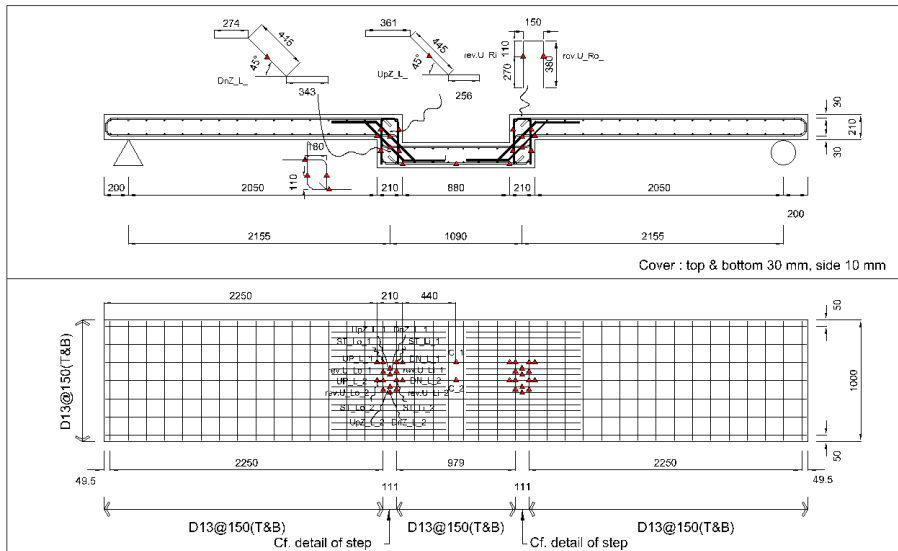


(b) Gauge location of specimen-2

Fig. 3.2.2 Drawing of specimen-2 image and the gauge location (mm)

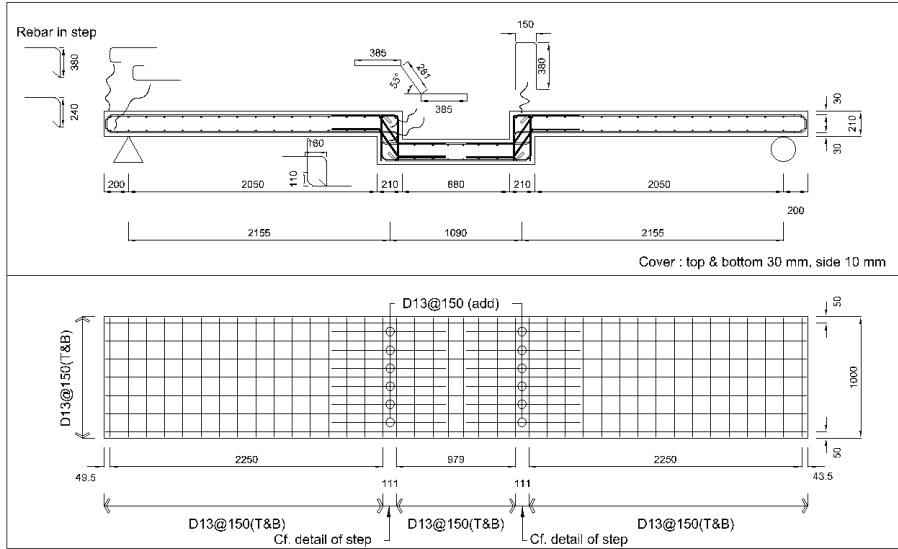


(a) Plane and sectional views of specimen-3

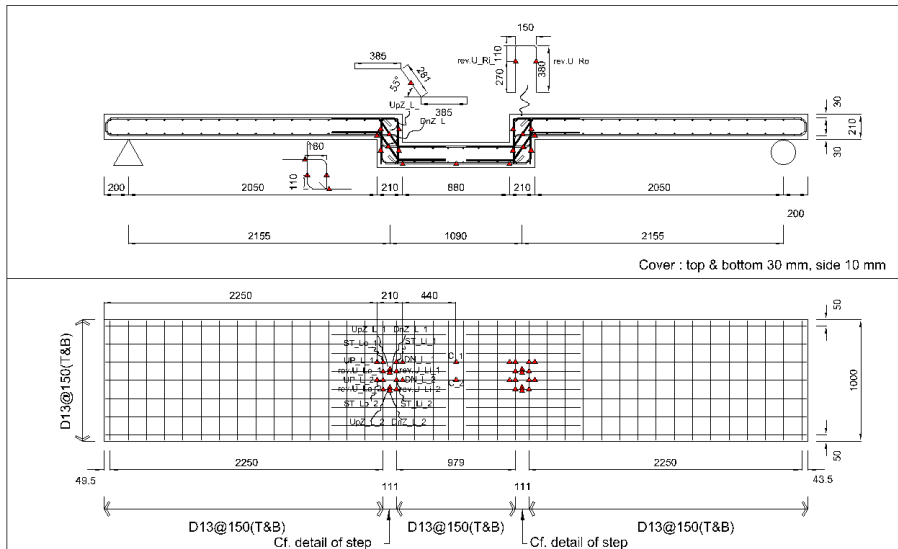


(b) Gauge location of specimen-3

Fig. 3.2.3 Drawing of specimen-3 image and the gauge location (mm)



(a) Plane and sectional views of specimen-4



(b) Gauge location of specimen-4

Fig. 3.2.4 Drawing of specimen-4 image and the gauge location (mm)

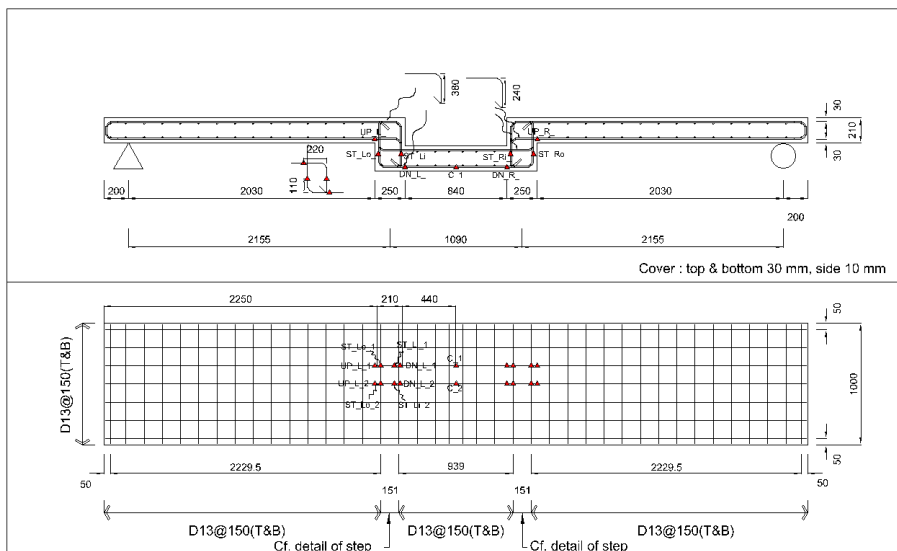
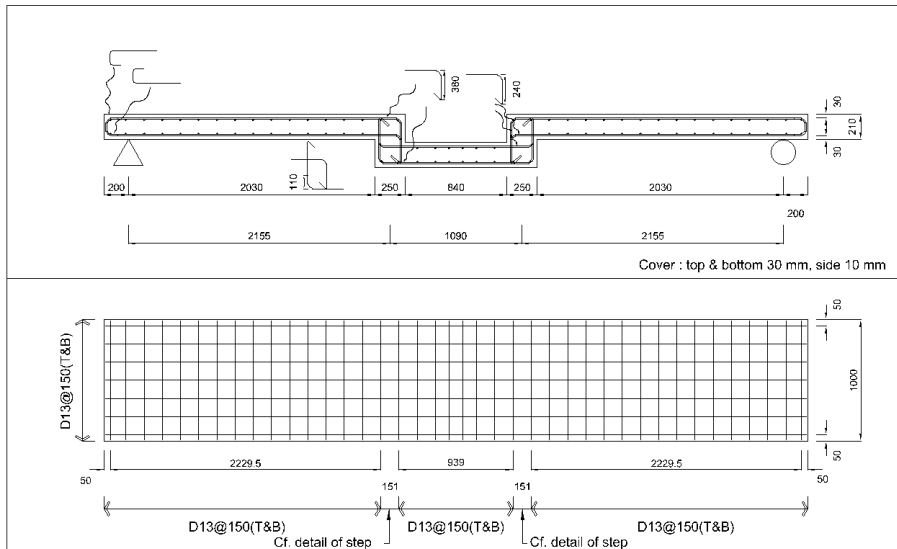
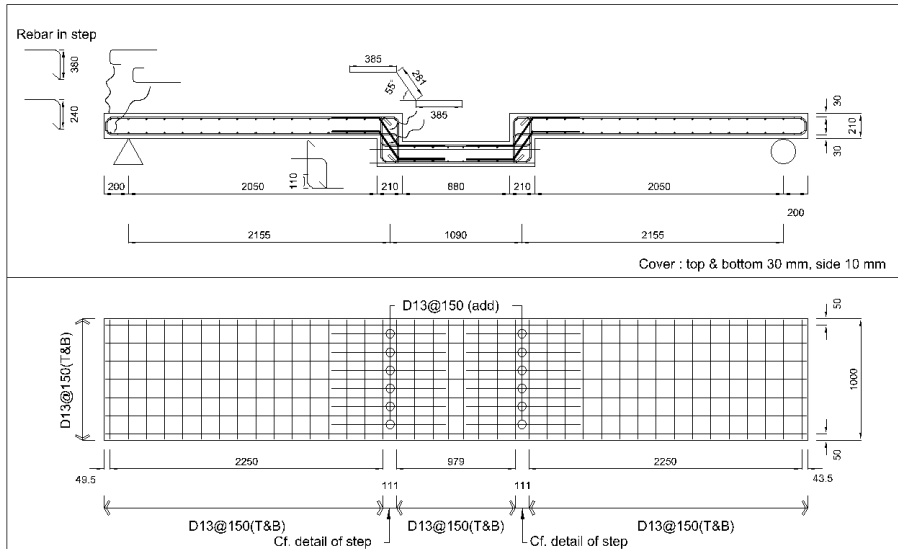
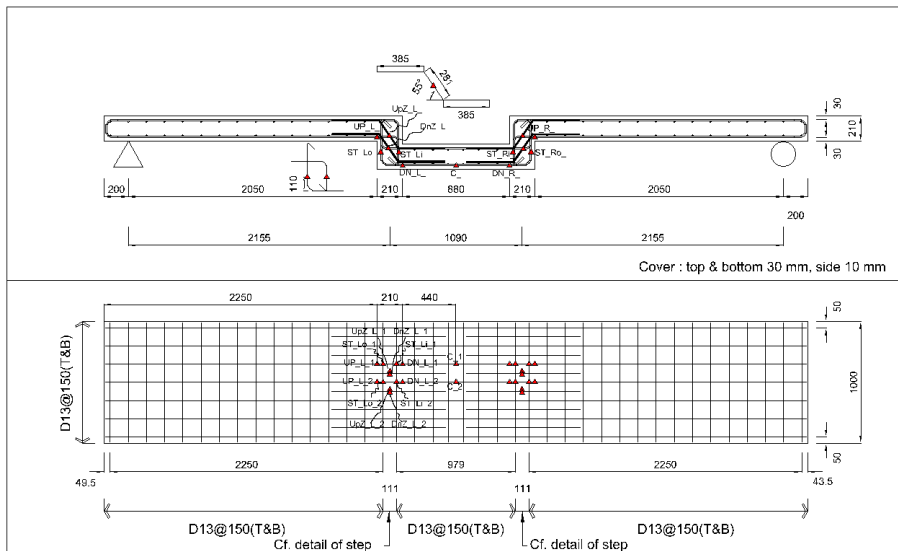


Fig. 3.2.6 Drawing of specimen-6 image and the gauge location (mm)

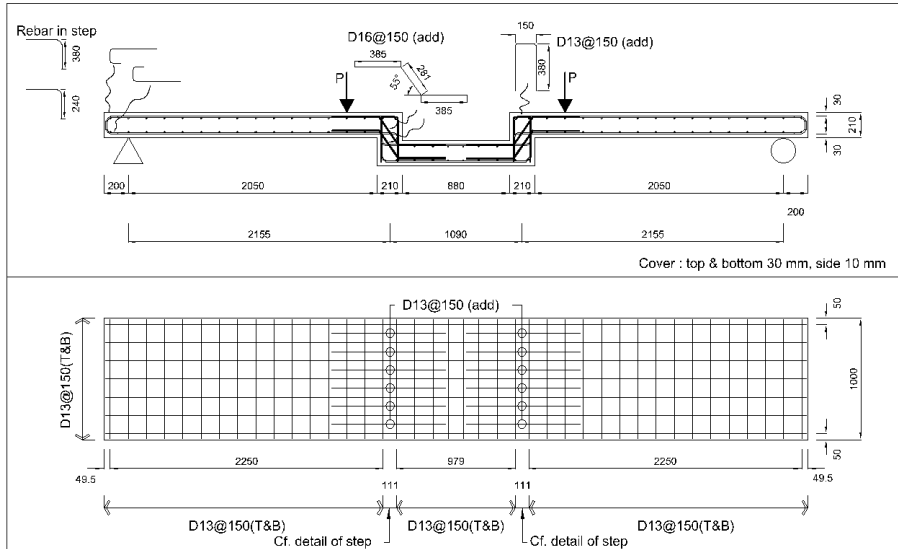


(a) Plane and sectional views of specimen-7

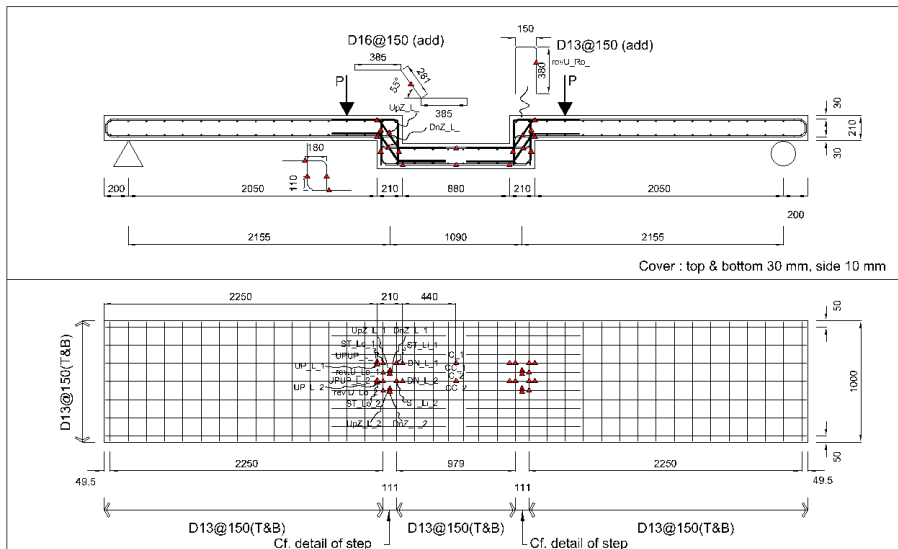


(b) Gauge location of specimen-7

Fig. 3.2.7 Drawing of specimen-7 image and the gauge location (mm)

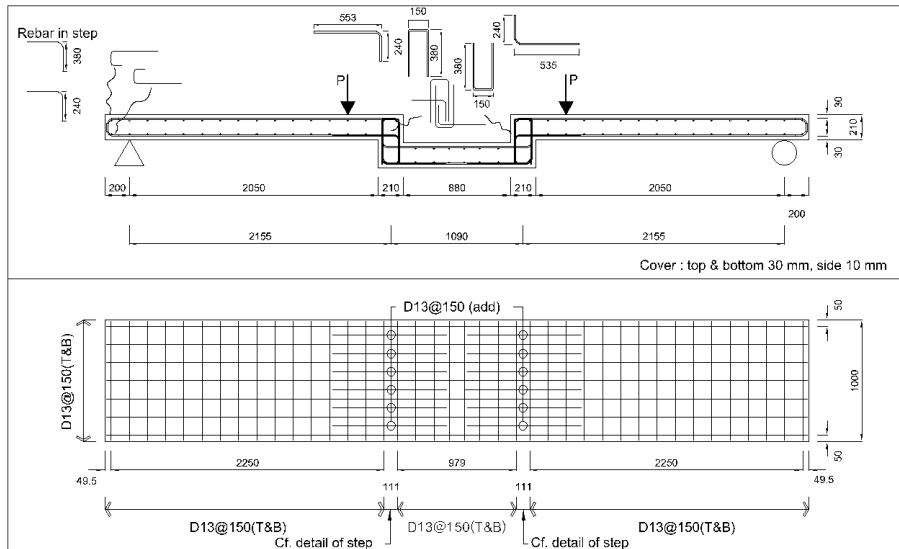


(a) Plane and sectional views of specimen-8

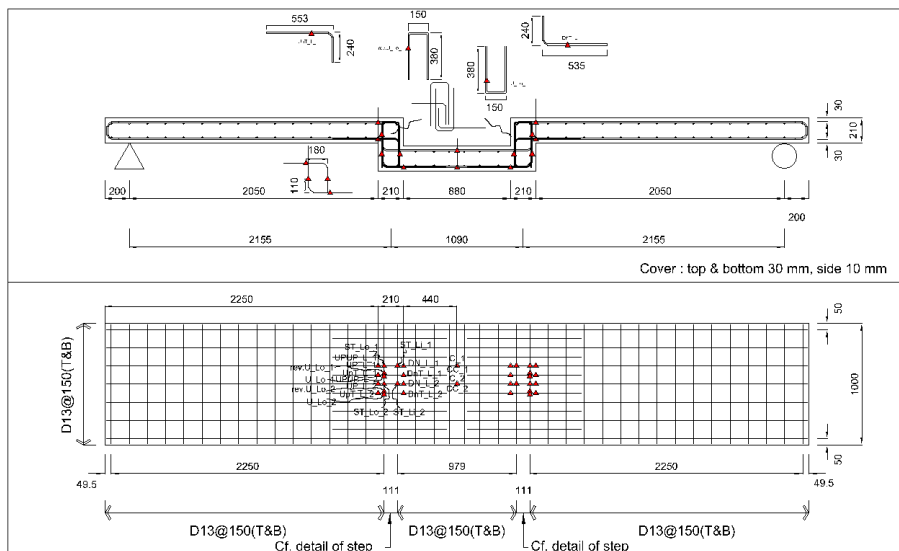


(b) Gauge location of specimen-8

Fig. 3.2.8 Drawing of specimen-8 image and the gauge location (mm)

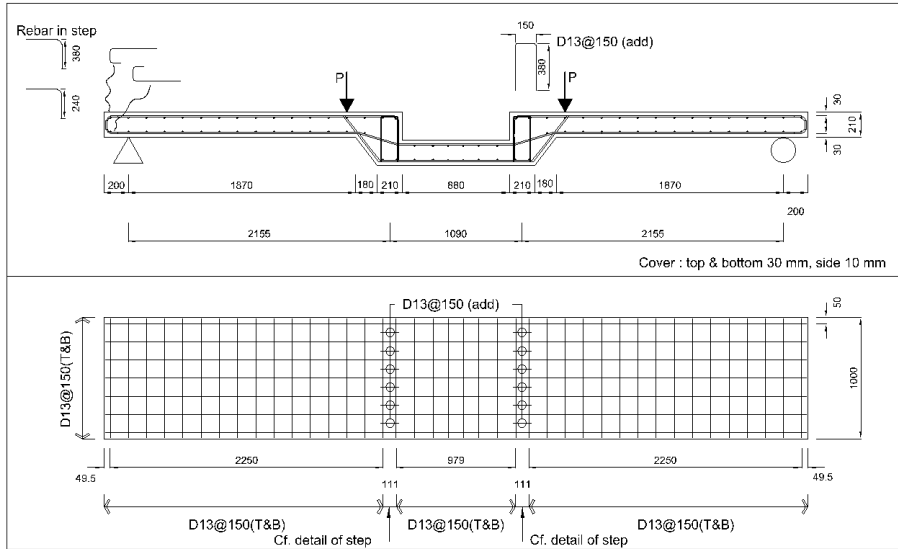


(a) Plane and sectional views of specimen-9

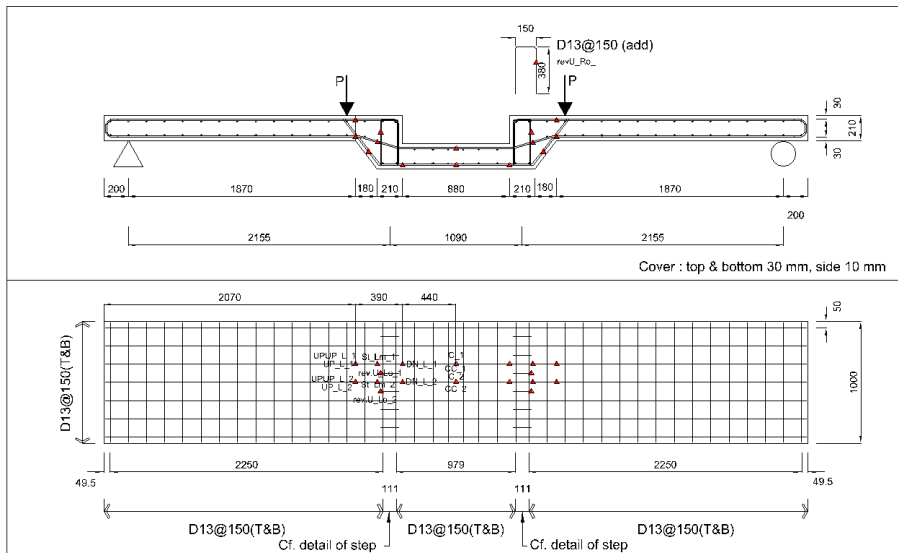


(b) Gauge location of specimen-9

Fig. 3.2.9 Drawing of specimen-9 image and the gauge location (mm)

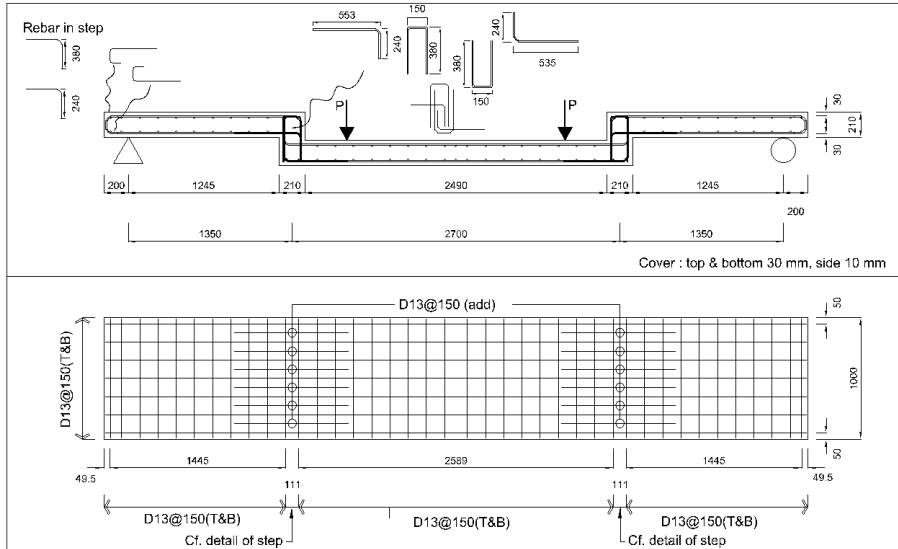


(a) Plane and sectional views of specimen-10

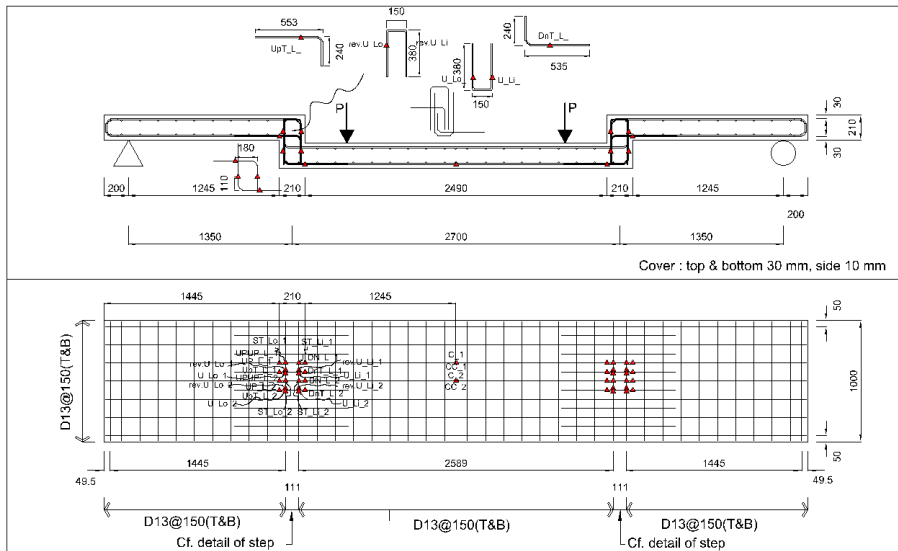


(b) Gauge location of specimen-10

Fig. 3.2.10 Drawing of specimen-10 image and the gauge location (mm)



(a) Plane and sectional views of specimen-12



(b) Gauge location of specimen-12

Fig. 3.2.12 Drawing of specimen-12 image and the gauge location (mm)

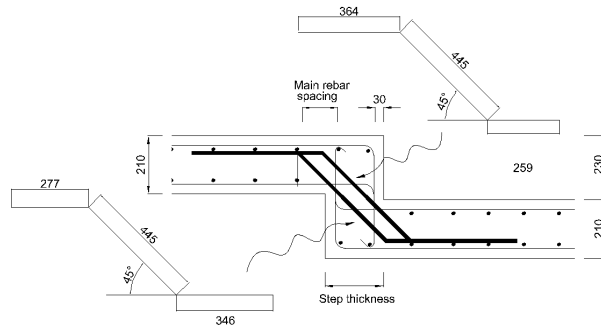


Fig. 3.2.17 Type-A additional rebar (mm)

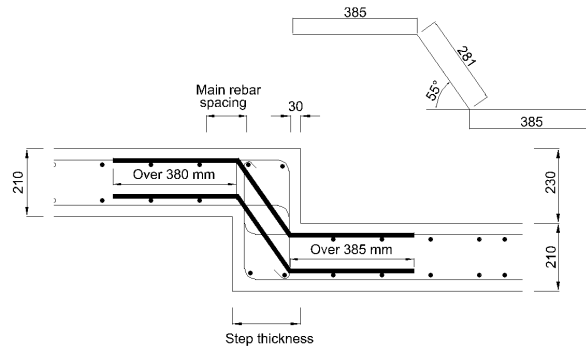


Fig. 3.2.18 Type-B additional rebar (mm)

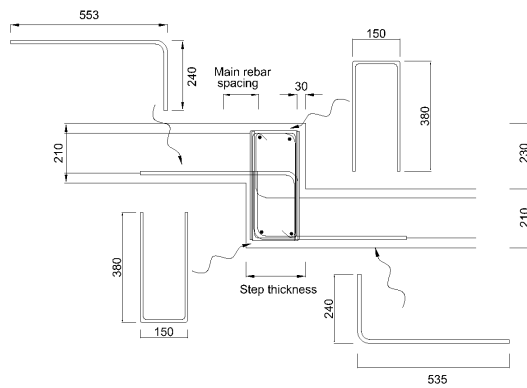


Fig. 3.2.19 Type-C additional rebar (mm)

3.3 Test Specimen Fabrication

The specimens were prepared at TotalPC Industries, Inc. located in Yeosu, Jeonnam-do, and the experiments were carried out at the laboratory of Hoseo university at Asan campus. The experiments were divided into two stages of the first preliminary test (Table 3.3.1) and the second follow-up test (Table 3.3.2). The preliminary experiment involved specimen-1 ~ specimen-7, and the follow-up test fabricated specimen-8 ~ specimen-12. Both tests involved the same fabrication process (Fig. 3.3.1 and 3.3.2) and preparation process (Fig. 3.3.3).

Table 3.3.1 Schedule of preliminary experiment (first test)

Test	Date	Specimen	Work	Re- marks
Preliminary test (1 st)	Aug. 2, 2012	Specimen-1 ~ specimen-3	Assembly of rebar and gauge installation	
	Aug. 3, 2012	Specimen-4 ~ specimen-7	Assembly of rebar and gauge installation	
	Aug. 11, 2012	Specimen-2 ~ specimen-6	Concrete placement	
	Aug. 13, 2012	specimen-1, 3, 4, 5, 7	Concrete placement	
	Aug. 23, 2012	Specimen-1 ~ specimen-7	Delivery of specimens	
	Aug. 29, 2012		Installation of the laboratory table	Hoseo Univ.
	Aug. 31, 2012	Specimen-1, 2, 6, 7	Testing	
	Sep. 3, 2012	Specimen-3, 4	Testing	
	Sep. 4, 2012	Specimen-5	Testing	

Table 3.3.2 Schedule of follow-up experiment (second test)

Test	Date	Specimen	Work	Re- marks
Follow-up test (2 nd)	Sep. 24, 2012	Specimen-8 Specimen-9 Specimen-12	Assembly of rebar and gauge installation	
	Sep. 25, 2012	Specimen-10 Specimen-11	Assembly of rebar and gauge installation	
	Oct. 9, 2012	Specimen-8 specimen-9	Concrete placement	
	Oct. 11, 2012	Specimen-11 Specimen-12	Concrete placement	
	Oct. 15, 2012	Specimen-10	Concrete placement	
	Oct. 19, 2012	Specimen-8 ~ specimen-12	Delivery of specimens	Hoseo Univ.
	Nov. 1, 2012	Specimen-8 Specimen-9	Testing	
	Nov. 2, 2012	Specimen-11 Specimen-12	Testing	
	Nov. 16, 2012	Specimen-10	Testing	



(a) Rebar processing



(b) Processed rebar



(c) Assembly of rebar



(d) Gauge installation



(e) Layout of the rebars in the step



(f) Completion of rebar assembly and gauge installation

Fig. 3.3.1 Process of rebar layout and gauge installation



(a) Form preparation



(b) Delivery of the assembled rebar



(c) Rebar placement and finishing work



(d) Concrete placement



(e) Vibration compaction and plastering



(f) Curing

Fig. 3.3.2 Form preparation and concrete placement process



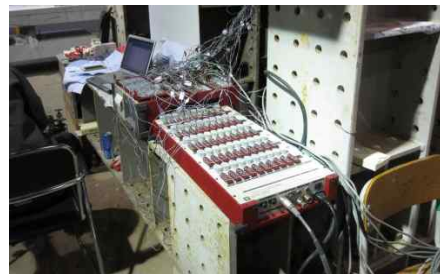
(a) Specimen delivery 1



(b) Specimen delivery 2



(c) Laboratory table installation



(d) Connection of data logger and gauge



(e) Specimen installation



(f) Testing

Fig. 3.3.3 Laboratory table installation and testing process

3.4 Test Method

This experiment was carried out with four point loading of simple span, and hinged end was installed 200 mm inside from both ends of the specimen so that the clear span would be 5400 mm. The distance between two loading points was set to be 1800 mm, and the experimental equipment was set up so that bending failure could be induced at a certain place of the moment between the loading points.

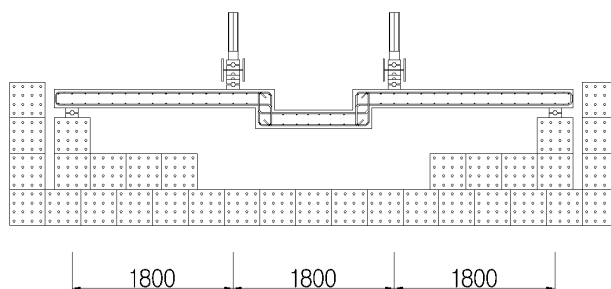


Fig. 3.4.1 Test set-up

Considering the characteristics of the slab specimen with unit width of 1000 mm, the loading device was installed so that line load could be exerted on the loading point, and the methods of installing line loading device differed a little in accordance with the specimen characteristics as discussed below.

Method 1 : Line load was exerted by using a roller and H-bar as shown in Fig. 3.4.2. The total weight of the roller and H-bar was 2.43 kN for each right and left side.

Method 2 : A roller and H-bar were used to apply line load as shown in Fig. 3.4.3 as the same as method 1, but the total

weight of the roller and H-bar was smaller at 1.55 kN for each right and left side due to the adjustment of the number of rollers caused by the spacing difference with oil jack.



Fig. 3.4.2 Method 1 of installing line loading device



Fig. 3.4.3 Method 2 of installing line loading device

Seven LVDT's were installed in order to measure the deflection of the specimen at the lower slab as shown in Fig. 3.4.4 for the sake of the analysis of the experimental result, and wire gauge was installed at upper step in order to measure the displacement due to the rotation of the step.

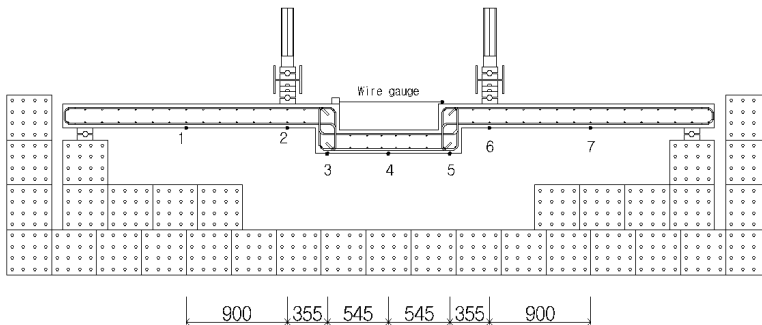


Fig. 3.4.4 Installation drawing of LVDT and wire gauge

Chapter 4

Experimental Results and Proposal of Detailing Design for the Step

4.1 Material Test Result

The physical properties of the concrete and rebars used for the experiments were investigated.

4.1.1 Result of concrete material test

The design strength of the concrete for the gravity load test was the same as 30 MPa, and the detail of the mix design is shown in Table 4.1.1. The Concrete used Portland Cement Type 1 and was placed within 30 minutes of the mixing. A cylindrical specimen of 100 mm diameter and 200 mm height was prepared and cured according to KS F 2405^[8] in order to find out the dynamic characteristics of unhardened concrete.

Table 4.1.1 Concrete mix design

Concrete placement date	Design strength (MPa)	Water-Cement ratio (W/C) %	Mix specification (kg/m ³)					Specimen
			Cement	Water	Fine aggregate	Coarse aggregate	Admixtures	
Aug. 11	30	43.1	392	169	825	952	1.91	#2, #6
Aug. 13	30	43.1	392	169	825	952	1.91	#1, #3, #4, #5, #7
Oct. 9	30	44.2	373	165	837	966	1.87	#8, #9
Oct. 11	30	44.2	373	165	837	966	1.87	#11, #12
Oct. 15	30	44.2	373	165	837	966	1.87	#10

The compressive strength test of the specimen was carried out with universal material tester after grinding the specimen surface to smoothen it out according to KS F 2405, and strength modification factor of 0.97 for the specimen was used pursuant to KBC 2009 Section 0502.2.24^[9].

Table 4.1.2 Concrete compressive strength

Specimen	Compressive strength (MPa)	Specimen	Compressive strength (MPa)
Specimen-1	28.0	Specimen-7	28.0
Specimen-2	23.9	Specimen-8	23.1
Specimen-3	29.8	Specimen-9	23.1
Specimen-4	29.8	Specimen-10	21.2
Specimen-5	30.0	Specimen-11	23.5
Specimen-6	23.9	Specimen-12	23.5

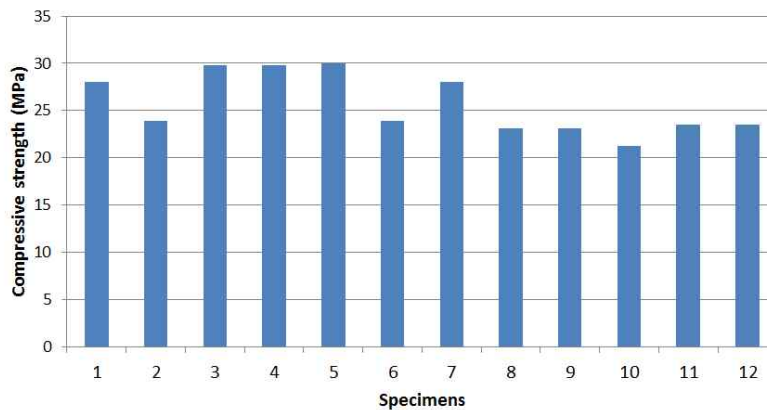


Fig. 4.1.1 Compressive strength of specimens

4.1.2 Result of rebar material test

SD500 D13 steel bar was used as main rebar. SD600 D16 rebar was used for specimen-11. Two D13 rebars, which were used in the preliminary test, were tested. The second experiment tested tensile specimens of D13 and D16 rebars.

Tensile strength test was performed in accordance with KS D 3504^[10], and the test result is shown in Table 4.1.3.

Table 4.1.3 Tensile strength of the rebars

Test	Deformed rebar	Specimen	Yield strength (MPa)	Tensile strength (MPa)
1 st test	D13	#1	594	709
		#2	582	697
		Average	588	703
2 nd test	D13	#1	576	680
		#2	567	673
		#3	564	670
		Average	569	674
	D16	#1	620	746
		#2	604	725
		#3	620	741
		Average	614	737

4.2 Cracking of the Specimens and the Failure Mode

Cracking and failure mode of all 12 specimens prepared for this experiment were recorded. The entire test process was video-recorded, and a pen was used to mark the cracks. Cracking patterns of specimen-2 ~ specimen-12 were similar except for specimen-1 and specimen-10. Cracking started from a bent corner and progressed to upper step. Then, it followed the cover of upper slab and extended until the failure. The detail of the failure process is discussed in Section 4.2.1 and depicted in Fig. 4.2.1.

4.2.1 Cracking stages of the slab and the failure mode

Cracking stages can be largely divided into eight stages from the beginning till the failure.

1) Early cracking stage

Early cracking occurs in the initial state of not applying the load with an actuator but takes place at the outer bent corner by its self-weight and line load device (Fig. 4.2.1(a)).

2) Progression of cracking at outer bent corner

As the load increased, initial cracking progressed diagonally up to about 30~60 mm (Fig. 4.2.1(b)).

3) Cracking of lower slab

Cracking took place at lower slab between stage 2) and stage 4). This lower slab cracking did not propagate a whole lot more until the end of the experiment (Fig. 4.2.1(c)).

4) Expansion of cracking

The cracking starting from outer bent corner expanded in two directions – one perpendicular to the loading point and the other parallel to inner bent corner (Fig. 4.2.1(d)).

5) Diagonal cracking of upper step

As the load increased, noticeable diagonal cracking took place from left upper step to right lower step. In most cases, load drops suddenly with this diagonal cracking (Fig. 4.2.1(e)).

6) Cracking around the inner bent corner

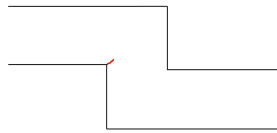
Several cracks were observed toward the inner bent corner (Fig. 4.2.1(f)).

7) Cracking of upper slab

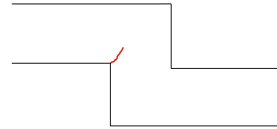
Cracking, which occurred at upper step in stages 5) and 6), followed upper cover layer of upper slab and headed toward the point of support (Fig. 4.2.1(g)).

8) Failure of upper slab

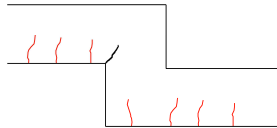
As the load increased, compressive failure of upper cover layer at the intersection of upper slab and step was observed to end the experiment (Fig. 4.2.1(h)).



(a) Early cracking stage



(b) Progression of cracking at outer bent corner



(c) Cracking of lower slab



(d) Expansion of cracking



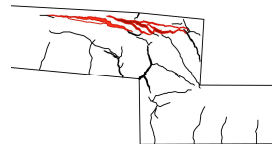
(e) Diagonal cracking of upper step



(f) Cracking around the inner bent corner



(g) Cracking of upper slab



(h) Failure of upper slab

Fig. 4.2.1 Stages of cracking and failure of the step

4.2.2 Cracking of the specimens and the failure mode

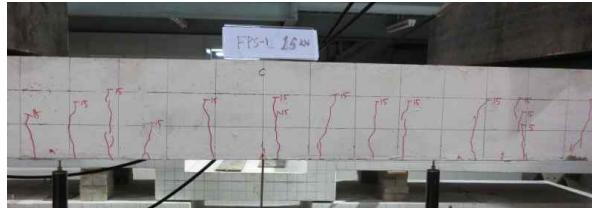
1) Cracking and failure mode of specimen-1

Specimen-1 is a control specimen with typical flat slab without step. It exhibited initial cracking at the load of 13.2 kN, and, as the load increased, cracking propagated to upper direction with greater width of the crack. Additionally, the lower crack, which took place between the loading points, propagated between the loading point and the point of support as the load increased (Fig. 4.2.2(a),(b)). With greater load, crack propagation stopped, and compressive failure of the concrete on top of the specimen was observed when the maximum load was 84.5 kN (Fig. 4.2.2(c)).

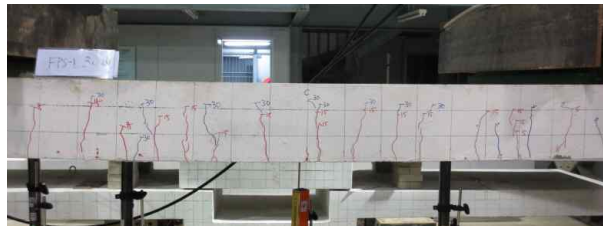
2) Cracking and failure mode of specimen-2

Specimen-2 is a slab with a step, and cracking also took place at outer bent corner due to its self-weight and line load device. As the load applied, the outer bent corner exhibited vertical cracking toward the loading point and horizontal cracking toward inner bent corner as the same as the cracking stage 4). Then, cracking gradually propagated throughout the specimen at lower part. The cracking propagated for a while and then stopped. No additional cracking was observed until large diagonal cracking occurred as the same as cracking stage 5) (Fig. 4.2.3(a)). As the load increased, a lot of cracking was observed as upper step (Fig. 4.2.3(b)). Finally, compressive failure occurred at the upper part of the

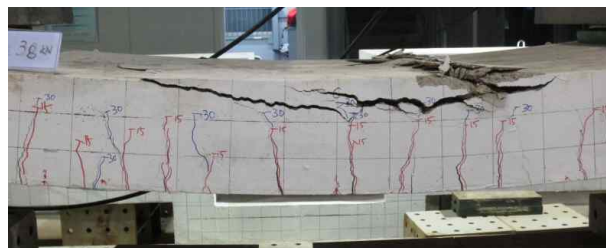
intersection between upper right slab and the step at the applied load of 27 kN (Fig. 4.2.3(c)).



(a) Cracking of specimen-1 at applied load = 36 kN

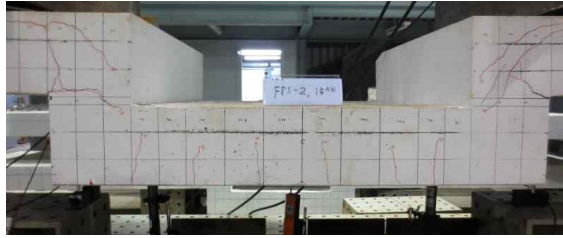


(b) Cracking of specimen-1 at applied load = 67 kN

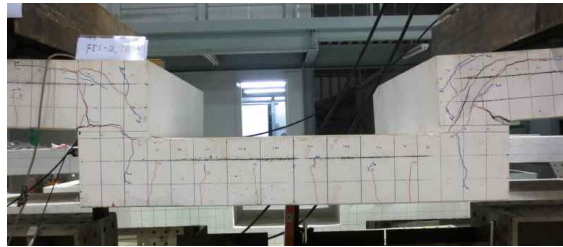


(c) Cracking failure of specimen-1 at applied load = 84 kN

Fig. 4.2.2 Cracking of specimen-1 by loading stage



(a) Cracking of specimen-2 at applied load = 22 kN



(b) Cracking of specimen-2 at applied load = 26 kN



(c) Cracking failure of specimen-2 at applied load = 27 kN

Fig. 4.2.3 Cracking of specimen-2 by loading stage

3) Cracking and failure mode of specimen-3

The step of specimen-3 was reinforced with Type-A and revU bar. Until the load of 14 kN continued, cracking progressed up to 50 mm at 45° angle from the outer bent corner. The cracking starting from the outer bent corner divided at the applied load of about 23 kN as the same as cracking stage 4). At the similar time when the cracking

divided, cracking was observed at lower part of the entire specimen, and then diagonal cracking was noted at upper step at the applied load of about 31 kN (Fig. 4.2.4(a)). As the load increased, cracking concentrated around the inner bent corner as the same as cracking stage 6) (Fig. 4.2.4(b)). Finally, compressive failure of the concrete took place at the applied load of 42 kN (Fig. 4.2.4(c)).

4) Cracking and failure mode of specimen-4

The step of specimen-4 was reinforced with Type-B and revU-bar. Until the load of 14 kN continued, cracking progressed up to 60 mm at 45° angle from the outer bent corner. About the time when the cracking from the outer bent corner subsided, cracking occurred at the lower part of the entire slab. Afterwards, cracking divided in vertical and horizontal direction as the same as cracking stage 4), and then diagonal cracking took place at upper step when the applied load reached about 34 kN (Fig. 4.2.5(a)). As the load increased, more cracking occurred around the inner bent corner and at upper part of the intersection of upper slab and step as the same as cracking stage 6) and 7). Especially, cracking was observed more at upper step (Fig. 4.2.5(b)). Finally, compressive failure of the concrete occurred at the applied load of 49 kN (Fig. 4.2.5(c)).



(a) Cracking of specimen-3 at applied load = 36 kN



(b) Cracking of specimen-3 at applied load = 58 kN

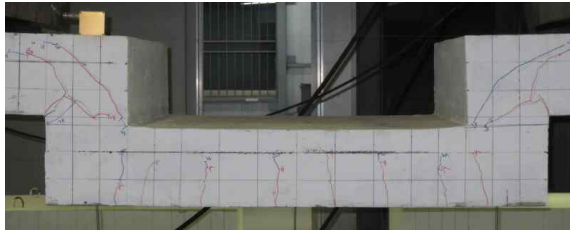


(c) Cracking failure of specimen-3 at applied load = 59 kN

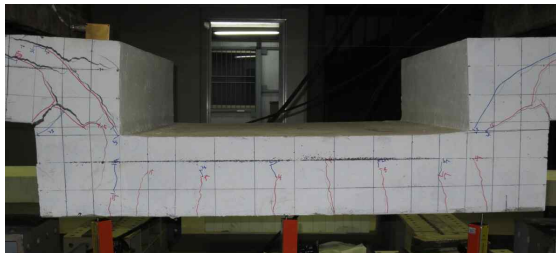
Fig. 3.2.4 Cracking of specimen-3 by loading stage



(a) Cracking of specimen-4 at applied load = 34 kN



(b) Cracking of specimen-4 at applied load = 53 kN



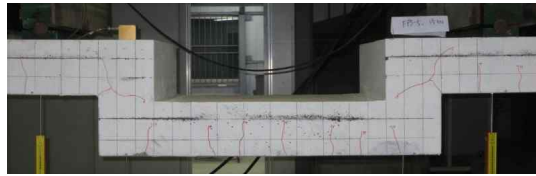
(c) Cracking failure of specimen-4 at applied load = 61 kN

Fig. 4.2.5 Cracking of specimen-4 by loading stage

5) Cracking and failure mode of specimen-5

The step of specimen-5 was reinforced with Type-C. Until the load of 14 kN continued, cracking progressed up to 50 mm diagonally from the outer bent corner of the step. Cracking took place at lower part of the entire slab at about this time, and the divided cracking propagation toward the loading point and inner bent corner slowed

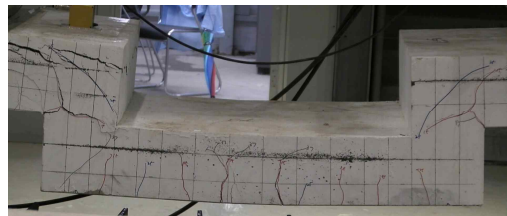
down at the applied load of about 23 kN (Fig. 4.2.6(a)). There was no further cracking observed for a while as the load increased, and then diagonal cracking occurred at upper step at the load of 38 kN. As the load increased, the diagonal cracking lengthened (Fig. 4.2.6(b)). Ultimately, compressive failure of the concrete occurred at upper slab of the step when the applied load reached 78.6 kN (Fig. 4.2.6(c)).



(a) Cracking of specimen-5 at applied load = 31 kN



(b) Cracking of specimen-5 at applied load = 50 kN



(c) Cracking failure of specimen-5 at applied load = 79 kN

Fig. 4.2.6 Cracking of specimen-5 by loading stage

6) Cracking and failure mode of specimen-6

The step of specimen-6 was 250 mm thick and was not reinforced. The thickness of upper slab and lower slab was 210 mm as the same as other specimens. As the specimen was lifted up to be placed on the lab table, cracking occurred at the outer bent corner of the step due to construction load. The cracking starting from the outer bent corner divided as the load was applied in the manner of cracking stage 4). A large diagonal crack was observed at the applied load of about 21 kN, and the length of the diagonal crack increased gradually (Fig. 4.2.7(a)). Then, compressive failure of the concrete at upper slab of the step took place at the applied load of 37 kN (Fig. 4.2.7(b)).



(a) Cracking of specimen-6 at applied load = 21 kN

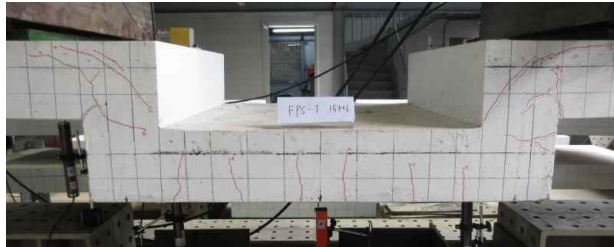


(b) Cracking failure of specimen-6 at applied load = 37 kN

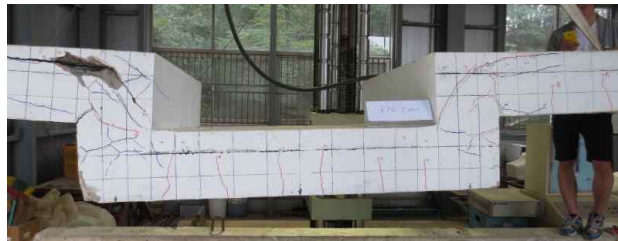
Fig. 4.2.7 Cracking of specimen-6 by loading stage

7) Cracking and failure mode of specimen-7

The step of specimen-7 was reinforced with Type-B. As the load increased, cracking extended up to 60 mm at 45° angle from the outer bent corner of the step. Then, the cracking divided in vertical and horizontal direction to slow down at about 24 kN. Diagonal cracking then took place at upper step at the applied load of about 31 kN, and the length of the diagonal crack at upper step increased as the load was continuously applied (Fig. 4.2.8(a)). As the load increased, the width and size of the crack increased to bring about compressive failure of the concrete at the applied load of 47 kN (Fig. 4.2.8(b)).



(a) Cracking of specimen-7 at applied load = 24 kN



(b) Cracking failure of specimen-7 at applied load = 47 kN

Fig. 4.2.8 Cracking of specimen-7 by loading stage

8) Cracking and failure mode of specimen-8

The step of specimen-8 was reinforced with Type-B and revU-bar. The rebar used for diagonal reinforcement of Type-B was SD600 D16, and the step to the end of the main rebar was straight. As the applied load of 13 kN continued, cracking propagated up to 30 mm at 45° angle from the outer bent corner of the step. The cracking starting from outer bent corner divided vertically and horizontally (Fig. 4.2.9(a)). The divided crack propagation slowed down at the applied load of about 24 kN, and diagonal cracking at upper step took place at the applied load of about 43 kN. As the load was continuously applied, the size and width of the diagonal crack at upper step increased (Fig. 4.2.9(b)). Subsequently, compressive failure of the concrete occurred at the applied load of 57.2 kN (Fig. 4.2.9(c)).

9) Cracking and failure mode of specimen-9

The step of specimen-9 was reinforced with Type-C, and the step to the end of the main rebar was straight without 135° hook. As the load of about 11 kN continued, cracking progressed up to 80 mm at 45° angle from the outer bent corner of the step to be divided in vertical and horizontal direction afterwards. The cracking starting from the outer bent corner slowed down at the applied load of about 24 kN, and cracking of lower slab was observed during this time. Simultaneously, the cracking starting from the outer bent corner divided in vertical and horizontal direction (Fig. 4.2.10(a)). Diagonal cracking was

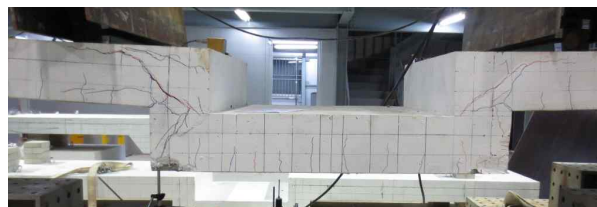
observed at upper step when a load of about 39 kN was applied. As the load was continuously applied, the diagonal cracking of the upper step became more severe to bring about cracking around the inner bent corner (Fig. 4.2.10(b)). When the applied load reached 74.9 kN, compressive failure of the concrete was observed at the intersection of the upper slab and the step (Fig. 4.2.10(c)).



(a) Cracking of specimen-8 at applied load = 34 kN



(b) Cracking of specimen-8 at applied load = 51 kN

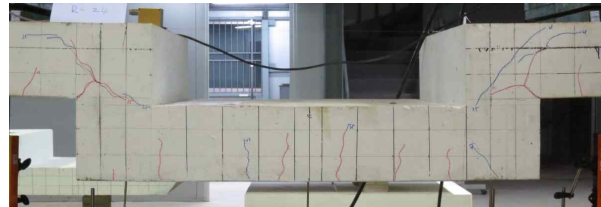


(c) Cracking failure of specimen-8 at applied load = 57 kN

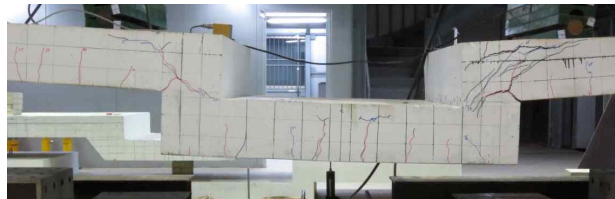
Fig. 4.2.9 Cracking of specimen-8 by loading stage



(a) Cracking of specimen-9 at applied load = 33 kN



(b) Cracking of specimen-9 at applied load = 53 kN



(c) Cracking failure of specimen-9 at applied load = 74.9 kN

Fig. 4.2.10 Cracking of specimen-9 by loading stage

10) Cracking and failure mode of specimen-10

Specimen-10 possesses 180 mm inclined step added to 210 mm step thickness. Additionally, the lower main rebars of right and left upper slabs were connected to the upper main rebar of lower slab. The specimen exhibited cracking during the process of delivery four days after the concrete placement (Fig. 4.2.11(a)). As the load was applied, cracking progressed up to 10 mm diagonally from the outer bent corner and then divided in vertical and

horizontal direction (Fig. 4.2.11(b)). As the load increased, the width of the vertical and horizontal cracking widened more, and the vertical and horizontal cracking propagated toward the point of support and the inner bent corner, respectively. The width of the vertical and horizontal cracking increased with increased load, and the specimen yielded finally to failure at the applied load of 50.6 kN (Fig. 4.2.11(c)). Particularly, there was no diagonal cracking observed at upper step.



(a) Cracking image of specimen-10 prior to load test



(b) Cracking of specimen-10 at applied load = 28 kN



(c) Cracking failure of specimen-10 at applied load = 50.6 kN

Fig. 4.2.11 Cracking of specimen-10 by loading stage

11) Cracking and failure mode of specimen-11

The step thickness of specimen-11 was set at 400 mm, and the step was reinforced additionally with revU-bar. The specimen exhibited cracking of about 10 mm at the outer bent corner of the step even with line load device only. While the cracking starting from the outer bent corner progressed, cracking was observed at lower part of the entire specimen at the applied load of 15 kN. Cracking from the outer bent corner continued up to 150 mm toward the upper cover layer. The applied load was about 27 kN at this time. Afterwards, the cracking from the outer bent corner progressed toward inner bent corner at the applied load of about 36 kN (Fig. 4.2.12(a)). As the load increased, the horizontal cracking progressed toward inner bent corner, and additional cracking around the inner bent corner took place. Diagonal cracking at upper step was observed at the applied load of about 53 kN (Fig. 4.2.12(b)). Finally, compressive failure of the concrete at upper step was manifested when the applied load reached 70.9 kN (Fig. 4.2.12(c)).

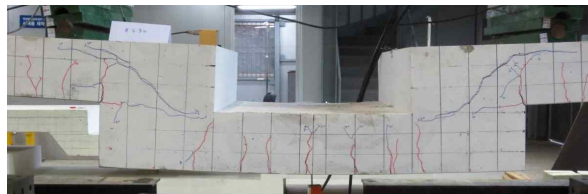
12) Cracking and failure mode of specimen-12

The step of specimen-12 was reinforced with Type-C detail, and the distance between the steps shortened to 5400 mm. As the load increased, cracking took place at the lower slab between the loading points as well as the step (Fig. 4.2.13(a)). The cracking pattern was similar to other specimens with step (Fig. 4.2.13(b)). However, while the lower cracking of other specimens did not increase a whole lot more, specimen-12 exhibited a great deal of

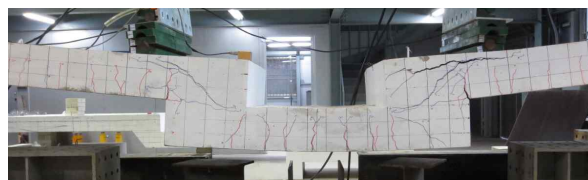
cracking at lower slab between the loading points as the load increased. The load test stopped at the applied load of 70.9 kN due to the lack of stroke. Thus, actual maximum load and final failure mode could not be ascertained (Fig. 4.2.13(c)).



(a) Cracking of specimen-11 at applied load = 42 kN

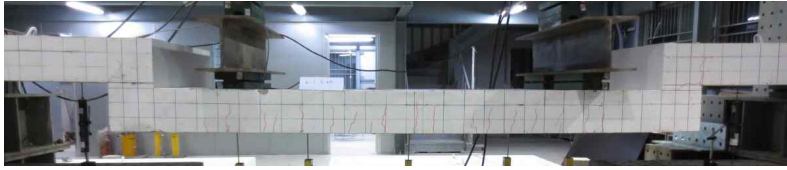


(b) Cracking of specimen-11 at applied load = 61 kN



(c) Cracking failure of specimen-11 at applied load = 70.9 kN

Fig. 4.2.12 Cracking of specimen-11 by loading stage



(a) Cracking of specimen-12 at applied load = 33 kN



(b) Cracking of specimen-12 at applied load = 63 kN



(c) Cracking of specimen-12 at applied load = 70.9 kN

Fig. 4.2.13 Cracking of specimen-12 by loading stage

4.3 Analysis of the Experimental Results

The next subsection 4.3.1 discusses the comparison analysis of the test results. It compared specimens of equivalent bending (flexural) strength in terms of the flexural performance by the rebar type, the influence of the step on flexural performance, etc.

4.3.1 Overview of experimental result analysis

Various test results of the specimens were analyzed for the following 1)~ 5) topics.

1) Center applied load-displacement relations

The curve depicts the relationship between measured load and displacement of the center point of the specimens.

2) Load-measured value of wire displacement gauge relations

A wire gauge installed at upper step measured the shortened distance between the steps. The curve depicts the relationship between the shortened distance and the load.

3) Deflection distribution curve of the slab by the loading stage

The curve shows the deflection as measured from LVDT-1 ~ LVDT-7 in the longitudinal direction of the slab by loading stage.

4) Applied load-rotational angle relationship curve

θ_1 is the angle from upper left slab as measured from LVDT1 and LVDT2 (Fig. 4.3.1). In other words, θ_1 is the rotation angle of upper joint of left step. Likewise, θ_2 is

the rotation angle of lower joint of left step as measured by LVDT3 and LVDT4. θ_3 is the rotational angle of lower joint of right step as measured by LVDT5 and LVDT6, and θ_4 is the rotational angle of upper joint of right step as measured by LVDT7 and LVDT8.

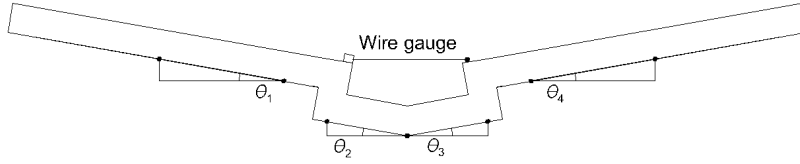


Fig. 4.3.1 Location of rotational angle

5) Maximum strain and load-strain curve

The strain measured the values (UP_L series) of gauge located near the main rebar in the left outer bent corner of left upper slab, while the measured strain values of UP_R series were taken from the gauge installed near the main rebar of right outer bent corner of right upper slab. Additionally, the strain values of C-series were measured from the gauge installed at the center of the lower main rebar of lower slab. DN_L and DN_R series of values are the strain values measured from the gauge installed at the point of interface with left step and right step, respectively. The curve depicts the relationship between the applied load and measured strain values.

4.3.2 Analysis of experimental result

Table 4.3.1 shows nominal bending moment (M_n) as computed from the physical properties of the concrete (Section 4.1) and rebar (Section 4.2). Since the maximum bending moment (M_{\max}) as measured from the specimen was greater than the design nominal bending moment (M_n) as computed from the physical properties, the experiment was well carried out in conclusion.

Table 4.3.1 Maximum bending strength of each specimen

Specimen	$M_{\text{actuator load}}$ ($kN \cdot m$)	$M_{\text{self weight}}$ ($kN \cdot m$)	Measured M_{\max} ($kN \cdot m$)	M_{\max}/M_n (%)
Specimen-1	76.1	17.9	94.0	119
Specimen-2	24.7	20.4	45.1	57
Specimen-3	53.1	20.4	73.5	93
Specimen-4	55.0	20.4	75.4	95
Specimen-5	70.7	20.4	91.1	115
Specimen-6	33.7	20.8	54.5	69
Specimen-7	42.1	20.4	62.5	79
Specimen-8	51.5	20.4	71.9	91
Specimen-9	67.4	20.4	87.8	111
Specimen-10	45.5	21.4	66.9	85
Specimen-11	63.8	22.6	86.4	109
Specimen-12	67.4	20.4	87.8	111

The specimens, which manifest the bending moment equivalent to specimen-1, were specimen-5 with Type-C reinforcement, specimen-9 and specimen-12, and these specimens exhibited nominal bending moment of greater than 100 % of M_n to M_{\max} ratio. Specimen-5, specimen-9, and specimen-12 showed 6.7 % less maximum bending moment

on the average in comparison to specimen-1 (Table 4.3.1, Fig. 4.3.2). This small difference could be explained by the SD500 7-D13 main rebar with $A_s f_y$ of 443.5 kN and the fact that the specimens with step had reinforcements such as revU-bar, SD500 6-D13, and Type-C so that stiffness reduction due to early cracking of the step and lowering of bending force transfer capacity did not take place.

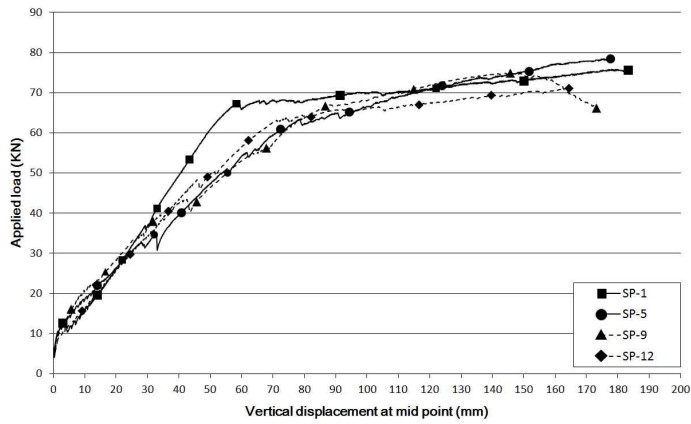


Fig. 4.3.2 Center applied load-displacement relations (specimens-1, 5, 9, 12)

Flat slab specimen and specimen with step but no reinforcement were compared in order to compare the performance with or without step. Specimen-1 is a flat slab and specimen-2 is a specimen with a step but no reinforcement. Specimen-2 exhibited 57 % M_n to M_{max} ratio in comparison to that of specimen-1 (Table 4.3.1, Fig. 4.3.3). Cracking of outer bent corner was observed at the early stage of the experiment. It progressed rapidly with increased load, and θ_2 of specimen-2 did not surpass 0.001 (Fig. 4.3.4). The maximum measured values of C_1 and C_2 gauges of

specimen-2 was 1314 *ms*. That is, bending of lower slab took place very little, because the moment did not get transferred through the step. In conclusion, the load applied to upper slab did not get transferred to the lower slab due to rapid stiffness reduction of the step (i.e., plastic hinge occurrence).

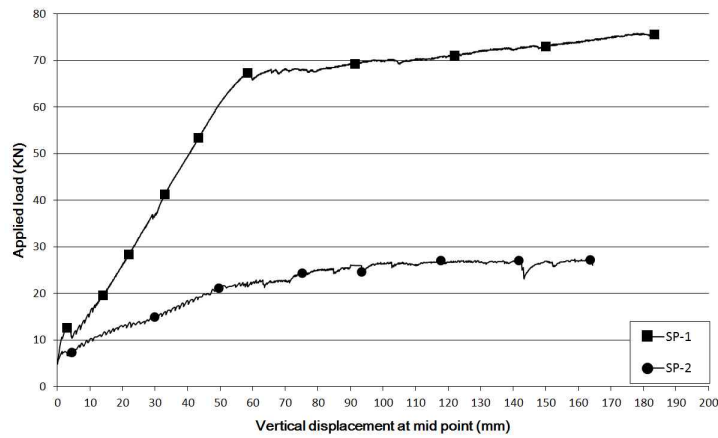


Fig. 4.3.3 Center applied load-displacement relations (specimens-1 and 2)

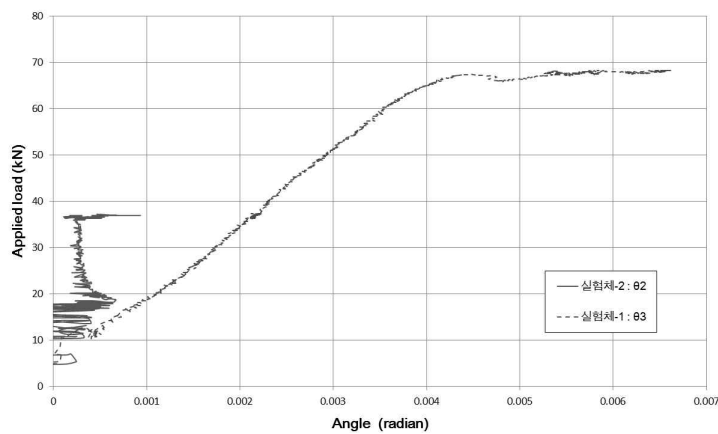


Fig. 4.3.4 Comparison of load-rotational angle of specimen-2

The performance differed greatly with the step type. Specimen-6 exhibited 9.4 kN · m greater M_{max} than SP-2 due to its increase in the step thickness by 40 mm. Specimen-10 and specimen-11 respectively manifested 85 % and 109 % to M_n (Table 4.3.1, Fig. 4.3.5). Particularly, the early secant stiffness of specimen-6 with a step but no reinforcement was 2.27 kN/mm, showing its excellence over that (1.39 kN/mm) of specimen-1, but it dropped rapidly to 0.75 kN/mm later (Table 4.3.2). In other words, the stiffness of the specimen-6 becomes larger with the step figure. However, the stiffness dropped rapidly with the propagation of cracking, and its maximum moment was much less than that of specimen-1. Nonetheless, specimen-10 and specimen-11 had the step reinforced with revU-bar, and this reinforcement alone was adequate to manifest significantly greater maximum moment than that of specimen without such revU-bar reinforcement. Thus, it can be seen that it is hard to manifest the equivalent maximum load by simply increasing the step thickness only.

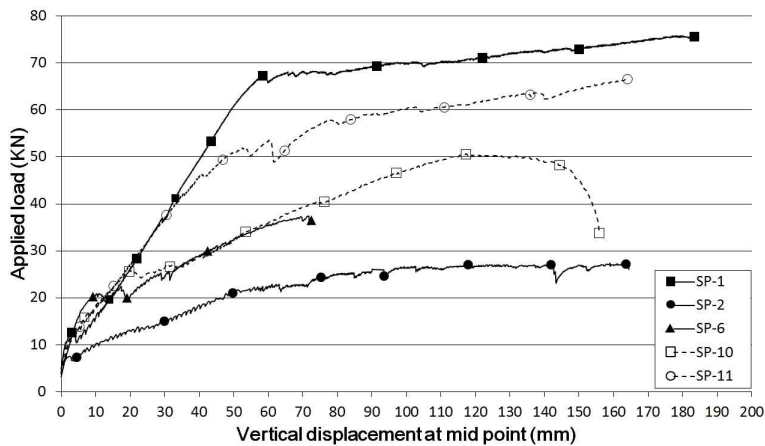


Fig. 4.3.5 Center applied load-displacement relations
(specimens-1, 2, 6, 10, 11)

Table 4.3.2 Secant stiffness at the applied load of 20 kN and $(3/4)P_{max}$

Specimens	Δ_{20kN} (mm)	$K_{sec, 20kN}$ (kN/mm)	$\Delta_{(3/4)P_{max}}$ (mm)	$K_{sec, (3/4)P_{max}}$ (kN/mm)
Specimen-1	14.4	1.39	52.7	1.20
Specimen-2	46.0	0.43	47.7	0.43
Specimen-3	15.3	1.31	58.2	0.76
Specimen-4	12.8	1.56	55.7	0.82
Specimen-5	11.6	1.72	68.9	0.86
Specimen-6	8.8	2.27	37.3	0.75
Specimen-7	19.0	1.05	67.9	0.52
Specimen-8	8.7	2.30	39.3	1.09
Specimen-9	9.7	2.06	67.5	0.83
Specimen-10	12.3	1.63	65.1	0.58
Specimen-11	12.0	1.67	67.0	0.79
Specimen-12	14.2	1.41	59.7	0.94

Specimen-10 has 180 mm inclined step added to 210 mm step thickness. Its maximum moment was 66.9 kN · m (Table 4.3.1). The specimen-10 with the inclined step showed greater stiffness in the beginning than that of flat slab specimen without step and exhibited less deflection until the applied load of 25 kN was applied (Fig. 4.3.6). However, the stiffness rapidly dropped after large cracking occurred at the applied load of 25 kN. The load applied to upper slab did not get transferred to lower slab from this time. θ_3 did not increase, after 25 kN load was applied, and approached 0 due to the lack of moment transfer capacity of right step (Fig. 4.3.7).

Specimen-5 and specimen-9 were prepared in the same condition except for the treatment of the longitudinal end of the main rebar. Although specimen-5 had a hook of 135° angle at the end of the main rebar in the step, the main rebar of specimen-9 had a straight end. M_{max} of specimen-5 and specimen-9 were 94.0 kN · m and 87.8 kN · m, respectively,

and was a little less than that of specimen-9 (Table 4.3.1).

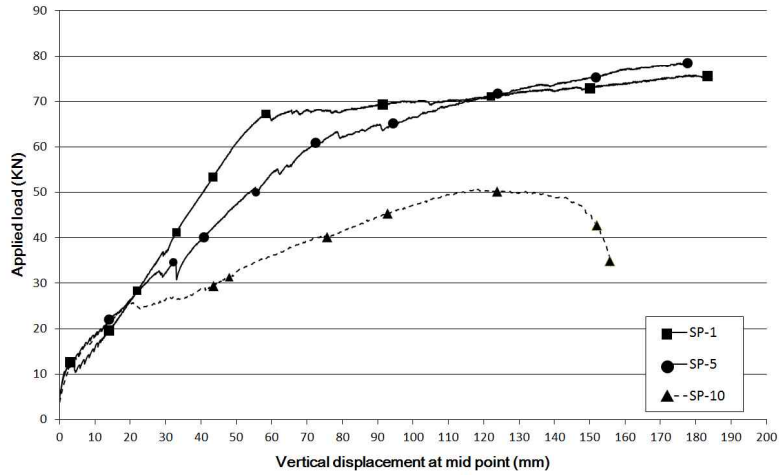


Fig. 4.3.6 Center applied load-displacement relations (specimens-1, 5, 10)

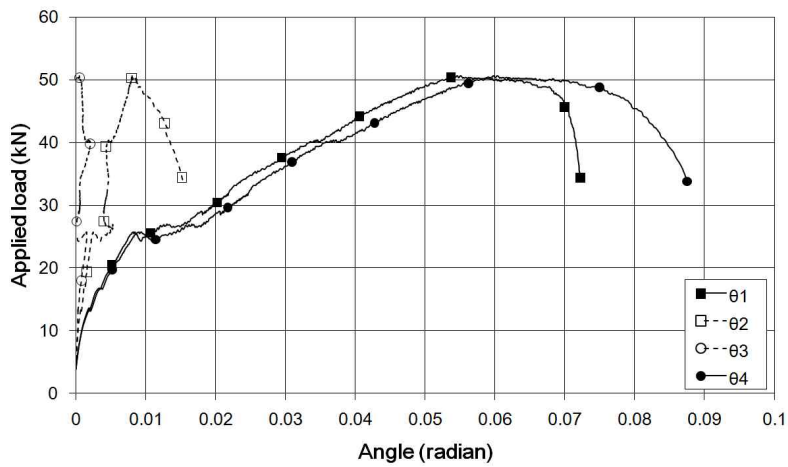


Fig. 4.3.7 Applied load-angle relations of SP-10

Nonetheless, examining load-displacement graph of Fig. 4.3.8, the trend of displacement of the two specimens in response to the applied load is similar. The compressive strengths of

specimen-5 and specimen-9 were 30.0 MPa and 23.1 MPa, respectively, and the difference in the concrete compressive strength affected M_{max} however little. Thus, it was found that there is no significant need for the treatment of the end of the main rebar of the slab with a hook of 135° angle.

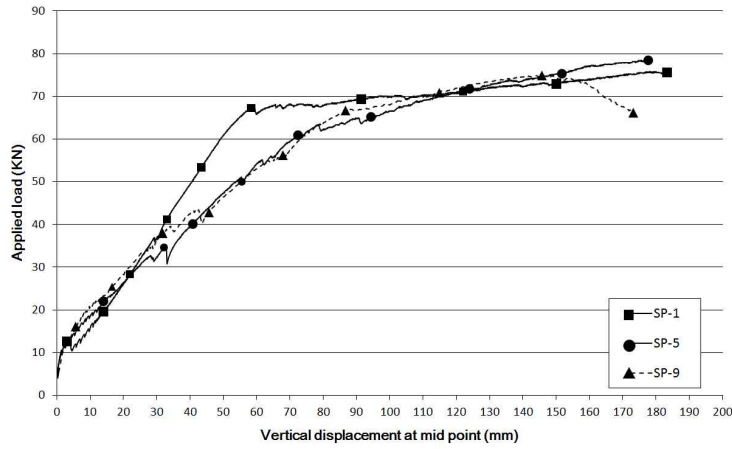


Fig. 4.3.8 Center applied load-displacement relations (specimens-1, 5, 9)

Specimen-4 had the step reinforced with Type-B and revU-bar, and specimen-7 reinforced the step with Type-B only. M_{max} of specimen-4 and specimen-7 were $75.4 \text{ kN} \cdot \text{m}$ and $62.5 \text{ kN} \cdot \text{m}$, respectively, with a difference of $12.9 \text{ kN} \cdot \text{m}$ (Table 4.3.1, Fig. 4.3.9). The maximum moment was greatly affected by the level of revU-bar to control the cracking of the upper step. Fig. 4.3.10 depicts the representative values of revU_Lo series and revU_Ro series readings from the strain gauges on revU-bar of specimen-4. The figure shows the strain value of revU_Lo_2 at the interface of left revU-bar and upper slab to be $6432 \text{ } \mu\text{m}$. This indicates the revU-bar bears a great force and controls diagonal cracking.

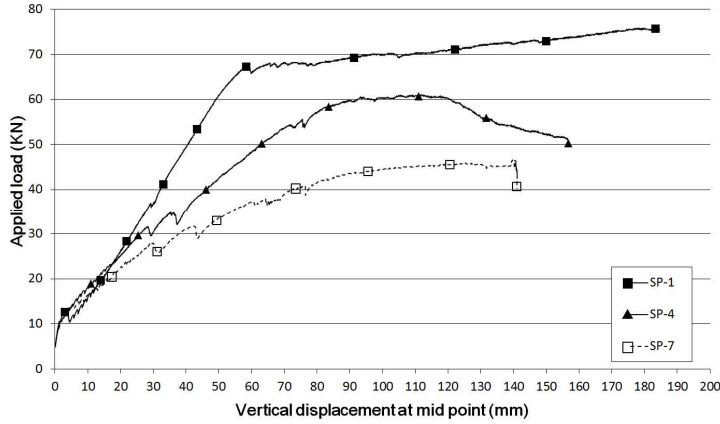


Fig. 4.3.9 Center applied load-displacement relations
(specimens-1, 4, 7)

Evaluating flexural performance of additional reinforcement bars Type-A ~ Type-C, the maximum moment of specimen-3 ~ specimen-5 were 73.5, 75.4, and 91.1 kN · m, respectively (Table 4.3.1, Fig. 4.3.11). Considering that all these specimens (specimen-3 ~ specimen-5) installed revU-bar to control diagonal cracking at the same level, the combination of U-bar, revL-bar, and L-bar was more effective in securing the bending performance than inclined rebar alone. Particularly, because the upper inclined rebar was subjected to compression more than tension, Type-A and Type-B rebars did not perform their role adequately.

Both specimen-4 and specimen-8 reinforced the step with revU-bar, and the only difference is $A_s f_y$ of the inclined rebar. $A_s f_y$ of specimen-4 and specimen-8 were increased by using the inclined rebars of SD500 D13 and SD600 D16, respectively.

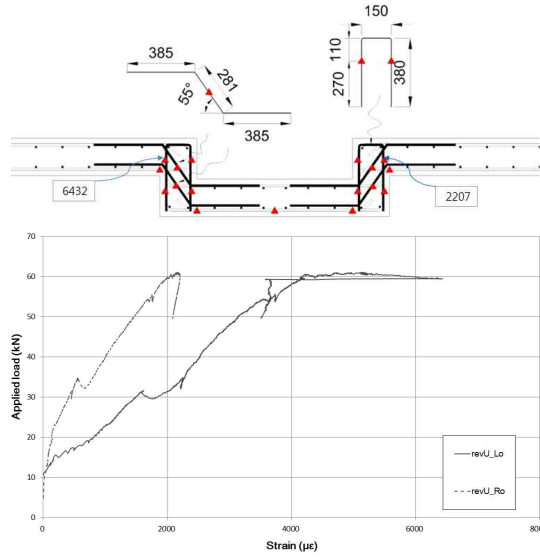


Fig. 4.3.10 Strain of specimen-4 with revU-bar

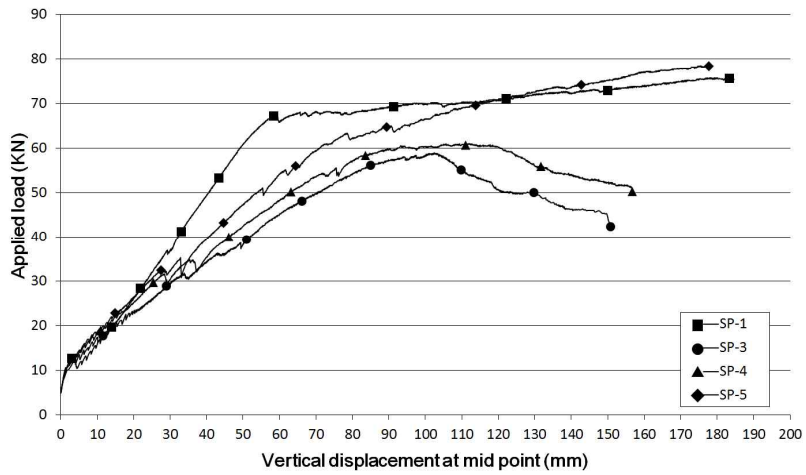


Fig. 4.3.11 Center applied load-displacement relations
(specimens-1, 3, 4, 5)

The test results of $A_s f_y$ of specimen-4 and specimen-8 were 75.4 kN and 71.9 kN, respectively, with a little difference (Table 4.3.1, Fig. 4.3.12). Considering the concrete compressive

strengths of specimen-4 and specimen-8 were 29.8 MPa and 23.1 MPa, respectively, the increase in the inclined rebar was not influential, and it can be concluded that inclined rebars were not so effective in reinforcing the step.

Comparing the readings of strain gauges on the inclined rebars as shown in Fig. 4.3.13 and Fig. 4.3.14, the inclined rebars did not bear a great force. Especially, the gauges on the upper inclined rebars (UpZ_L series, UpZ_R series) showed compressive values in the same direction as diagonal cracking. On the contrary, because the strain gauges on the lower inclined rebars (Dn_L series, Dn_R series) were in perpendicular direction to diagonal cracking, the readings were tensile values.

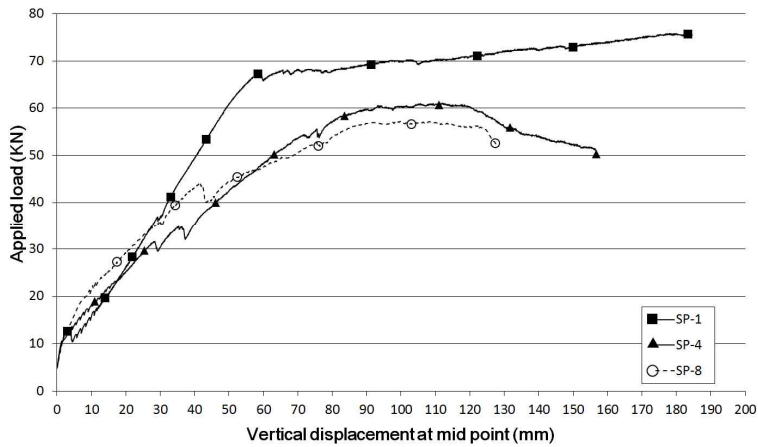


Fig. 4.3.12 Center applied load-displacement relations (specimens-1, 4, 8)

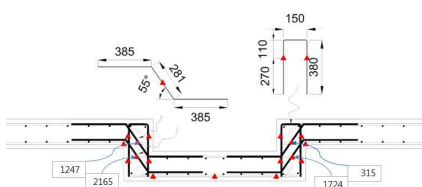


Fig. 4.3.13 Strain of inclined rebar of specimen-4

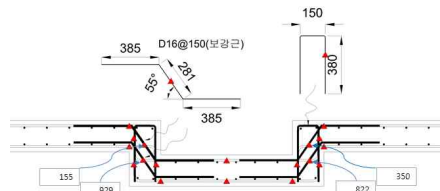


Fig. 4.3.14 Strain of inclined rebar of specimen-8

Specimen-12 placed the step between the point of support and loading point so that it could be subjected to shear and bending. This experimental set-up was to compare it with simple flexural test specimen (Table 4.3.1, Fig. 4.3.15). Comparing the strain of main rebars, the strain readings of the gauge placed at the interface of left upper slab and the step (Up_L series) was 1883 ms , and the strain readings of the gauge placed at the interface of lower slab and the step (Dn_L series) was smaller at 1509 ms (Fig. 4.3.16). On the contrary, the strain readings of the gauge placed between loading points and near lower main rebar of lower slab (C series) was 40799 ms . If enough stroke was applied, compressive failure of the lower slab between the loading points is expected.

On the contrary, specimen-9 with the step laid out between loading points manifested failure of the step, given the same experimental condition. Thus, it is explained that the slab with step was harder on the step when it is subjected to simple bending force than simultaneous shear and bending force.

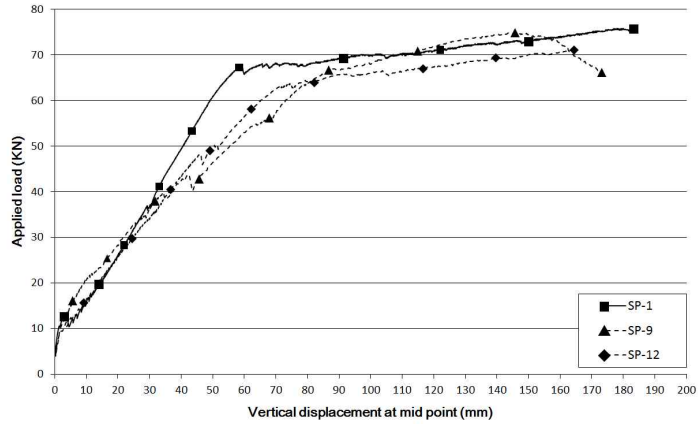


Fig. 4.3.15 Center applied load-displacement relations (specimens-1, 9, 12)

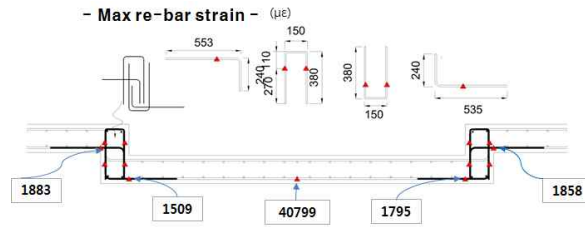


Fig. 4.3.16 Strain of the main rebar of specimen-12

4.4 Concept of Step Reinforcement Design

The following details are presented to restrain the yield of rebars in the joint area of the slab with step and to secure their bonding as well as prevention of diagonal tensile cracking.

- 1) L-bar was additionally placed at the lower slab to the flexural rebar of existing slab, at which positive moment occurred (Fig. 4.4.1(a), (b)) to restrain the flexural yield with increased bonding by increasing the flexural strength of the joint. In other words, it aimed at changing the location of flexural yield

- from the step to flat slab. L-bar was reinforced at upper step at which negative moment took place (Fig. 4.4.1©, ④).
- 2) revU-bar was placed at the step to prevent diagonal cracking (Fig. 4.4.1©) Additionally, U-bar was placed at lower to anchor the vertical element of revU-bar (Fig. 4.4.1⑥). When negative moment was to apply, the role of revU-bar and U-bar changed.
- 3) The quantity of Type-C rebars (rebars of 1) and 2)) was determined by the main rebar of the slab. One combination of rebars with the same size as the main rebar was placed.
- 4) Fillet was installed at the corner of tensile side of the slab to prevent early cracking by reducing the concrete stress (Fig. 4.4.1⑧).

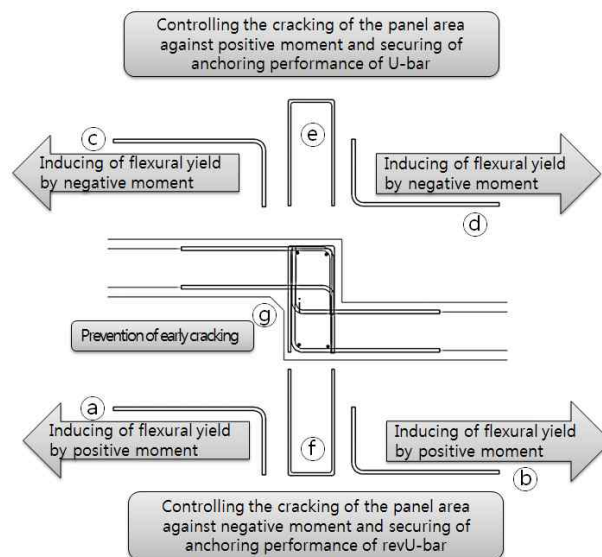


Fig. 4.4.1 Concept drawing of rebar placement at the step area

4.4.1 Additional reinforcement quantity of revU-bar

The stress flow at upper panel area and lower panel area of the step is shown as follows (Figs. 4.4.2 and 4.4.3).

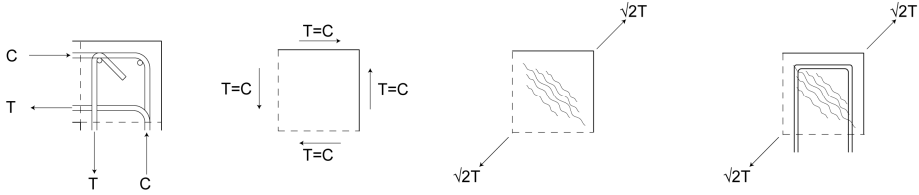


Fig. 4.4.2 Stress flow at upper step

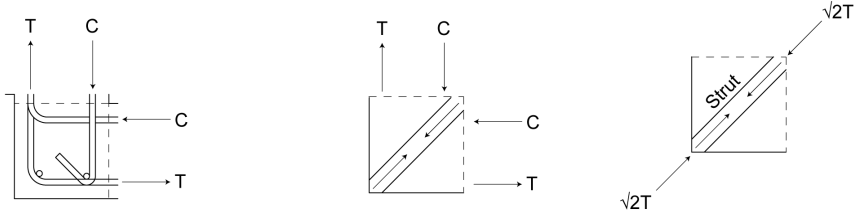


Fig. 4.4.3 Stress flow at lower step

Since tensile force occurs diagonally in the upper panel area, rebar is necessary to prevent cracking. The quantity of revU-bar for this purpose is computed as follows.

$$\sqrt{2} T = 2A_{rU}f_{y-rU} / \sqrt{2} \quad (\text{Eq. 4.4.1})$$

$$\sqrt{2} A_b f_y = \sqrt{2} A_{b-rU} f_{y-rU} \quad (\text{Eq. 4.4.2})$$

$$A_b f_y = A_{rU} f_{y-rU} \quad (\text{Eq. 4.4.3})$$

That is, revU-bar with equivalent strength as one rebar against bending tension of the slab should be placed.

4.4.2 Additional reinforcement quantity of U-bar

U-bar as the same quantity as revU-bar was placed at lower panel area in order to secure the anchoring performance of revU-bar. U-bar was laid out at this time for workability prior to the perpendicular placement of rebar in the slab.

4.4.3 Additional reinforcement quantity of L-bar and revL-bar

L-bar and revL-bar were placed at the step area in order to induce flexural yield at flat slab area away from the step area. When positive moment took place, L-bar and revL-bar were placed at lower slab. When negative moment took place, they were placed at upper slab. Rebars should be placed in upper and lower slab at the point where both positive and negative moment could occur due to seismic load. The rebar ratio of L-bar and revL-bar should be the same as the main rebar of the slab at this time.

4.5 Proposal of Step Reinforcement Design

1) Necessity for the reinforcement of step in the slab

It was found the step area is very sensitive to concrete cracking even with very light gravity load. Additionally, the bending strength of step in the slab was below 50% in comparison to flat slab. Thus, its reinforcement is necessary in order to secure the usability of equivalent performance and safety to flat slab.

2) Application scope

The slab thickness of 210 mm and step height of 230 mm is appropriate for its application. Additionally, the step thickness can vary from the same thickness as the slab, i.e. 210 mm, or above.

4.5.1 Anchoring of main rebar in the slab

The rebars in upper and lower slab is anchored with a hook of 90° angle.

- 1) The upper main rebar of upper slab (Fig. 4.5.1) is anchored with a hook as close to the bottom of lower slab. Likewise, the lower main rebar of lower slab is anchored with a hook as close to the top of upper slab (Eq. 4.5.1).

$$\text{Rebar hook \#1} = (\text{slab thickness} + \text{step height}) - 2 \times \text{cover thickness} - d_b - \text{inner radius at bent section} \quad (\text{Eq. 4.5.1})$$

- 2) The lower main rebar of upper slab is anchored as close to the bottom of lower slab (Fig. 4.5.2). Likewise, the upper main rebar of lower slab is anchored as close to the top of upper slab (Eq. 4.5.2).

$$\text{Rebar hook \#2} = \text{step height} - \text{inner radius at bent section} \quad (\text{Eq. 4.5.2})$$

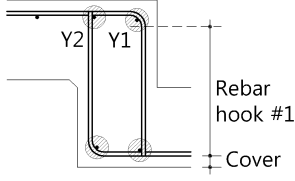


Fig. 4.5.1 Rebar termination #1

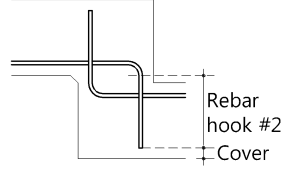


Fig. 4.5.2 Rebar termination #2

- 3) Four perpendicular rebars are placed at four corners of reinforcement are as shown in Fig. 4.5.1. Existing flexural rebar in the slab can be used for the corner rebar.

4.5.2 Design of revU-bar and U-bar

The quantity of revU-bar and U-bar were determined. The quantity of revU-bar is computed as follows (Fig. 4.5.3, Eq. 4.5.3).

$$A_s f_y \leq A_{s_rU} f_{y_rU} \quad (\text{Eq. 4.5.3})$$

The quantity of U-bar is computed as follows (Fig. 4.5.4, Eq. 4.5.4).

$$A_s f_y \leq A_{s_U} f_{y_U} \quad (\text{Eq. 4.5.4})$$

where the height (h) and width (w) of revU-bar and U-bar are computed as follows (Eq. 4.5.5, Eq. 4.5.6)

$$h_{rU} = h_U = \text{slab thickness} + \text{step height} - 2 \times \text{cover thickness} \quad (\text{Eq. 4.5.5})$$

$$w_{rU} = w_U = \text{step thickness} - 2 \times \text{cover thickness} \quad (\text{Eq. 4.5.6})$$

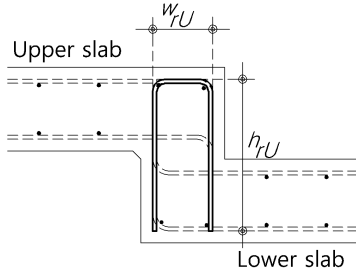


Fig. 4.5.3 revU-bar in upper slab

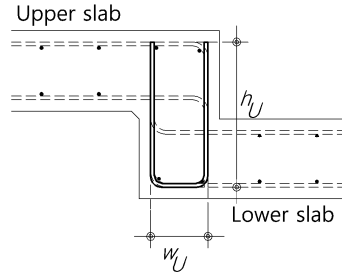


Fig. 4.5.4 U-bar in lower slab

4.5.3 Design of revL-bar and L-bar

1) Case of positive moment

revL-bar is placed in the same size and spacing as lower main rebar in upper slab. Likewise, L-bar is placed in the same size and spacing as lower main rebar in lower slab. The straight anchoring length of revL-bar in upper slab ($l_{a,rL}$ of Fig. 4.5.5) and the straight anchoring length of L-bar in lower slab ($l_{a,L}$ of Fig. 4.5.6) are computed pursuant to KCI 2012 Section 8.2. The anchoring of revL-bar and L-bar with a hook of 90° angle is carried out in the manner of the most straight zone. The 90° hook for revL-bar is extended to the lower main rebar of lower slab. Additionally, the 90° hook for L-bar is extended to the lower main rebar of upper slab.

2) Case of negative moment

revL-bar is placed in the same size and spacing as upper main rebar in upper slab. Likewise, L-bar is placed in the

same size and spacing as upper main rebar in lower slab. The straight anchoring length of revL-bar in upper slab ($l_{a,rL}$ of Fig. 4.5.7) and the straight anchoring length of L-bar in lower slab ($l_{a,L}$ of Fig. 4.5.8) are computed pursuant to KCI 2012 Section 8.2. The anchoring of revL-bar and L-bar with a hook of 90° angle is carried out in the manner of the most straight zone. The 90° hook for revL-bar is extended to the upper main rebar of lower slab. Additionally, the 90° hook for L-bar is extended to the upper main rebar of upper slab.

- 3) Case of positive · negative moment due to seismic load
revL-bar and L-bar are placed together in the same manner as discussed in Sections 4.5.2 and 4.5.3 (Figs. 4.5.9 and 4.5.10).

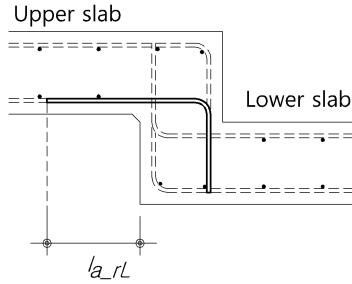


Fig. 4.5.5 revL-bar of upper slab

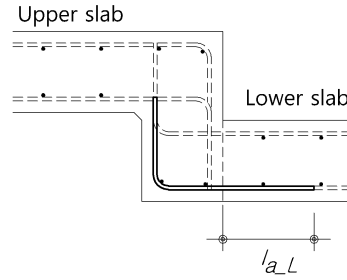


Fig. 4.5.6 L-bar of lower slab

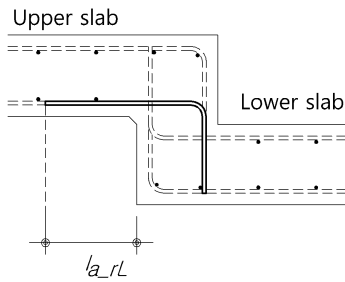


Fig. 4.5.7 revL-bar of upper slab

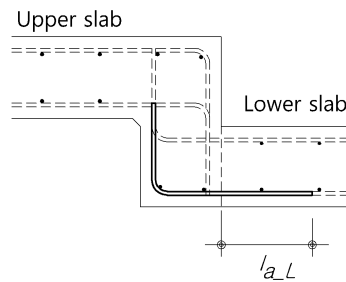


Fig. 4.5.8 L-bar of lower slab

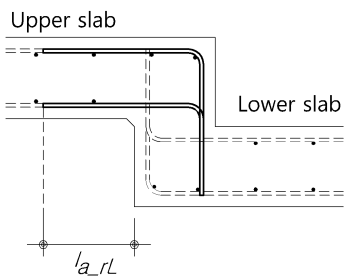


Fig. 4.5.9 revL-bar of upper slab

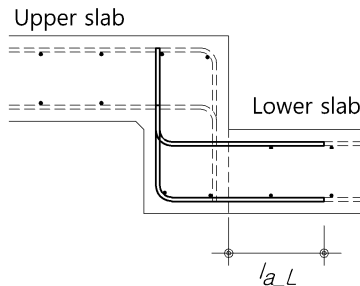


Fig. 4.5.10 L-bar of lower slab

4.5.4 Construction sequence

The main rebar and additional reinforcement in the slab are concentrated around the step. The workability can be improved with proper construction sequence.

- 1) Longitudinal placement of lower main rebar in lower slab: determined by such factors as bending moment, etc. (Fig. 4.5.11).
- 2) Placement of U-bar: The same size and type of U-bar as the main rebar in slab is placed one each between the main rebars (Fig. 4.5.12).

- 3) Placement of L-bar: The same size and type of L-bar as the main rebar in slab is placed one each between the main rebars and then is adjacent to U-bars (Fig. 4.5.13).
- 4) Perpendicular placement of lower rebar in lower slab: determined by such factors as perpendicular bending moment, etc. Two are placed inside U-bar (Fig. 4.5.14).
- 5) Longitudinal placement of lower main rebar in upper slab: determined by factors such as bending moment, ect. (Fig. 4.5.15).
- 6) Placement of revL-bar: The same size and type of revL-bar as the main rebar in slab is placed one each between the main rebars and then is adjacent to U-bars and L-bars (Fig. 4.5.16).
- 7) Perpendicular placement of upper main rebar in lower slab: determined by factors such as bending moment, ect. (Fig. 4.5.17).
- 8) Longitudinal placement of upper main rebar in lower slab: determined by factors such as bending moment, ect. (Fig. 4.5.18).
- 9) Perpendicular placement of lower main rebar in upper slab: determined by factors such as bending moment, ect. (Fig. 4.5.19).

- 10) Perpendicular placement of upper main rebar in upper slab: determined by factors such as bending moment, ect. (Fig. 4.5.20).
- 11) Longitudinal placement of upper main rebar in upper slab: determined by factors such as bending moment, ect. (Fig. 4.5.21).
- 12) Placement of revU-bar: The same size and type of revU-bar as the main rebar in slab is placed one each between the main rebars and then U-bar, L-bar, and revL-bar (Fig. 4.5.22).

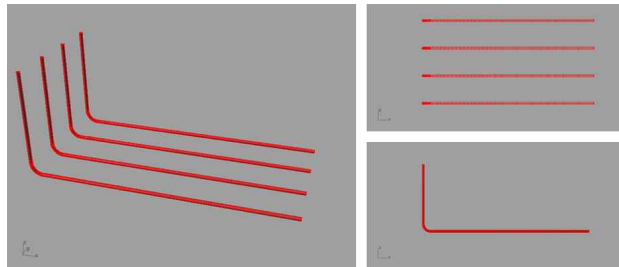


Fig. 4.5.11 Longitudinal placement of lower main rebar in lower slab

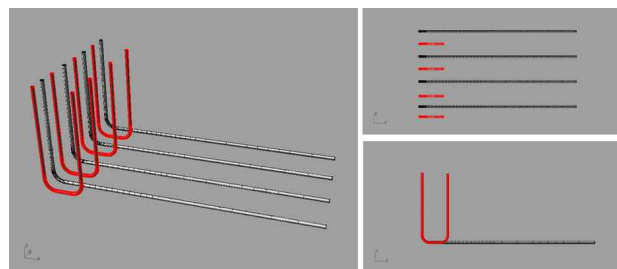


Fig. 4.5.12 Placement of U-bar

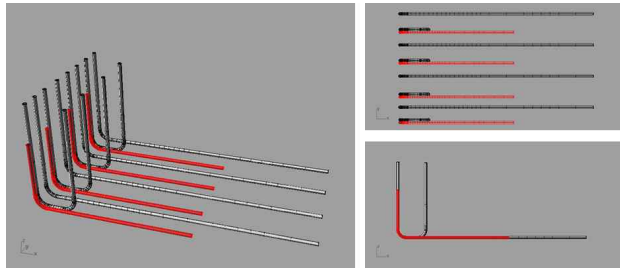


Fig. 4.5.13 Placement of L-bar

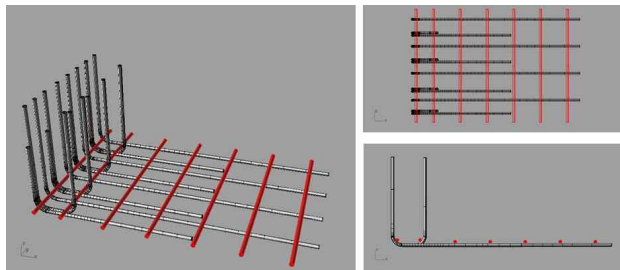


Fig. 4.5.14 Perpendicular placement of lower main rebar in lower slab

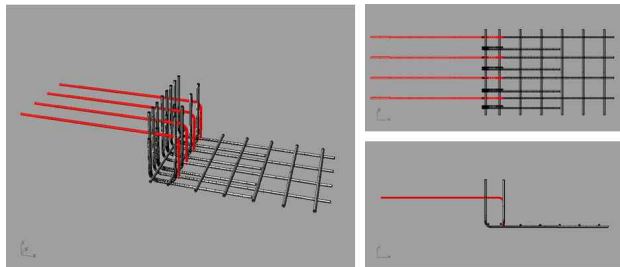


Fig. 4.5.15 Longitudinal placement of lower main rebar in upper slab

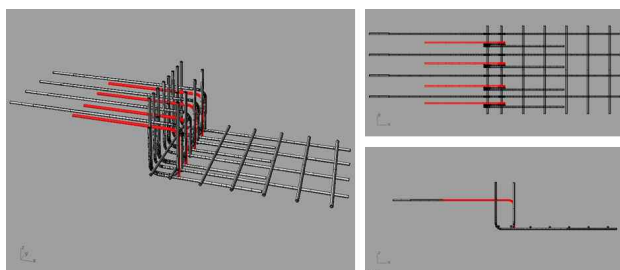


Fig. 4.5.16 Placement of revL-bar

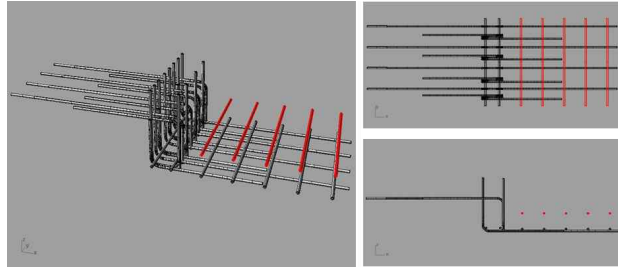


Fig. 4.5.17 Perpendicular placement of upper main rebar in lower slab

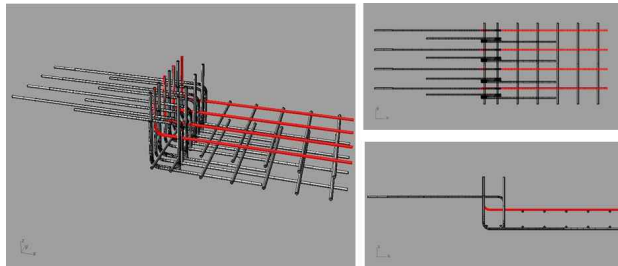


Fig. 4.5.18 Longitudinal placement of upper main rebar in lower slab

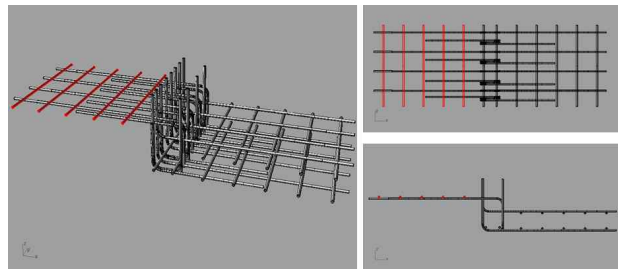


Fig. 4.5.19 Perpendicular placement of lower main rebar in upper slab

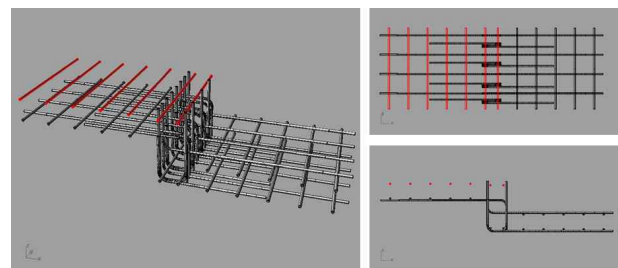


Fig. 4.5.20 Perpendicular placement of lower main rebar in upper slab

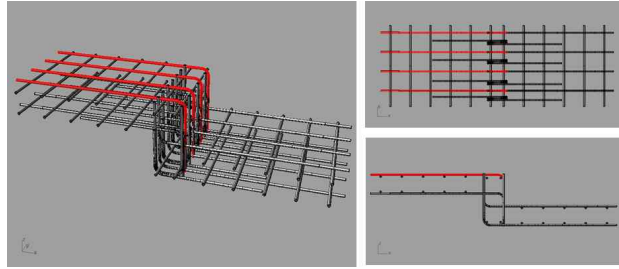


Fig. 4.5.21 Longitudinal placement of upper main rebar in upper slab

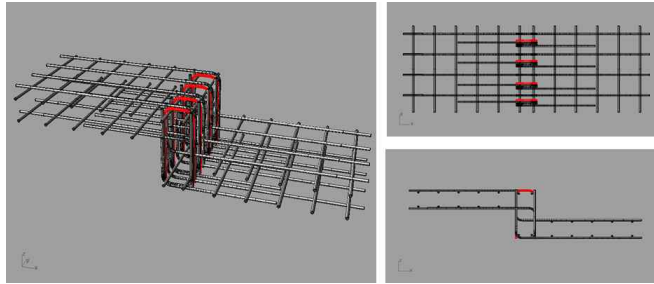


Fig. 4.5.22 Placement of revU-bar

4.6 Necessity of Stiffness Analysis Based on the Experimental Result

The test result of twelve specimens indicates the slabs with steps can manifest the bending performance equivalent to flat slab if they are provided with adequate reinforcement detail. However, there was a significant difference in secant stiffness by the shape, size, and reinforcement method of the steps. Thus, the stiffness of steps is investigated based on the aforementioned experimental results to apply it to stiffness analysis of the slab in two directions against the lateral load. Additionally, a simplified stiffness design method in consideration of the stiffness reduction of the step in the slab during structural design is proposed in Chapter 5.

4.7 Summary of Results

- 1) The specimen with Type-C reinforcement detail manifested a bending moment equivalent to the computed nominal bending moment of 79.1 kN. There were a total of three specimens, which manifested greater than the nominal bending moment, and all these specimens had the commonness of possessing Type-C reinforcement detail.
- 2) The specimen without reinforced step manifested only 57 % of nominal bending moment. Thus, the reinforcement of the step is necessary to manifest the safety and usability as equivalent to flat slab.
- 3) If the cross section of the step gets larger, its initial stiffness was better. However, its maximum strength manifestation was a problem. It exhibited better bending stiffness than the flat slab in the beginning, but its stiffness quickly dropped after the occurrence of a large crack. As the step was thicker, its initial stiffness was satisfactory. However, its stiffness rapidly dropped after a large crack, and the inclined step did not manifest initial cracking. Thus, making the step inclined or fillet can control initial cracking.
- 4) It is alright not to treat the main rebar of the slab in the step with a hook of 135° angle. Specimen-5 (with 135° hook) and specimen-9 (straight end) were the same except for the treatment of anchoring the main rebar in the step of the slab. However, this difference did not affect the bending strength of

these two specimens.

- 5) Inclined rebar reinforcement was not effective because its inclination was in the same direction as diagonal cracking. Additionally, since inclined rebar was not effective as reinforcement, its increase in size was not effective, also.

Chapter 5

Stiffness Analysis in Consideration of Steps

Commercialized stiffness analysis programs use nodes and elements. These programs typically assume completely rigid or completely hinged at the node. Thus, stiffness of elements at the nodes is constant. Modelling of the nodes without completely rigid or hinged uses elastic link of the commercialized analysis program. Two nodes can be connected with the spring (elastic link) of desired stiffness as designed, and this spring can manifest flexible stiffness including rotation at the node. This study applied the spring (elastic link) for the rotation to carry out stiffness analysis with a variety of variables. Then, the result of the stiffness analysis is used to determine the step modification factor (γ), which can be additionally considered in existing effective width models.

5.1 Input Method through Elastic Link

The stiffness analysis programs basically rigidly connects an element with other element at the node. It is not appropriate to apply the rigid connection to the bent area of the slab with step. It is because the connection will have the stiffness between rigid and hinged as cracking takes place in the step to reduce the bonding gradually. In other words, if the inner and outer angle of the step are set to be θ_1 and θ_2 , respectively, as shown in Fig.

5.1.1. Then the angle of the bent area of the step changes $\theta_1 \rightarrow \theta_3, \theta_2 \rightarrow \theta_4$. That is, the phenomenon depicted in Fig. 5.1.2 (the angles at the bent area, θ_1 and θ_2 , do not change and remain as θ_1 and θ_2 even at the ultimate strength) is not realistic. In reality, the angle at the bent area increases in proportion to the rotational moment at the center of the bent area, and the stiffness analysis program should additionally apply elastic link, i.e. a rotational spring, between the nodes in order to reflect this rotational behavior.

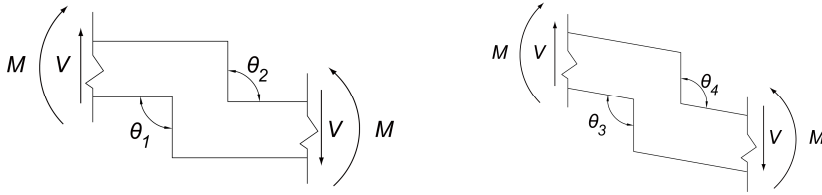


Fig. 5.1.1 Actual behavior of the step

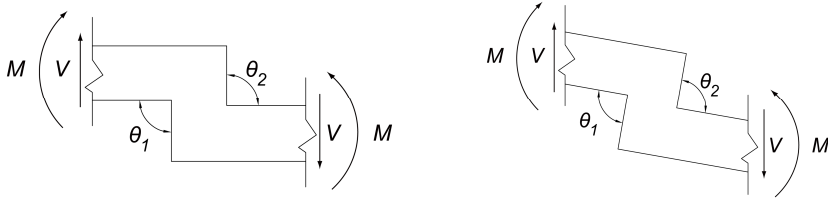


Fig. 5.1.2 Behavior of stiffness analysis program

This study carried out an analysis similar to the actual behavior of the step by reflecting the rotational stiffness in the stiffness analysis program instead of basic rigid analysis. The analysis program uses elastic link. It has the following characteristics.

Typical stiffness of elastic link can be analyzed by three coordinates and rotational stiffness. In other words, it can be

expressed in terms of force per unit length (kN/m) in three directional coordinates (x, y, z) and moment per rotational angle (kN · m/[rad]) (Fig. 5.1.3). Tensile component and compressive component can be attributed to elastic link, and, in this case, stiffness in axial direction of the element coordinates only is necessary. Additionally, rigid characteristics can be attributed to elastic link to connect two nodes.^[11]

This study considered rotational stiffness at the node at which two members interface. Especially, the stiffness of slab against lateral load and story drift are investigated in consideration of the rotational stiffness for SRy. The three stiffness in axial directions (SDx, SDy, SDz) and two rotational stiffness (SRx, SRz) are given infinite (∞) stiffness to mimic the actual behavior (Fig. 5.14).

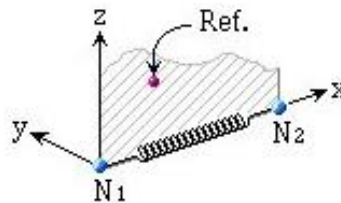


Fig. 5.1.3 Element coordinates

SDx	10000000	kN/m
SDy	10000000	kN/m
SDz	10000000	kN/m
SRx	10000000	kN-m/(rad)
SRy	12597	kN-m/(rad)
SRz	10000000	kN-m/(rad)
<input type="checkbox"/> Shear Spring Location Distance Ratio From End I SDy: 0.5 SDz: 0.5		
Beta Angle : 0 [deg]		
2 Nodes :		

Fig. 5.1.4 Input form for rotational stiffness

5.2 Computation and Application of Rotational Stiffness

The worst condition (the largest rotational angle and the least rotational stiffness) for the same story drift ratio is expressed as follows (Fig. 5.2.1 and Fig. 5.2.2).

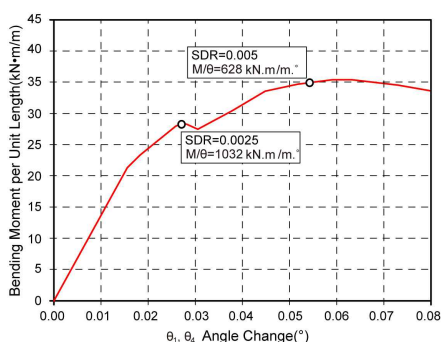


Fig. 5.2.2 Relationship of moment
-rotational angle (+)
per unit length

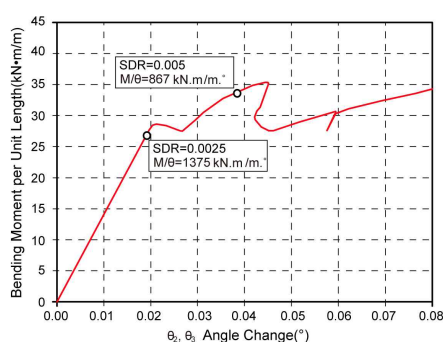


Fig. 5.2.1 Relationship of moment
-rotational angle (-)
per unit length

- 1) Story drift ratio 0.0025 : 1032 kN/° (rotational angle (+))
1375 kN/° (rotational angle (-))
- 2) Story drift ratio 0.005 : 628 kN/° (rotational angle (+))
867 kN/° (rotational angle (-))

Thus, the rotational stiffness of the step to be applied to linear analysis can use the rotational stiffness of the worst condition, and rotational stiffness of 1032 kN/° for story drift ratio 0.0025 and rotational stiffness of 628 kN/° for story drift ratio 0.005 are conservatively applied regardless of increase or decrease in the rotational angle.

5.3 Procedure and Condition for the Computation of Step Modification Factor

Stiffness values among the rotational stiffness values of the step, which were determined in Section 5.2, are applied, because the stiffness of slab should be conservatively applied in the design for the total service load. This section aims at developing an analysis model of the stiffness change, which should be additionally considered for the case of the slab with step. The stiffness change due to the step can be considered through modification factor, which can be additionally applied to existing effective beam width methods. The modification factor γ for the step was obtained by controlling for the variables of the stiffness analysis model.

5.3.1 Rotational stiffness by the area of influence

Column strip width, which is similar to effective beam width or a little larger, was regarded as the length of the area of influence of rotational stiffness in width direction. The width of step differs by design. Even though the width of step changes every time, the width of step is generally more probable to be less than the width of column strip or effective beam width. Then, applying the rotational stiffness per unit length (M/θ), which was computed by nonlinear analysis, to design strip would cause an precise representation, because it is flat slab outside the step. Even if it is to be applied to column strip, of which the width would probably be larger than the step width, it would underestimate the rotational stiffness a little. Nevertheless,

the column strip width was regarded as the length of the area of influence of rotational stiffness in width direction in order to conservatively compute the lateral displacement, i.e. to make the rotational stiffness unfavorable, Then, the rotational stiffness, which was computed in consideration of effective beam width, was reflected to the design of slab reinforcement (Fig. 5.3.1).

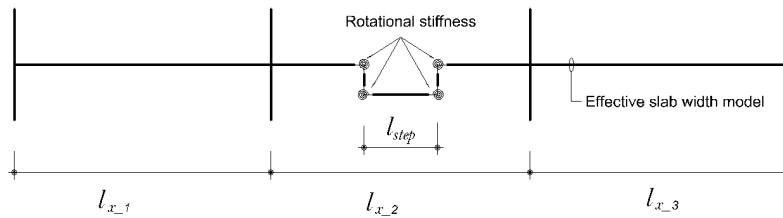


Fig. 5.3.1 Frame modeling

5.3.2 Procedure of modification factor computation

The computational procedure for step modification factor (γ) is as follows.

- 1) The flat slab with step was assumed to be a flat plate without step in order to compute effective beam width (application of Grossman's effective beam width method)
- 2) Computation of rotational stiffness by the area of influence (compute rotational stiffness for strength design and serviceability design)
- 3) Composition of the following three models for lateral load analysis

Model 1 : Model with the effective beam width computed from 1)

Model 2 : Model with effective beam width from 1) and the step within the effective beam width. Input rotational stiffness computed from 2)

Model 3 : Model with new effective beam width

- 4) Compute lateral force P when by the strength design from model 1 of 3) when δ_i does not surpass (height)/200 and the closest, then continue to compute lateral force P by the serviceability design when δ_i does not surpass (height)/400 and the closest (Step 1 of Fig. 5.3.2)
- 5) Compute new lateral displacement, δ_k , taking place when lateral force P from 4) of model 2 (Step 2 of Fig. 5.3.2)
- 6) Exert lateral force P from 4) of model 3 and compute the effective beam width, b_k , which results in the equivalent lateral displacement δ_k (Step 3 of Fig. 5.3.2)
- 7) Define effective beam width modification factor $\gamma(= b_k/b_i)$ by using the new effective beam width (b_k) from 6) relative to the effective beam width (b_i) of flat plate without step.

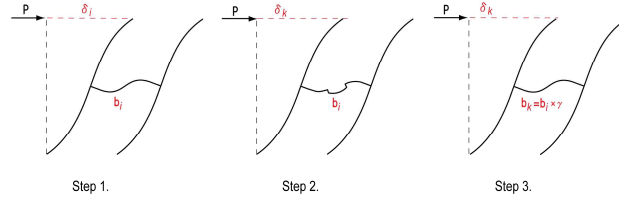


Fig. 5.3.2 Concept of modification factor (γ) computation through stiffness analysis

5.4 Analysis Result of Step Modification Factor

It is difficult to predict which variable will influence the stiffness of the slab with step. Thus, this section varies only condition as a variable and all other conditions are set to be the same in order to find out a single modification factor (γ'). Then, step modification factor (γ), which considers a variety of variables, can be finally obtained, if the single modification factors, which considered only one variable at a time, are multiplied as expressed in Eq. 5.4.1.

$$\gamma = \prod \gamma'_n = \gamma'_1 \times \gamma'_2 \times \gamma'_3 \cdots \gamma'_n \quad (\text{Eq. 5.4.1})$$

5.4.1 Basics of stiffness analysis

The prototype model for stiffness analysis and basic specification are presented in Table 5.4.1 and Fig. 5.4.1. In this given condition, the rotational stiffness has the values of 206952 kN · m/radian and 125937 kN · m/radian when the story drift ratios are 0.0025 and 0.005, respectively.

Table 5.4.1 Specification of the basic model for stiffness analysis

Column size	600 × 600 mm	Column spacing	7000 mm
Slab thickness	210 mm	Load	D.L.: 8 kN/m ² L.L.: 3 kN/m ²
Step height	230 mm		
Step thickness	210 mm		

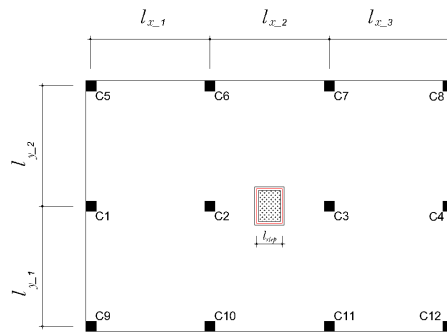


Fig. 5.4.1 Basic plane view for stiffness analysis

5.4.2 Relationship between variables and single modification factor

Firstly, modification factor by the location of step and change of the step length was investigated. It was analyzed with the simultaneous variables of step length (l_{step}) and location as discussed in Section 5.4.1 of the basic condition. Since the step location and step length together affected the stiffness of slab, the two variables were controlled simultaneously for the analysis. The locations of step were designated at eight points - 2/4 (center), 3/4 and 4/4 of inner span, and 0/4, 1/4, 2/4, 3/4 and 4/4 of outer span. The step length (l_{step}) was increased by 10 % of slab span to vary between 0 % ~ 90 %.

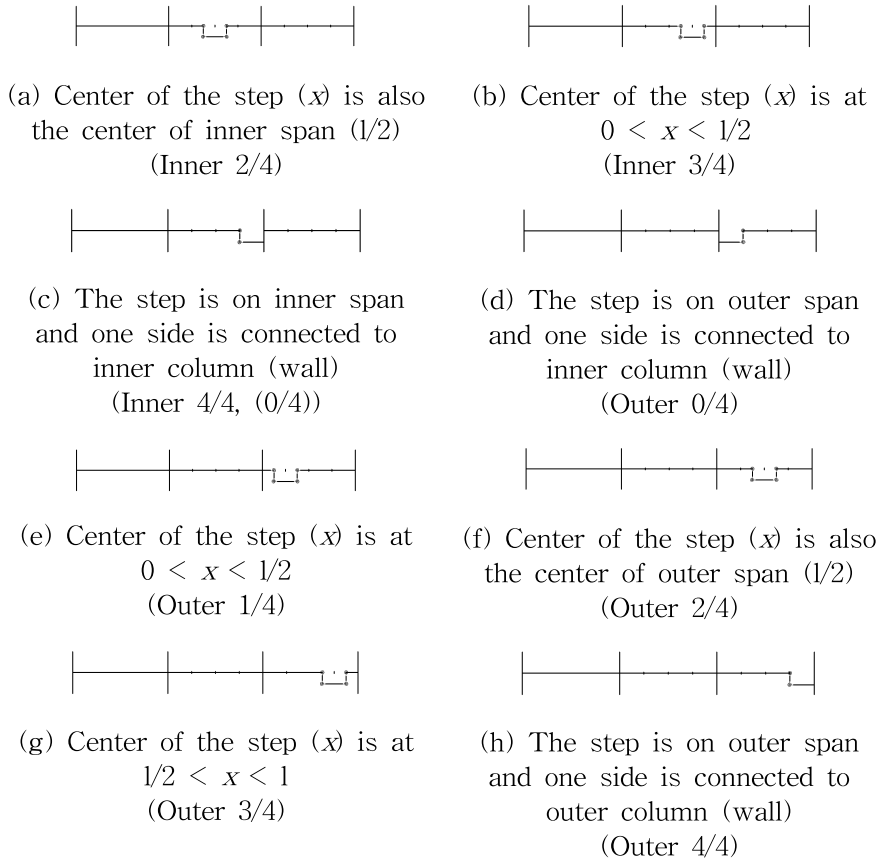


Fig. 5.4.2 Location of the step

New effective beam width (b_k), which manifested lateral displacement equivalent to the frame of slab with step by step location and step length, was divided by effective beam width (b_i) of the flat plate without step to compute single modification factor (γ') (Table 5.4.2, Table 5.4.3). Examining the values of strength design and serviceability design, lateral load transfer capacity was affected by the combination of step location and step length. The cases of the step location – the vertical member connected to one side of the

step (0/4 and 4/4 location), the center of step being the center of slab (2/4 location), and the center of the step not being the center of slab (1/4 and 3/4 location) exhibited the same trend.

Secondly, the modification factor by the increase in step thickness was investigated. The step length of 3,500 mm and step location at inner 2/4 point as discussed in basic condition of Section 5.4.1 and Section 5.4.2 were fixed to analyze the analysis result with step thickness as the only variable. The step thickness increased from 210 mm, the same as the thickness of slab, by 10% of the slab thickness, i.e. to 230 mm, 250 mm, etc., in order to attain the effective beam width (b_k) in consideration of the step. Then, its ratio (b_k/b_i) to the effective beam width of flat plate without step (b_i) was computed. Then, the inverse ratio (b_i/b_k) was computed based on the standard step thickness of 210 mm, i.e. the step thickness of 0 % in Table 5.4.4, to compute a single modification factor (γ') by the change of step thickness. Examining the analysis result, it was found that the lateral stiffness of the slab with step increased with increased thickness of the step.

Thirdly, the modification factor by the increase in step height was investigated. The step length of 3,500 mm and step location at inner 2/4 point as discussed in basic condition of Section 5.4.1 and Section 5.4.2 were fixed to analyze the analysis result with step height as the only variable. The step height increased from 230 mm by 10 %,

i.e. to 250 mm, 275 mm, etc., in order to attain new effective beam width (b'_k) in consideration of the step. Then, its ratio (b_k/b_i) to the effective beam width of flat plate without step (b_i) was computed. Afterwards, the inverse ratio (b_i/b_k) was computed based on the standard step height of 230 mm, i.e. the step height of 0 % in Table 5.4.5, to compute a single modification factor (γ') by the change of step thickness. Examining the analysis result, it was found that the lateral stiffness of the slab with step decreased with increased height of the step.

Fourthly, the modification factor by the increase in the length of the slab, which was adjacent to the middle step interior slab in both sides, was investigated. The step length of 3,500 mm and step location at inner 2/4 point as discussed in basic condition of Section 5.4.1 and Section 5.4.2 were fixed to analyze the analysis result with the length (l_{x_1} , l_{x_3}) of the slab, which was adjacent to the step in both sides, as the only variable. The length of the slab in both sides was increased by 10 % to compute new effective beam width (b'_k), and then its ratio (b_k/b_i) to the effective beam width of flat slab without step (b_i) was computed. Afterwards, the inverse ratio (b_i/b_k) was computed based on the standard slab length of 7,000 mm, i.e. the slab length of 0 % in Table 5.4.6, to compute a single modification factor (γ') by the change of the length of the slab, which was adjacent to the step in both sides. Examining the analysis result, it was found that the lateral stiffness decreased with increased length of the slab which

was adjacent to the middle step slab in both sides.

Fifthly, the modification factor by the increase in the length of the slab, which was adjacent to the middle step interior slab in one side, was investigated. The step length of 3,500 mm and step location at inner 2/4 point as discussed in basic condition of Section 5.4.1 and Section 5.4.2 were fixed to analyze the analysis result with the length (l_{x_3}) of the slab, which was adjacent to the span with step one side, as the only variable. The length of the slab in one side was increased by 10 % to compute new effective beam width (b'_k), and then its ratio (b_k/b_i) to the effective beam width of flat slab without step (b_i) was computed. Afterwards, the inverse ratio (b_i/b_k) was computed based on the standard slab length of 7000 mm, i.e. the slab length of 0 % in Table 5.4.7, to compute a single modification factor (γ') by the change of the length of the slab, which was adjacent to the step in one side. Examining the analysis result, it was found that the lateral stiffness decreased with increased length of the slab which was adjacent to the middle step slab in one side.

Sixthly, the modification factor by the increase in the column size was investigated. The step length of 3,500 mm and step location at inner 2/4 point were fixed to find out the change of modification factor by the increase in the column size [C1 ~ C4 column size ($b \times h$)]. The size variables of b and h of C1 ~ C4 columns were increased by

10 % to compute new effective beam width (b'_k), and then its ratio (b_k/b_i) to the effective beam width of flat slab without step (b_i) was computed. Then, the inverse ratio (b_i/b_k) was computed based on the standard column size of 600×600 mm, i.e. the size of 0 % in Table 5.4.8, to compute a single modification factor (γ') by the change of the column size. Examining the analysis result, it was found that the lateral stiffness decreased with increased size of the column.

Seventhly, the modification factor by the increase in the number of continuous slabs with steps was investigated. The step length of 3,500 mm and step location at inner 2/4 point were fixed to find out the change of modification factor by the increase in the number of slabs with steps, i.e. 1, 2, 3, 4, 5, in order to compute new effective beam width (b'_k), and then its ratio (b_k/b_i) to the effective beam width of flat slab without step (b_i) was computed. Afterwards, the inverse ratio (b_i/b_k) was computed based on the standard number of column, i.e. 1 slab in Table 5.4.9, to compute a single modification factor (γ') by the change of number of continuous slabs. Examining the analysis result, it was found that the lateral stiffness was not affected by the number of continuous slabs with steps.

5.4.3 Parametric analysis and proposal of step modification factor

When several variables such as step length, step location,

slab-step thickness and step height are considered in combination, the final modification factor for the step can be computed based on the single modification factor, which was computed in consideration of only one variable at a time. If the single modification factor by step location and length, slab-step thickness, and step height are denoted as γ'_1 , γ'_2 , and γ'_3 , respectively, then multiplying each of these single modification factor would yield the final modification factor for the step in consideration of these variables as expressed in the following Eq. 5.4.2.

$$\gamma = \gamma'_1 \times \gamma'_2 \times \gamma'_3 \quad (\text{Eq. 5.4.2})$$

Using the values of γ computed from Eq. 5.4.2 and the research method as described in Section 4.3, the values in consideration of the model with simultaneous multiple variables could be obtained (Table 5.4.10). In the table, values of step modification factor (γ) are presented by multiplying all single modification factors, which were attained by controlling for only one variable at a time. The value of (b_{cal}/b_k) in Table 5.4.10 compares the effective beam width (b_{cal}) with the effective beam width (b_k), which was obtained by applying all variables simultaneously. They were very similar. Nonetheless, the two values differed somewhat noticeable for the cases of very small effective beam width and excessively large step length or height. Then, these cases are seldom encountered in actual practice. Thus, it is deemed that the method of computing step modification

factor for several variables as expressed in Eq. 4.5.2 is appropriate.

For example, the stiffness reduction around the step was examined through gravity load test and nonlinear analysis. The reduced rotational stiffness was quantified through nonlinear analysis, and this value was applied to stiffness analysis in order derive the step modification factor.

Table 5.4.2 Analysis result by the change of step length and location
for strength design

Outer 4/4			Outer 3/4		
Length change	b_k	γ'	Length change	b_k	γ'
10%	1583	0.89	10%	1546	0.87
20%	1521	0.85	20%	1506	0.84
30%	1621	0.91	30%	1254	0.70
40%	2017	1.13	40%	951	0.53
50%	2612	1.46	50%	710	0.40
60%	2175	1.22	60%	554	0.31
70%	1730	0.97	70%	542	0.30
80%	1608	0.90	80%	714	0.40
90%	1569	0.88	90%		
Outer 2/4			Outer 1/4		
Length change	b_k	γ'	Length change	b_k	γ'
10%	1767	0.99	10%	1552	0.87
20%	1732	0.97	20%	1510	0.85
30%	1677	0.94	30%	1263	0.71
40%	1607	0.90	40%	967	0.54
50%	1524	0.85	50%	731	0.41
60%	1433	0.80	60%	578	0.32
70%	1315	0.74	70%	571	0.32
80%	1216	0.68	80%	746	0.42
90%	1119	0.63	90%		
Outer 0/4			Inner 4/4		
Length change	b_k	γ'	Length change	b_k	γ'
10%	1570	0.88	10%	1763	0.89
20%	1536	0.86	20%	1731	0.87
30%	1625	0.91	30%	1860	0.94
40%	2018	1.13	40%	2316	1.17
50%	2615	1.47	50%	2997	1.51
60%	2096	1.17	60%	2452	1.24
70%	1698	0.95	70%	1967	0.99
80%	1594	0.89	80%	1819	0.92
90%	1514	0.85	90%	1722	0.87
Inner 3/4			Inner 2/4		
Length change	b_k	γ'	Length change	b_k	γ'
10%	1722	0.87	10%	1967	0.99
20%	1669	0.84	20%	1924	0.97
30%	1404	0.71	30%	1856	0.94
40%	1086	0.55	40%	1768	0.89
50%	831	0.42	50%	1667	0.84
60%	664	0.34	60%	1558	0.79
70%	646	0.33	70%	1446	0.73
80%	816	0.41	80%	1335	0.67
90%			90%	1229	0.62

Table 5.4.3 Analysis result by the change of step length and location
for serviceability design

Outer 4/4			Outer 3/4		
Length change	b_k	γ'	Length change	b_k	γ'
10%	1990	0.89	10%	1907	0.86
20%	1633	0.73	20%	1851	0.83
30%	1635	0.73	30%	1395	0.63
40%	2137	0.96	40%	887	0.40
50%	3060	1.37	50%	508	0.23
60%	2416	1.08	60%	290	0.13
70%	1793	0.80	70%	310	0.14
80%	1761	0.79	80%	661	0.30
90%	1931	0.87	90%	–	–
Outer 2/4			Outer 1/4		
Length change	b_k	γ'	Length change	b_k	γ'
10%	2205	0.99	10%	1912	0.86
20%	2171	0.97	20%	1876	0.84
30%	2119	0.95	30%	1468	0.66
40%	2047	0.92	40%	1003	0.45
50%	1960	0.88	50%	650	0.29
60%	1864	0.84	60%	442	0.20
70%	1705	0.76	70%	469	0.21
80%	1590	0.71	80%	797	0.36
90%	1475	0.66	90%	–	–
Outer 0/4			Inner 4/4		
Length change	b_k	γ'	Length change	b_k	γ'
10%	1960	0.88	10%	2220	0.90
20%	1642	0.74	20%	1860	0.75
30%	1621	0.73	30%	1874	0.76
40%	2139	0.96	40%	2463	0.99
50%	3125	1.40	50%	3551	1.43
60%	2335	1.05	60%	2740	1.11
70%	1813	0.81	70%	2082	0.84
80%	1800	0.81	80%	2036	0.82
90%	1830	0.82	90%	2111	0.85
Inner 3/4			Inner 2/4		
Length change	b_k	γ'	Length change	b_k	γ'
10%	2130	0.86	10%	2463	0.99
20%	2061	0.83	20%	2418	0.98
30%	1597	0.64	30%	2346	0.95
40%	1076	0.43	40%	2254	0.91
50%	681	0.27	50%	2144	0.87
60%	450	0.18	60%	2024	0.82
70%	475	0.19	70%	1899	0.77
80%	822	0.33	80%	1772	0.72
90%	–	–	90%	1647	0.66

Table 5.4.4 Analysis result by the change of step thickness

Thickness change	Strength design				Serviceability design			
	b_i	b_k	(b_k/b_i)	γ'	b_i	b_k	(b_k/b_i)	γ'
0%	1982	1667	0.84	1.00	2478	2144	0.87	1.00
10%	1982	1695	0.86	1.02	2478	2167	0.87	1.01
20%	1982	1704	0.86	1.02	2478	2183	0.88	1.02
30%	1982	1712	0.86	1.03	2478	2195	0.89	1.02
40%	1982	1717	0.87	1.03	2478	2203	0.89	1.03
50%	1982	1721	0.87	1.03	2478	2210	0.89	1.03
60%	1982	1724	0.87	1.03	2478	2215	0.89	1.03
70%	1982	1726	0.87	1.04	2478	2219	0.90	1.03
80%	1982	1728	0.87	1.04	2478	2222	0.90	1.04
90%	1982	1730	0.87	1.04	2478	2225	0.90	1.04
100%	1982	1731	0.87	1.04	2478	2227	0.90	1.04

Table 5.4.5 Analysis result by the change of step height

Height change	Strength design				Serviceability design			
	b_i	b_k	(b_k/b_i)	γ'	b_i	b_k	(b_k/b_i)	γ'
0%	1982	1667	0.84	1.00	2478	2144	0.87	1.00
10%	1982	1660	0.84	1.00	2478	2135	0.86	1.00
20%	1982	1653	0.83	0.99	2478	2126	0.86	0.99
30%	1982	1646	0.83	0.99	2478	2117	0.85	0.99
40%	1982	1640	0.83	0.98	2478	2108	0.85	0.98
50%	1982	1633	0.82	0.98	2478	2099	0.85	0.98
60%	1982	1626	0.82	0.98	2478	2091	0.84	0.98
70%	1982	1620	0.82	0.97	2478	2082	0.84	0.97
80%	1982	1613	0.81	0.97	2478	2073	0.84	0.97
90%	1982	1607	0.81	0.96	2478	2065	0.83	0.96
100%	1982	1600	0.81	0.96	2478	2056	0.83	0.96

Table 5.4.6 Analysis result by the increase in the length of slab adjacent in both sides

Length change	Strength design				Serviceability design			
	b_i	b_k	(b_k/b_i)	γ'	b_i	b_k	(b_k/b_i)	γ'
0%	1982	1667	0.84	1.00	2478	2144	0.87	1.00
10%	2038	1708	0.84	1.00	2548	2199	0.86	1.00
20%	2097	1751	0.84	0.99	2621	2256	0.86	0.99
30%	2156	1795	0.83	0.99	2695	2313	0.86	1.00
40%	2217	1839	0.83	0.99	2772	2373	0.86	0.99
50%	2280	1884	0.83	0.98	2850	2432	0.85	0.99
60%	2343	1929	0.82	0.98	2929	2492	0.85	0.98
70%	2408	1975	0.82	0.98	3010	2554	0.85	0.98
80%	2473	2021	0.82	0.97	3092	2616	0.85	0.98
90%	2540	2067	0.81	0.97	3175	2678	0.84	0.97
100%	2607	2114	0.81	0.96	3258	2740	0.84	0.97

Table 5.4.7 Analysis result by the increase in the length of slab adjacent in one side

Length change	Strength design				Serviceability design			
	b_i	b_k	(b_k/b_i)	γ'	b_i	b_k	(b_k/b_i)	γ'
0%	1982	1667	0.84	1.00	2478	2144	0.87	1.00
10%	2010	1687	0.84	1.00	2513	2171	0.86	1.00
20%	2024	1697	0.84	1.00	2550	2200	0.86	1.00
30%	2069	1730	0.84	0.99	2587	2229	0.86	1.00
40%	2100	1753	0.83	0.99	2625	2258	0.86	0.99
50%	2131	1775	0.83	0.99	2664	2288	0.86	0.99
60%	2163	1799	0.83	0.99	2704	2319	0.86	0.99
70%	2195	1822	0.83	0.99	2744	2349	0.86	0.99
80%	2228	1845	0.83	0.98	2785	2381	0.85	0.99
90%	2261	1869	0.83	0.98	2827	2413	0.85	0.99
100%	2295	1894	0.83	0.98	2868	2444	0.85	0.98

Table 5.4.8 Analysis result by the increase in the column size

Size change	Strength design				Serviceability design			
	b_i	b_k	(b_k/b_i)	γ'	b_i	b_k	(b_k/b_i)	γ'
0%	1982	1667	0.84	1.00	2478	2144	0.87	1.00
10%	2026	1699	0.84	1.00	2533	2187	0.86	1.00
20%	2070	1731	0.84	0.99	2588	2230	0.86	1.00
30%	2115	1764	0.83	0.99	2643	2273	0.86	0.99
40%	2159	1796	0.83	0.99	2698	2315	0.86	0.99
50%	2203	1829	0.83	0.99	2752	2357	0.86	0.99
60%	2247	1860	0.83	0.98	2809	2401	0.85	0.99
70%	2291	1892	0.83	0.98	2864	2443	0.85	0.99
80%	2335	1923	0.82	0.98	2919	2485	0.85	0.98
90%	2379	1955	0.82	0.98	2974	2527	0.85	0.98
100%	2423	1986	0.82	0.97	3029	2568	0.85	0.98

Table 5.4.9 Analysis result by the number of continuous slabs

Number of slabs	Strength design				Serviceability design			
	b_i	b_k	(b_k/b_i)	γ'	b_i	b_k	(b_k/b_i)	γ'
1 slab	1982	1667	0.84	1.00	2478	2144	0.87	1.00
2 slabs	1982	1667	0.84	1.00	2478	2144	0.87	1.00
3 slabs	1982	1667	0.84	1.00	2478	2144	0.87	1.00
4 slabs	1982	1667	0.84	1.00	2478	2144	0.87	1.00
5 slabs	1982	1667	0.84	1.00	2478	2144	0.87	1.00

Table 5.4.10 Complex analysis result in simultaneous consideration of several variables

	Step length	Step locat-ion	Step thk.	Step height	γ'_1	γ'_2	γ'_3	γ	b_{cal}	b_k	$\frac{b_{cal}}{b_k}$
S t r e n g t h d s I g n	40%	Outer 4/4	250	230	1.14	1.02	1.00	1.16	2074	2033	1.02
	40%	Outer 2/4	315	230	0.90	1.03	1.00	0.93	1654	1639	1.01
	60%	Inner 4/4	355	230	1.21	1.04	1.00	1.26	2494	2485	1.00
	60%	Outer 3/4	210	275	0.31	1.00	0.99	0.31	548	485	1.13
	30%	Outer 1/4	210	345	0.71	1.00	0.98	0.70	1241	1235	1.01
	30%	Inner 2/4	210	460	0.94	1.00	0.96	0.91	1794	1825	0.98
	70%	Outer 0/4	250	250	0.95	1.02	1.00	0.97	1729	1726	1.00
	20%	Outer 2/4	420	460	0.97	1.04	0.96	0.97	1728	1745	0.99
	50%	Inner 3/4	315	300	0.42	1.03	0.99	0.43	849	952	0.89
S e r v i c e a b i l i t y d e s i g n	40%	Outer 4/4	250	230	1.14	1.02	1.00	1.16	2074	2033	1.02
	40%	Outer 2/4	315	230	0.90	1.03	1.00	0.93	1654	1639	1.01
	60%	Inner 4/4	355	230	1.21	1.04	1.00	1.26	2494	2485	1.00
	60%	outer 3/4	210	275	0.31	1.00	0.99	0.31	548	485	1.13
	30%	Outer 1/4	210	345	0.71	1.00	0.98	0.70	1241	1235	1.01
	30%	Inner 2/4	210	460	0.94	1.00	0.96	0.91	1794	1825	0.98
	70%	Outer 0/4	250	250	0.95	1.02	1.00	0.97	1729	1726	1.00
	20%	Outer 2/4	420	460	0.97	1.04	0.96	0.97	1728	1745	0.99
	50%	Inner 3/4	315	300	0.42	1.03	0.99	0.43	849	952	0.89

5.5 Summary of Results

When a structural analysis of slabs with steps is performed with effective beam width, the reduction of lateral stiffness of the slab in the step area should be considered. Thus, step modification factor ($\gamma < 1.0$) was multiplied to the effective beam width, which was computed with the assumption of flat plate, so as to reduce the effective beam width. The step modification factor was computed by multiplying three single modification factors, which affected the slabs with steps and obtained by controlling for one variable at a time among potentially influential variables of Section 5.4. The three influential variables were step length and location (Table 5.5.1), step thickness (Table 5.5.2), and step height (Table 5.5.3).

$$\text{Step modification factor } (\gamma) = \prod \gamma'_n = \gamma'_1 \times \gamma'_2 \times \gamma'_3 \quad (\text{Eq. 5.5.1})$$

Table 5.5.1 Single modification factor by step length and location

Design type	Location of step	Step length / span length									
		None	0.1	0.2	0.3	0.4	0.5	0.6	0.7	0.8	0.9
Strength design	One side of the step connects to the vertical member	1	0.89	0.86	0.92	1.14	1.48	1.21	0.97	0.90	0.87
	Center of the step is also the center of the slab	1	0.99	0.97	0.94	0.90	0.85	0.79	0.73	0.68	0.62
	Center of the step is NOT the center of the slab	1	0.87	0.84	0.71	0.54	0.41	0.32	0.32	0.41	–

Service- ability design	Connected to the vertical member	1	0.88	0.73	0.73	0.96	1.37	1.05	0.80	0.79	0.82
	Center of the step is also the center of the slab	1	0.99	0.97	0.95	0.91	0.87	0.82	0.76	0.71	0.66
	Center of the step is NOT the center of the slab	1	0.86	0.83	0.63	0.40	0.23	0.13	0.14	0.30	–

Table 5.5.2 Single modification factor by step thickness

Design type	Step thickness / Slab thickness										
	1	1.1	1.2	1.3	1.4	1.5	1.6	1.7	1.8	1.9	2
Strength design	1	1.02	1.02	1.03	1.03	1.03	1.03	1.04	1.04	1.04	1.04
Serviceability design	1	1.01	1.02	1.02	1.03	1.03	1.03	1.03	1.04	1.04	1.04

Table 5.5.3 Single modification factor by step height

Design type	Step height / standard step height										
	1	1.1	1.2	1.3	1.4	1.5	1.6	1.7	1.8	1.9	2
Strength design	1	1	0.99	0.99	0.98	0.98	0.98	0.97	0.97	0.96	0.96
Serviceability design	1	1	0.99	0.99	0.98	0.98	0.98	0.97	0.97	0.96	0.96

Standard step height : 230 mm

Chapter 6

Conclusions

The drainage of existing bathroom is to drill its floor and is installed on the ceiling of lower floor. Thus, there have been problems of flushing noise and difficulty in repair of the leakage. This study aimed at lowering the floor of the slab in the bathroom by 230 mm to confine it within the household in order to deal with these problems.

Therefore, this study investigated the structural behavior of the RC slab with 230 mm step through gravity load test. The test result was used to examine the stress flow of the step, and then appropriate reinforcement details were proposed to manifest the bending performance equivalent to flat slab. Then, step modification factor, which can reflect the flexural stiffness against lateral load in the structural design, was suggested. The following conclusions were derived.

- 1) It was found that more quantity of rebars than that required for strut-tie model were necessary. Typical strut-tie model computes the quantity of rebar by using the balance of compression (strut) and tension (tie) force at each randomly assumed node. It was also found that the size of the randomly assumed node was too small to properly manifest the balance of force and instead the force was transferred by bonding of the rebar throughout the entire area of the panel joint. Therefore, it is appropriate to treat the entire joint panel

area as one node.

- 2) Unlike typical joint area of exterior column and beam, the joint panel area of the step in the slab is subjected to diagonal tensile force, and it is relatively very brittle to manifest early damage and failure due to tensile cracking. It is very difficult to manifest ductility of the joint itself due to the influence of diagonal tension in the joint panel area. Therefore, it is important to restrain the yield of flexural rebar, which is anchored in the joint panel area, and to prevent the damage of the joint by securing adequate bonding capacity for the purpose of securing bending strength and ductility of the flat slab during its design. In other words, it is desirable to use capacity design method, which induces flexural yield not in the joint panel area but in the flat slab area. Flexural rebar should be added in the step to prevent early flexural yield for this purpose.
- 3) It was observed that a great deal of diagonal cracking took place due to diagonal tensile force at upper step of the specimens. Since concrete is very susceptible to tensile damage, rebar reinforcement is necessary to restrain the diagonal cracking. revU-bar reinforcement at the upper step is desirable for this purpose. While diagonal compressive stress takes place at lower step, the reinforcement of lower step may not be necessary, because concrete is resistant to compressive stress. Nonetheless, additional U-bar reinforcement is necessary to manifest the anchoring capacity of revU-bar and to secure the reinforcement against negative moment, and this

study proposes Type-C reinforcement among the reinforcement details of this experiment.

- 4) Reduction of stiffness due to the step inside the flat slab can be analyzed with rotational stiffness around the step, and the lateral bending stiffness can be designed by a simplified method of multiplying appropriate step modification factor to existing effective beam width models. The effect of step is influenced by step length and location, step thickness and step height. This study suggested single modification factor, which can reflect the influence of each variable. Additionally, one step modification factors, γ , can be computed by multiplying each single modification factor for the case of considering the influence of a combination of several variables. Applying the step modification factor, which was developed and suggested in this study, the result was very similar to the linear analysis result in consideration of several variables simultaneously. Therefore, the reliability of the proposed step modification factor could be ascertained.

References

- [1] Lee, J. W. and Jeong, G. C., "Investigation of Lowering the Toilet Flushing Noise", 10th Anniversary Proceedings of The Korean Society for Noise and Vibration engineering, Vol. 2000, No. 1, 2000, pp. 165~171.
- [2] Korea Land & Housing Corporation, Bureau of Mechanic Design, "Establishment of Design Standard for Drainage Layout at the Floor for the Noise Reduction in the Bathroom (Proposal)", Korea Land & Housing Corporation, 2011, 5.
- [3] American Concrete Institute, "Detailing Corner : Steps in Beams", Concrete International, June 2012, pp. 41~44
- [4] Kang, D. E., Oh, S. H., Kang, Y. W., and Lee, W. H., "Experimental Study of Structural Behavior of the Slab with Step", Korea Concrete Institute, 2007 Autumn Academic Proceedings, Vol. 19, No. 2, 2007, pp. 37~40.
- [5] Grossman, J. S., "Verification of Proposed Design Methodologies for Effective Width of Slabs in Slab-Column Frames," ACI Structural Journal, V. 94, No. 2, March-April, 1997, pp. 181~196.
- [6] Hwang, S. J., and Moehle, J. P., "An Experimental study of Falt-Palate Structures under Vertical and Lateral Loads," No. UCB/EERC-93/03, University of California, Berkely, Feb. 1993, 278 pp.
- [7] Korea Concrete Institute, Cases of Strut-Tie Model Design of Concrete Structural Member, Gimoondang, 2007.

- [8] Korean Agency for Technology and Standards, Concrete Compressive Strength Test Method, KS F 2405:2010, Bulletin No. 2010-0654, Korean Standards Association, 2010.
- [9] Architectural Institute of Korea, Architectural Structure Standard, 2009.
- [10] Korean Agency for Technology and Standards, Steel Bar for Reinforced Concrete, KS D3504:2011, Bulletin No. 2011-0042, Korean Standards Association, 2011.
- [11] Kim, Y. M., “Analysis with Nonlinear Elastic Link”, MIDAS, 2010
- [12] Korea Land & Housing Corporation, “Development of Analysis and Design Method in Consideration of Flat Hybrid Structure of Slab with Step”, Report of Korea Land & Housing Corporation, 2012.

국 문 초 록 (Korean Abstract)

제 목 : 단차가 있는 철근콘크리트 슬래브의 구조설계에 관한 연구

지도교수 : 강 현 구

제 출 자 : 김 상 희

단차가 있는 철근콘크리트 슬래브의 설계를 위하여 실험연구와 강성보정계수를 위한 해석연구를 수행하였다. 실험연구는 콘크리트 단차슬래브의 성능을 평가하고 단차가 없는 평슬래브와 동등한 휨강도를 발현할 수 있는 보강상세를 제안하는데 그 목적이 있다. 본 연구에서는 단순지간 4점 재하 실험을 통하여 다양한 보강상세를 가진 12개 실험체의 성능을 서로 비교하였다. 추가보강근이 없는 단차슬래브는 휨강도, 강성, 처짐, 균열 등에서 평슬래브와 비교하여 매우 낮은 성능을 가졌으며, 특히 단차 내에서 균열이 빠르게 진전되어 조기에 힌지현상이 발생하였다. 반면 역U형철근, U형철근, 역L형철근, L형철근 등의 추가 보강상세를 가지는 단차슬래브는 평슬래브와 동등한 휨강도를 발현하였다. 역U형철근과 U형철근은 단차의 사인장 균열을 제어하는데 효과적이었고, 역L형철근과 L형철근은 일관적으로 단차 밖 평슬래브로 슬래브 주근의 휨항복을 유도하는 것으로 나타났다.

해석연구는 단차슬래브의 단차부위의 강성변화를 반영한 강성보정계수를 제안하고자 한다. 단차슬래브의 단차는 실험에서도 증명하였듯이 평슬래브에 비해 약하며 회전강성이 떨어진다. 그래서 6개의 모델을 비선형해석을 수행하여 단차부위의 회전강성을 산출한다. 그리고, 앞서 산출한 회전강성값을 강성해석프로그램의 회전스프링에 대입하여 변화된 횡방향 휨강성을 파악한다. 이 때, 단차 길이, 단차

높이, 단차 위치, 단차 두께 등의 1개의 변수를 통제하며 단일보정계수를 산정하였다. 여러개의 변수통제를 통하여 단일보정계수의 곱에 의한 단차보정계수의 검토하였다. 결과를 살펴보면, 단차보정계수는 단차길이와 위치, 단차 높이, 단차 두께에 영향을 받으며, 도출된 단차보정계수는 기존의 유효보폭법에 적용하여 구조설계에 쉽게 적용이 가능하다.

주요어 : 단차, 무량판, 보강근, 보정계수, 유효보폭법

학번 : 2012-20548